THE ASTROPHYSICAL JOURNAL

AN INTERNATIONAL REVIEW OF SPECTROSCOPY AND ASTRONOMICAL PHYSICS

VOLUME 88 NOVEMBER 1938 NUMBER 4

THE MATHEMATICAL CHARACTERISTICS OF SUNSPOT VARIATIONS

JOHN Q. STEWART AND H. A. A. PANOFSKY*

ABSTRACT

This paper mathematically defines the course of the Wolf sunspot numbers during the sixteen completed cycles since 1755. The usual periodic or "superposition" point of view is rejected in favor of the "outburst" hypothesis of Halm and Waldmeier, which is here independently confirmed in detail. Each successive cycle or "outburst" is regarded as a fresh phenomenon, following, however, a standard pattern.

As a new addition to the "Wolf" sunspot data published by W. Brunner in the Zurich statistics, the zero, first, and second moments for each cycle are calculated about the times of minimum, and all the observed data are employed to show that the empirical form $R = F\theta^a e^{-b\theta}$ represents, to a good first approximation, the course of spot numbers during a single outburst or cycle (of, on the average, eleven years). Here R is the Wolf number, θ is the interval in years after the time of beginning, s, of the outburst, and F, a, and b are parameters which differ for different cycles but remain constant for a single cycle. Values of these four parameters, s, a, b, and F, are tabulated for each cycle, and the goodness of fit is discussed.

There are small random discrepancies, year by year, averaging no more than half-a-dozen Wolf numbers, between observed and computed spot numbers; and an important systematic discrepancy which is particularly evident when the interval between the time of maximum and of centroid is examined. According to the form suggested, the centroid should always come after the maximum, but actually this is the case only for cycles of higher maximum. For the group of cycles of low maximum the observed centroid precedes the maximum; the interval between the two shows a strong correlation with the height of maximum. This means that in a second approximation the suggested formula for R will require modification.

The computed parameters are examined for possible mutual dependence, and the indication is that F and b can be taken as rough functions of a. The even-numbered cycles have smaller values of a than any odd-numbered cycle. In view of the strong family resemblance shown by this study among apparently rather dissimilar cycles, the conventional periodogram analysis of spot numbers definitely must be abandoned, because such resemblance would be too improbable as the result of the superposition of independent periodic factors. Long-range prediction of spots will remain impracticable, but short-range prediction will be facilitated by the methods outlined in this paper.

* The extensive contributions to this study by Mr. Panofsky represent his Senior thesis as a student of astronomy, toward his A.B., Princeton, 1938.

I. THE SUPERPOSITION HYPOTHESIS VERSUS THE OUTBURST HYPOTHESIS

Many years ago Halm[1] briefly pointed out that Spörer's well-known rule of sunspot latitudes[2] suggests that each successive spot-cycle represents a new outburst independent of previous cycles. The appearance, near solar latitudes 30° north and south, of the first spots in each successive new outburst, followed by the gradual creeping toward the sun's equator of the two zones of greatest activity, is an indication that each spot-cycle represents a fresh recurrence of a phenomenon which always follows a standard pattern of development. Each rise in the number of spots from minimum to maximum, together with the subsequent fading-back to minimum, constitutes a single outburst. Halm's suggestion was less than conclusive, however, and several careful analyses of sunspot numbers have held to the older superposition hypothesis, which interprets the rough eleven-year period as due to the combination of several continuously acting harmonic or pseudo-harmonic variations.[3] These laborious analyses without exception have failed to predict the future rise and fall of spots.

In an important paper, Waldmeier[4] has brought support to the outburst hypothesis. He suggested that the course of sunspot numbers during each outburst, from minimum to minimum, could be represented by one particular curve of a family of curves. He gave the graphical, but not the mathematical, form of sample curves of the family. The present paper suggests a simple mathematical form (eqs. [1] and [2]) and applies statistical methods of curve-fitting to prove that this form approximately represents all the annual sunspot numbers.

The outburst hypothesis, therefore, becomes so definitely substantiated that the conventional superposition approach must be abandoned.

The analysis here presented deals with the annual Wolf numbers[5]

[1] *A.N.*, **156**, 44, 1901.

[2] G. Abetti, *Handbuch der Astrophysik*, **4**, 96, 1929.

[3] H. Kimura, *M.N.*, **73**, 543, 1913; S. Oppenheim, *A.N.*, **232**, 369, 1928; H. Turner, *M.N.*, **73**, 549 and 714, 1913. But see Yule, "A Method of Investigating Periodicities, etc." *Phil. Trans.*, A, **226**, 267, 1927.

[4] *Astr. Mitt.*, Zürich, **133**, 105–30, 1935. (A good bibliography is included.)

[5] *Handbuch der Astrophysik*, **4**, 95 and 99, 1929. (These are the well-known spot

over the available years 1755–1937. These are reprinted in Table 1, in a somewhat novel form.

During these years there were sixteen successive complete spot-cycles or outbursts from minimum to maximum and down again to minimum. It is shown in Sections V and VI that a fit, rough to

TABLE 1*

WOLF SUNSPOT NUMBERS

Cycle Number	Minimum Year	Spot Numbers for Years after Minimum													
		0	1	2	3	4	5	6	7	8	9	10	11	12	13
1	1755	9.6	10.2	32.4	47.6	54.0	62.9	85.9	61.2	45.1	36.4	20.9	....	....	...
2	1766	11.4	37.8	69.8	106.1	100.8	81.6	66.5	34.8	30.6	....	....	....	....	...
3	1775	7.0	19.8	92.5	154.4	125.9	84.8	68.1	38.5	22.8	....	....	....	....	...
4	1784	10.2	24.1	82.9	132.0	130.9	118.1	89.9	66.6	60.0	46.9	41.0	21.3	16.0	6.4
5	1798	4.1	6.8	14.5	34.0	45.0	43.1	47.5	42.2	21.1	10.1	8.1	2.5	....	...
6	1810	0.0	1.4	5.0	12.2	13.9	35.4	45.8	41.1	30.4	23.9	15.7	6.6	4.0	...
7	1823	1.8	8.5	16.6	36.3	49.7	62.5	67.0	71.0	47.8	27.5	....	....	....	...
8	1833	8.5	13.2	56.9	121.5	138.3	103.2	85.8	63.2	36.8	24.2	....	....	....	...
9	1843	10.7	15.0	40.1	61.5	98.5	124.3	95.9	66.5	64.5	54.2	39.0	20.6	6.7	...
10	1856	4.3	22.8	54.8	93.8	95.7	77.2	59.1	44.0	47.0	30.5	16.3	....	....	...
11	1867	7.3	37.3	73.9	139.1	111.2	101.7	66.3	44.7	17.1	11.3	12.3	....	....	...
12	1878	3.4	6.0	32.3	54.3	59.7	63.7	63.5	52.2	25.4	13.1	6.8	....	....	...
13	1889	6.3	7.1	35.6	73.0	84.9	78.0	64.0	41.8	26.2	26.7	12.1	9.5	....	...
14	1901	2.7	5.0	24.4	42.0	63.5	53.8	62.0	48.5	43.9	18.6	5.7	3.6	....	...
15	1913	1.4	9.6	47.4	57.1	103.9	80.6	63.6	37.6	26.1	14.2	....	....	....	...
16	1923	5.8	16.7	44.3	63.9	69.0	77.8	65.0	35.7	21.2	11.1	....	....	....	...
17	1933	5.7	8.7	36.1	80.4	114.4	....	....	....	....	....	....	....	....	...

* E.g., the spot number for the year 1850 = 1843 + 7 is 66.5; and in this paper this number is attributed to the data 1850.5, since it is the *average* number for a calendar year. Numbers for 1749.5 through 1754.5 are, respectively, 80.9, 83.4, 47.7, 47.8, 30.7, 12.2.

excellent, for each of these sixteen outbursts can be obtained by suitable choices of four disposable parameters, F, a, b, and s, in the family of curves,

$$R = F(r - s)^a e^{-b(r-s)}, \tag{1}$$

where R is the Wolf number for the varying year r. During a single cycle F, a, b, and s are to be taken as constant. Here s is the time of the start of the new outburst; F is a scale factor; a is a pure number; the parameter b expresses the amount of damping and has the dimensions of inverse time; r runs with the time from s to plus infinity. For $r < s$, R is taken as zero.

numbers of Wolf, Wolfer, and Brunner. Values after 1927 are direct from the *Astr. Mitt.*).

II. RELEVANT PROPERTIES OF THE SUGGESTED FAMILY OF CURVES

Writing $\theta = r - s$, the time in years since the start of the outburst,

$$R = F\theta^a e^{-b\theta} . \tag{2}$$

This is Pearson's Type III distribution;[6] but for present purposes the form must be examined afresh. The following results are readily verified.

a) The time at which maximum occurs is

$$v = s + \frac{a}{b} . \tag{3}$$

b) The spot number V at maximum is

$$V = \frac{Fa^a e^{-a}}{b^a} . \tag{4}$$

c) The area or zero moment for the outburst is

$$M_0 = \int_0^\infty F\theta^a e^{-b\theta} d\theta = \frac{F\Gamma(a+1)}{b^{a+1}} , \tag{5}$$

where $\Gamma(a+1)$ is the ordinary gamma function.[7]

d) The first moment with respect to the arbitrary time t is

$$M_1 = \int_0^\infty (r-t)\dot{R}dr = \frac{F\Gamma(a+2)}{b^{a+2}} + M_0(s-t) .$$

In the integration R is taken as zero for values of $r < s$; we write

$$(r-t) = \theta + (s-t) .$$

The centroid of the outburst comes at time

$$w = t + \frac{M_1}{M_0} = s + \frac{a+1}{b} , \tag{6}$$

since $\Gamma(a+2) = (a+1)\,\Gamma(a+1)$.

[6] *Phil. Trans.*, A, **186**, 373, 1895.

[7] Tabulated, e.g., by J. Brownlee to seven decimal places in *Tracts for Computers*, No. 9, Cambridge University Press, 1923.

e) The second moment with respect to t is

$$M_2 = \int_0^\infty (r - t)^2 R dr = \frac{F\Gamma(a + 3)}{b^{a+3}} + 2M_1(s - t) + M_0(s - t)^2 .$$

Thus, the invariant σ^2 (independent of $s - t$) is

$$\sigma^2 = \frac{M_2}{M_1} - \left(\frac{M_1}{M_0}\right)^2 = \frac{a + 1}{b^2} . \tag{7}$$

This is a measure of the dispersion of the sunspot numbers during an outburst. (For a frequency curve σ^2 so defined comes out the square of the standard deviation.)

f) Another useful relation is

$$\frac{V}{M_0} = \frac{ba^a e^{-a}}{\Gamma(a + 1)} = b\phi(a) , \tag{8}$$

where

$$\phi(a) = \frac{a^a e^{-a}}{\Gamma(a + 1)} . \tag{9}$$

Numerical values of $\phi(a)$, $a\phi(a)$, and $(a + 1)\phi(a)$ have been computed in Table 4.

The flexibility of the form (1) or (2) is worth emphasizing. When γ is any positive exponent,

$$R^\gamma = F^\gamma \theta^{\gamma a} e^{-\gamma b\theta} ,$$

but, writing $F^\gamma = F'$, $\gamma a = a'$, $\gamma b = b'$, this is just the original form (2). Accordingly, *the rather successful agreement with observation described below establishes little as to the physical meaning of the scale of Wolf numbers.*

III. THE OBSERVATIONAL CRITERIA

To fit a particular curve of the family (1) or (2) to any one of the sixteen available outbursts since 1749, a suitable value of each of the four adjustable constants, F, a, b, and s, must be determined. In

the Zurich statistics[8] three quantities especially applicable to this purpose are published for each cycle, namely:

The exact time of minimum, which will be designated by u

The time of maximum, designated here by v

The sunspot number, V, at maximum (the tabulated "maximum smoothed monthly number").

In addition, the area M_0 can be readily approximated by summing the published annual sunspot numbers (of Table 1) between suc-

TABLE 2

OBSERVED DATA

Cycle Number	s	t	u	v	w	M_0	M_1	M_2	M_1/M_0	σ^2
1	1754.60	55.5	55.2	61.5	61.33	467	2652	17,710	5.68	5.68
2	1766.35	66.5	66.5	69.7	70.79	537	2226	11,266	4.14	3.81
3	1775.37	75.5	75.5	78.4	79.72	615	2502	12,124	4.07	3.17
4	1784.53	84.5	84.7	88.1	90.05	843	4555	31,184	5.40	7.19
5	1797.59	98.5	98.3	05.2	04.00	277	1482	9,227	5.35	4.68
6	1810.09	10.5	10.6	16.4	17.38	236	1591	11,880	6.73	4.95
7	1822.65	23.5	23.3	29.9	29.35	392	2233	14,357	5.70	4.19
8	1833.74	33.5	33.9	37.2	38.37	653	3083	17,158	4.72	3.97
9	1843.18	43.5	43.5	48.1	49.51	694	4068	28,354	5.86	6.50
10	1855.75	56.5	56.0	60.1	61.58	547	2698	16,375	4.93	5.61
11	1867.03	67.5	67.2	70.6	71.92	620	2647	13,929	4.27	4.25
12	1878.52	78.5	78.9	83.9	83.78	382	1960	11,757	5.13	4.44
13	1889.30	89.5	89.6	94.1	94.83	463	2395	14,853	5.18	5.24
14	1901.37	01.5	01.7	06.4	07.11	373	2038	12,873	5.46	4.67
15	1913.36	13.5	13.6	17.6	18.39	444	2105	11,633	4.74	3.71
16	1923.25	23.5	23.6	28.4	28.35	410	1928	10,443	4.70	3.38
17	.....	33.5	33.8	.....	.....	.....	.....	.....	.....	.....

cessive minima, and this we have done. Similarly, we have approximated the first and second moments, M_1 and M_2, about an arbitrary time t—taken as the time of the minimum near the beginning of an outburst (but see Sec. IV).

Values of these seven quantities, together with values of two others, s and w, obtained as explained below, are presented in Table 2. (Century numbers are omitted before the years, except for values of s.) The following specific example shows exactly how the tabulated values of M_0, M_1, and M_2 were obtained. Cycle number 2 (Table 1) begins with the minimum of about 1766.5 and ends with the minimum of about 1775.5. The annual spot numbers for Cycle

[8] *Astr. Mitt.*, Zürich, **124**, 77, 1930.

2—years 1766.5–1775.5, inclusive—are 11.4, 37.8, 69.8, 106.1, 100.8, 81.6, 66.5, 34.8, 30.6, and 7.0. In computing the moments, the two minimum values are regarded as shared with the preceding and following cycles, and therefore (as a rough allowance) are reduced to one-half in the computation. So M_0 is approximately $5.7 + 37.8 + 69.8, + \ldots + 30.6 + 3.5 = 537$. The value of t was uniformly taken as the year of the initial minimum annual number—here 1775.5. Thus M_1 is $(0)(5.7) + (1)(37.8) + (2)(69.8) + \ldots + (8)(30.6) + (9)(3.5) = 2226$. Similarly M_2 is $(0)(5.7) + (1)(37.8) + (2^2)(69.8) + \ldots + (8^2)(30.6) + (9^2)(3.5) = 11266$. (All numerical computations were carried out on a late-model Monroe or a Marchant computing machine.) In each cycle the computations of the moments were carried in this manner from minimum to minimum annual numbers. (These rounded-off annual minima are not to be confused with the Zurich times u estimated for exact minima.)

Empirical tests with idealized cases showed that the errors involved in taking the integrals for M_0, M_1, M_2 (of Sec. II) as equivalent to the summations (formed as just described) are negligible here.

It is worth noting that the values of V used in Table 2 doubtless are not quite the best values that could have been adopted for the particular purposes of this paper. In place of using these Zurich maxima from smoothed monthly numbers, maxima could have been adopted from smoothed annual numbers. Such maxima would have been slightly smaller in many cycles. Their use would have reduced a little the systematic discrepancies discussed below—but by no means would they have eliminated them. In order to keep our study wholly "objective," however, and since general conclusions would not have been affected, we employed the Zurich values.

IV. OVERLAP AND END CORRECTION

An outburst of the form (1), although damped out rapidly for large values of $r - s$, still retains a slight vitality even after the beginning of its successor outburst (Table 7). The spot numbers for several years after each minimum represent the sum of the effects of the new, growing cycle and the preceding, not yet quite negligible, cycle. The computation of the moments, however, ran only from

minimum to minimum. Since the theoretical moments represent summations to infinity, there are positive end corrections to be applied to the values of M_1 and M_2 presented in Table 2. These corrections can be approximated in detail for particular cases (when a and b are known) by reference to tables for the incomplete gamma function.[9] (In general, only a negligible correction is indicated for M_0 because the loss of area after the arbitrary cut-off at the second minimum is statistically balanced by the gain of area from the tail

TABLE 3

OBSERVED DATA: THE OBSERVATIONAL CRITERIA

Cycle Number	V	M_0	V/M_0	$v-u$	$v-s$	$w-s$	$w-v$
1	86.5	467	0.185	6.3	6.90	6.73	−0.17
2	115.8	537	.216	3.2	3.35	4.44	+1.09
3	158.5	615	.257	2.9	3.03	4.35	+1.32
4	141.2	843	.167	3.4	3.57	5.52	+1.95
5	49.2	277	.178	6.9	7.61	6.41	−1.20
6	48.7	236	.206	5.8	6.31	7.29	+0.98
7	71.7	392	.183	6.6	7.25	6.70	−0.55
8	146.9	653	.225	3.3	3.46	4.63	+1.17
9	131.6	694	.190	4.6	4.92	6.33	+1.41
10	97.9	547	.179	4.1	4.35	5.83	+1.48
11	140.5	620	.227	3.4	3.57	4.89	+1.32
12	74.6	382	.195	5.0	5.38	5.26	−0.12
13	87.9	463	.190	4.5	4.80	5.53	+0.73
14	64.2	373	.172	4.7	5.03	5.74	+0.71
15	105.4	444	.237	4.0	4.24	5.03	+0.79
16	78.1	410	0.190	4.8	5.15	5.10	−0.05

of the preceding outburst incorrectly included after the initial minimum.)

It turns out that the additive corrections so indicated for the various values of M_2 are so large as to render the values of M_2, and consequently of σ^2, in Table 2 rather unreliable (see Sec. VIII). Fortunately, only slight end corrections are indicated, by detailed study, for the values of M_1. The uniform correction to M_1/M_0 of +0.15 year, while somewhat arbitrary, seemed sound enough for use. The values in Table 2 are without this correction, however. Further discussion of these points is omitted for the sake of brevity.

The Zurich data, of course, do not give the times of start, s, of

[9] *Tables of the Incomplete* Γ-*Function*. Karl Pearson, ed., London, 1922.

the outbursts but—disregarding random fluctuations in the spots—these must always a little precede the minima. Such precedence is because the observed spot-curve represents, as has been said, the sum of the effects of the fading and the fresh outbursts, and the new outburst at first is gaining less rapidly than the old one falls.[10] Our examination of the individual cases with reference to appropriate curves of the family (1) showed that an adequate empirical first approximation to s is

$$s = u - 0.015(v - u)^2 , \tag{10}$$

where v, it will be remembered, is the Zurich time of maximum, and u of minimum. The values of s in Table 2 were so derived and, strictly speaking, are not "observed data"; but the correction $-0.015\ (v - u)^2$ is always small.

Again, detailed discussion is omitted for brevity's sake. The small corrections described in the two immediately preceding paragraphs are undeniably in the right direction and are of about the right magnitude. Any reasonable quantitative changes in them would not make a significant difference.

V. FITTING THE INDIVIDUAL SIXTEEN CYCLES; THE FIVE CASES

Table 2 includes values of s computed by means of (10) from the Zurich values of u and v. It also presents values of w, defined as the times of the centroids of the outbursts, obtained by adding M_1/M_0 to t (eq. [6])—with the inclusion in each case of the adopted end correction, +0.15 year, to the tabulated M_1/M_0.

Any four of the five independent quantities, V, M_0, s, v, and w, suffice in each special cycle or outburst to determine, through the equations of Section II, the four adjustable constants, a, b, s, and F, of (1). Accordingly, five cases arise.

1. Adopt from Table 2 M_0, V, s, and v. Combination of (3) and (8) gives

$$(v - s)\frac{V}{M_0} = a\phi(a) . \tag{11}$$

[10] Waldmeier, *op. cit.*, p. 107, Fig. 1.

But by Table 4 the value of $a\phi(a)$ so found determines a. Then, by (3),

$$b = \frac{a}{v - s}, \tag{12}$$

and we compute w by the second part of (6).

TABLE 4

AUXILIARY TABLE REPRESENTING EQUATION 9

a	$\phi(a)$	$a\phi(a)$	$(a+1)\phi(a)$
1.0	0.3679	0.3679	0.7358
1.2	.3402	0.4083	0.7485
1.4	.3180	0.4452	0.7632
1.7	.2915	0.4955	0.7870
2.0	.2707	0.5413	0.8120
2.3	.2537	0.5835	0.8372
2.6	.2396	0.6230	0.8626
3.0	.2240	0.6720	0.8960
3.5	.2082	0.7288	0.9370
4.0	.1953	0.7815	0.9768
4.5	.1846	0.8308	1.0154
5.0	.1754	0.8774	1.0528
5.5	.1675	0.9217	1.0892
6.0	.1606	0.9637	1.1243
6.5	.1544	1.0042	1.1586
7.0	.1490	1.0430	1.1920
7.5	.1440	1.0805	2.0115
8.0	.1396	1.1167	1.2563
8.5	.1355	1.1518	1.2873
9.0	.1318	1.1858	1.3176
9.5	.1283	1.2189	1.3472
10.0	.1251	1.2511	1.3762
11.0	.1194	1.3132	1.4326
12.0	.1144	1.3724	1.4868
13.0	.1099	1.4292	1.5391
14.0	.1060	1.4839	1.5899
15.0	0.1024	1.5366	1.6390

2. Adopt from Table 2 M_0, V, s, and w. By (6) and (8),

$$(w - s)\frac{V}{M_0} = (a + 1)\phi(a), \tag{13}$$

determining a by Table 4. Then, by (8),

$$b = \frac{a + 1}{w - s}, \tag{14}$$

and we compute v by (3).

3. Adopt M_0, V, v, and w. By (3), (6), and (8)

$$b = \frac{1}{w - v}, \tag{15}$$

and

$$(w - v)\frac{V}{M_0} = \phi(a), \tag{16}$$

determining a by Table 4. We compute s by (3).

4. Adopt M_0, u, v, and w. Then (15) applies, but a is found from

$$a = \frac{v - s}{w - v}, \tag{17}$$

and we compute V by (8).

5. Adopt V, u, v, and w. Then (15) and (17) apply; so a and b are the same as in Case 4. We compute M_0 by (8).

Values of the quantities w, v, s, V, and M_0, so computed, will be designated by primes. In every case F is found by (5), which is equivalent to

$$\log F = (a + 1)\log b - \log \Gamma(a + 1) + \log M_0. \tag{18}$$

As a step in these computations, Table 3 presents values of M_0, $v-u$, $v-s$, $w-s$, and $w-v$ derived from Table 2, together with values of V[8] and V/M_0. The fact that $w-v$ is less than zero for Cycles 1, 5, 7, 12, and 16 is definite evidence that the suggested family of curves described by equation (1) cannot accurately fit these cases, for a negative value of b in (15) is meaningless. But these cycles, together with 6, are just the group of cycles of lowest maxima. For these the observed centroid precedes the observed maximum; but for all curves described by equation (1) the centroid must follow the maximum. The conclusion is that *the cycles of lowest maxima systematically deviate from the suggested form—their maxima come too late*. This discrepancy is discussed further in Sections VI and VII. It corresponds in the detailed fits of Section VI to definitely systematic but not very large differences between observed and computed spot numbers, especially for years near maxima of the group of low cycles.

Since the observed time v of maximum and the time w of centroid (Table 1) are both assumed in Cases 3, 4, and 5, these cases have meaning only when applied to the remaining cycles: viz., 2, 3, 4, 6, 8, 9, 10, 11, 13, 14, 15.

Table 5 gives for each of the sixteen cycles the values of a and b computed by the methods just described. The determination of the second decimal places in a and b is not precise. Only Cases 1 and 2 apply to all the cycles. Cases 4 and 5 give identical values as regards a, and Cases 3, 4, and 5 give identical values of b. Values of log F are included for Case 2 only; the others may be obtained from (18).

TABLE 5

COMPUTED PARAMETERS

Cycle Number	Case 1		Case 2			Case 3		Cases 4 and 5	
	a	b	a	b	log F	a	b	a	b
1	10.43	1.51	7.89	1.32	−0.763	.....	.....	.....	.....
2	3.44	1.03	3.75	1.07	+1.650	2.71	0.92	3.08	0.92
3	3.99	1.32	5.95	1.60	+1.390	1.20	0.76	2.30	0.76
4	2.41	0.68	3.35	0.79	+1.500	1.32	0.51	1.82	0.51
5	11.66	1.53	6.21	1.12	−0.233	.....	.....	.....	.....
6	10.80	1.71	12.30	1.83	−3.147	3.74	1.02	6.44	1.02
7	11.22	1.55	7.55	1.28	−0.682	.....	.....	.....	.....
8	3.97	1.15	4.86	1.27	+1.447	2.13	0.85	2.94	0.85
9	5.63	1.14	7.13	1.28	−0.103	2.06	0.71	3.49	0.71
10	3.97	0.91	4.88	1.01	+0.772	2.10	0.68	2.96	0.68
11	4.29	1.20	5.73	1.38	+1.095	1.61	0.76	2.71	0.76
12	7.07	1.31	4.62	1.07	+0.944	.....	.....	.....	.....
13	5.38	1.12	4.95	1.08	+0.823	8.10	1.37	6.58	1.37
14	4.88	0.97	4.14	0.89	+0.839	10.48	1.41	7.09	1.41
15	6.54	1.54	7.04	1.60	+0.550	4.36	1.27	5.38	1.27
16	6.20	1.20	3.92	0.96	+1.198	.....	.....	.....	.....

VI. DETAILED CURVES

The spread in Table 5, for the various cases, in the values of a and b, respectively, for an individual cycle, provides an indication of how well the suggested form (1) fits each separate outburst. (But see the last paragraph of Sec. VIII). If the fit were exact in every detail, there would be no spread. If only random departures existed, there would be no systematic spread. A serious systematic discrepancy has already been mentioned; it is discussed further

in the next section. Because of this discrepancy—which proves that the suggested form (1) requires modification—detailed fits are presented in Table 7 for only a few sample cycles and cases. Such fits are much better than a superficial inspection of the discrepancies of Table 5 would suggest.

For example, the suggested form (1) represents the annual spot numbers of the long Cycle 4 very fairly—notwithstanding small systematic deviations; as Table 7 shows. It will be remembered that

TABLE 6*

COMPUTED CRITERIA

Cycle Number	V'	M_0'	$w'-s$	$v'-s$	$v-s'$
1	.....	.....	7.57	5.98	.....
2	109.4	568	4.31	3.50	2.95
3	118.7	822	3.78	3.72	1.58
4	121.8	977	5.05	4.25	2.57
5	.....	.....	8.21	5.54	.....
6	37.4	308	6.90	6.72	3.67
7	.....	.....	7.88	5.90	.....
8	125.5	764	4.32	3.83	2.49
9	102.8	889	5.82	5.57	2.90
10	83.9	639	5.44	4.83	3.11
11	111.0	785	4.41	4.15	2.13
12	.....	.....	6.16	4.32	.....
13	97.5	418	5.70	4.58	5.91
14	77.9	307	6.06	4.65	7.44
15	95.4	490	4.90	4.40	3.44
16	.....	.....	6.00	4.08	.....

* The respective cases (Sec. V), left to right, are 4, 5, 1, 2, and 3. Cf. Table 3.

this cycle of 1784–98 seemed so abnormal to Newcomb that he rejected it in his statistical examination.[11] Such rejection is altogether unwarranted from the present point of view, and *invalidates Newcomb's conclusion that an underlying regularity of period governs the sunspot cycles.*

The late observed maximum of such a smallish outburst as Cycle 12 is associated with very appreciable systematic deviations between observed and computed spot numbers throughout the cycle; but even so the representation (according to Case 2) computed in Table 7 for Cycle 12 is in fair agreement with observation.

[11] *Ap.J.*, **13**, 1, 1901.

The computed spot numbers in Table 7 are obtained from the formula—another form of (2):

$$\log R' = \log F + a \log (r - s) - 0.43429\, b(r - s)\,, \qquad (19)$$

all logarithms being to Base 10. In Cycle 4, for example, r takes on the successive values, 1785.5, 1786.5, ...; and the constant s (by Table 2) is 1784.53; $\log F$, a, and b also are constant throughout the computation, and their values are taken from Table 5.

Examination of residuals O−C for the sunspot numbers, such as are presented in Table 7, indicates that a suitable mathematical form, replacing (1), which would eliminate the systematic discrepancies, *would represent each outburst with an average random deviation regardless of sign of no more than half-a-dozen Wolf numbers.* Thus, the hypothesis is confirmed that *the general course of sunspot numbers follows during each successive outburst an underlying and surprisingly definite trend.*

VII. SYSTEMATIC DEVIATIONS

A comparison of the computed values presented in Table 6 with the corresponding values of the "observational criteria" given in Table 3 brings out the nature of the systematic failure of equation (1) to fit exactly the course of sunspot numbers. The overdetermination of the four adjustable parameters permitted by the trustworthiness of the five observed quantities taken as criteria (Sec. III) fortunately makes possible this test of the applicability of the form (1).

The five cases represented in Table 6 must of necessity lead to the same conclusion with respect to the nature of the systematic discrepancies. It suffices to consider here in detail Case 2 only. The fit in Case 2, it will be recalled (Sec. V), is made by assuming M_0, the area; V, the maximum smoothed monthly spot number; s, the time of beginning of the outburst (from eq. [10]); and w, the time of centroid of the outburst (from the first part of eq. [6], with a uniform plus end correction of 0.15 year); and computing the time of maximum, v'. Table 8 compares these computed times, v' (Table 6), with the observed times of maximum v (of Table 2) in relation to the observed heights V of maximum. *Definitely, Table 8 shows $v-v'$ is*

large positively for the lower maxima and takes on negative values for the cycles of higher maxima.

TABLE 7*

COMPUTED SUNSPOT NUMBERS

t	Case 2		O−C	Case 2		O−C
	R'	R'		t	R'	
	Cycle 2				Cycle 12	
1766.5	0.3	.....	.....	1879.5	3.6	.....
67.5	22.1	.....	+15.7	80.5	25.5	+ 6.8
68.5	79.1	.....	− 9.3	81.5	56.8	− 2.5
69.5	113.5	.....	− 7.4	82.5	73.6	−13.9
70.5	109.6	.....	− 8.8	83.5	70.8	− 7.1
71.5	84.3	.....	− 2.7	84.5	56.4	+ 7.1
72.5	56.2	.....	+10.3	85.5	39.4	+12.8
73.5	34.0	.....	+ .8	86.5	25.0	+ 0.4
74.5	19.1	.....	+11.5	87.5	14.8	− 1.7
75.5	10.1	Cycle 3	− 3.1	88.5	8.3	− 1.5
76.5	5.1	8.3	+ 6.4	89.5	4.4	.....
77.5	2.5	73.1	+16.9	.....	.....	.....
78.5	1.2	145.5	+ 7.7	.....	.....	.....
79.5	0.5	153.1	−27.7	.....	.....	.....
80.5	0.2	112.2	−27.6	.....	.....	.....
81.5	0.1	65.6	+ 2.4	.....	.....	.....
82.5	.....	32.5	+ 6.0	.....	.....	.....
83.5	.....	14.3	+ 8.5	.....	.....	.....
84.5	Cycle 4	5.8	+ 4.4	.....	.....	.....
85.5	13.3	2.2	+ 8.6	Case 3, Cycle 4		
86.5	65.0	0.8	+17.1	1786.5	88.7	− 6.6
87.5	116.9	0.3	+14.8	87.5	135.2	− 3.5
88.5	140.3	0.1	− 9.5	88.5	139.0	− 8.2
89.5	135.5	.....	−17.4	89.5	122.2	− 4.1
90.5	114.0	.....	−24.1	90.5	98.4	− 8.5
91.5	87.1	.....	−20.5	91.5	75.0	− 8.4
92.5	62.1	.....	− 2.1	92.5	55.1	+ 4.9
93.5	41.9	.....	+ 5.0	93.5	39.4	+ 7.5
94.5	27.2	.....	+13.8	94.5	27.6	+13.4
95.5	17.0	.....	+ 4.3	95.5	19.0	+ 2.3
96.5	10.4	.....	+ 5.6	96.5	12.9	+ 3.1
97.5	6.2	.....	+ 0.2	97.5	8.6	− 2.2
98.5	3.6	.....	+ 0.5	98.5	5.3	.....

* Where two computed cycles overlap, as in 1776.5, the two values of R' were summed before computing O−C. (For the observed values see Table 1.)

The only marked exceptions to this correlation of $v - v'$ with V are Cycles 6 and 14. Cycle 6 in all statistical respects (Tables 3, 8, 9) behaves like a cycle of high maximum, although it is the lowest of all. In view of observational uncertainties for the earlier cycles and of possible displacements of maxima due to the undoubted "random" deviations in spot numbers from their indicated underlying trend, these exceptions are not necessarily significant. The

TABLE 8

THE SYSTEMATIC DISCREPANCY BETWEEN EQUATION (1) AND OBSERVATION

V	Cycle Number	Observed v	Computed v'	O−C $v-v'$
48.7	6	1816.4	1816.81	−0.41
49.2	5	1805.2	1803.12	+2.08
64.2	14	1906.4	1906.02	+0.38
71.7	7	1829.9	1828.55	+1.35
74.6	12	1883.9	1882.84	+1.06
78.1	16	1928.4	1927.33	+1.07
86.5	1	1761.5	1760.58	+0.92
87.9	13	1894.1	1893.88	+0.22
97.9	10	1860.1	1860.58	−0.48
105.4	15	1917.6	1917.76	−0.16
115.8	2	1769.7	1769.85	−0.15
131.6	9	1848.1	1848.75	−0.65
140.5	11	1870.6	1871.18	−0.58
141.2	4	1788.1	1788.78	−0.68
146.9	8	1837.2	1837.57	−0.37
158.5	3	1778.4	1779.09	−0.69

observed spot numbers for Cycle 14 obviously are a bit ragged—it seems that "random" deviations in the actual number of spots from their underlying trend are pronounced for that cycle. The discrepancies for Cycle 6 would be avoided if the observed maximum came later. On a flat-topped curve with random deviations such an error would not be surprising.

A rough empirical representation of Table 8 is

$$v - v' = \frac{108 - V}{40}. \tag{20}$$

Search for an improved mathematical form to be substituted for (1) should be guided, therefore, by (20). That is to say, a new family of curves should be looked for such that, when the height of maxi-

mum, V, area, M_0, time of start of outburst, s, and time of centroid of outburst, w, are fitted exactly, the new computed time of maximum v'' will follow the corresponding Case 2 computed time v' by roughly the quantity $(V - 108)/40$. This linear correlation with V need not be anything like exact.

The existence of the systematic deviations shown in Table 8 is definitely confirmatory of the hypothesis that a *suitably modified mathematical form rather similar to* (1) *will represent with fair accuracy the general course of sunspot numbers.* The various numerical tables already presented lead to the very tentative suggestion that *the true form replacing* (1) *likewise needs to have four adjustable parameters.* The wide variations in a, b, and log F (Table 5) permitted in almost equally good representations of individual cycles suggest that (1) uses four parameters to make adjustments for which only three would be sufficient—resulting in some indetermination. On the other hand, the inability of the form (1) to adjust itself generally to the observed relation between maximum and centroid (Sec. V, Cases 3, 4, 5; Cycles 1, 5, 7, 12, 16) shows that a fourth parameter is required in the true form to meet this condition.

VIII. THE SECOND MOMENTS

Were it not for the large, uncertainly determined end corrections which are required (Sec. IV, because of overlap, for the values of M_2 presented in Table 2, equation (7) would give a sixth control for the determination of a and b, and so would give an excellent further test of the applicability of form (1). In the actual circumstances this test is a weak one. Table 9 compares the computed values of $(a + 1)/b^2$ (from Table 7 for Case 2 only) with the observed values of σ^2 from Table 2. If form (1) applied without systematic discrepancy, the observed σ^2 of the cycle could not be systematically greater than the computed $(a + 1)/b^2$, for the expected end corrections to σ^2 are positive. But for Cycles 1, 3, 4, 6, 8, 9, 11, 13, 15, σ^2 is greater than $(a + 1)/b^2$. Of these only Cycle 1 is among the group of cycles of low maximum for which the centroid precedes the maximum. That group comprises (as has been said in Sec. V) Cycles 1, 5, 7, 12, 16. The condition that the observed σ^2 be less than the computed $(a + 1)/b^2$ is indeed met (when the fit is by Case 2) only by Cycles 2, 5, 7, 10, 12, 14, 16. (If Case 1 instead of Case 2 had been exam-

ined, the only change is the reversal of size of the O−C for Cycle 4.)

Accordingly, Table 9 gives further, although slighter, evidence, supplementing Table 8, that the suggested form (1) is systematically somewhat in error.

It is worth mentioning that the O−C in Table 9 for Cycle 2 is about what would be expected from end correction. Also, in Table 8 Cycle 2 shows only a small discrepancy. Therefore, equation (1) applied to Cycle 2 fits well all six criteria. The height of maximum

TABLE 9

THE SECOND MOMENTS

Cycle Number	$(a+1)/b^2$ (Case 2)	σ^2	O−C
1	5.11	5.68	+0.57
2	4.15	3.81	−0.34
3	2.71	3.17	+0.46
4	6.97	7.19	+0.22
5	5.75	4.68	−1.07
6	3.97	4.95	+0.98
7	5.21	4.19	−1.02
8	3.64	3.97	+0.33
9	4.96	6.50	+1.54
10	5.76	5.61	−0.15
11	3.53	4.25	+0.72
12	4.91	4.44	−0.47
13	5.10	5.24	+0.14
14	6.49	4.67	−0.82
15	3.14	3.71	+0.57
16	5.34	3.38	−1.96

of this cycle is intermediate between the two extreme groups, which indicates that *equation* (1) *is exact for cycles of intermediate height of maximum*, and the run of values of v–v^1 in Table 8 confirms this.

IX. REPRESENTATION OF THE COURSE OF SUNSPOTS BY A TWO-PARAMETER FAMILY

Referring to Table 5, Case 2, b and $\log F$ can be expressed with fair statistical approximation as functions of the corresponding a. The empirical approximations

$$b = 1.60 \log a + 0.03 , \tag{21}$$

$$\log F = -0.537a + 3.63 , \tag{22}$$

represent most of the sixteen cycles not badly (Table 10).

A series of curves R as a function of θ (eq. [2]) for different relevant values of a, and having b and F related to a by (21) and (22), could be computed and plotted on tracing paper. If all the sunspot numbers of Table 1 are plotted, then by sliding in time sample curves of this series the best fit with respect to values of a and s can be readily found for each cycle. *These two-parameter representations so found of the whole course of the sunspot numbers would be, in general, fair,* although in certain cycles not so good as the four-parameter

TABLE 10

CORRELATION OF a, b, AND F (CASE 2)

Cycle Number	a	log F	log a	b
4	3.35	+1.500	0.53	0.79
2	3.75	+1.650	0.57	1.07
16	3.92	+1.198	0.59	0.96
14	4.14	+0.839	0.62	0.89
12	4.62	+0.944	0.66	1.07
8	4.86	+1.447	0.69	1.27
10	4.88	+0.772	0.69	1.01
13	4.95	+0.823	0.69	1.08
11	5.73	+1.095	0.76	1.38
3	5.95	+1.390	0.77	1.60
5	6.21	−0.233	0.79	1.12
15	7.04	+0.550	0.85	1.60
9	7.13	−0.103	0.85	1.28
7	7.55	−0.682	0.88	1.28
1	7.89	−0.763	0.90	1.32
6	12.30	−3.147	1.09	1.83

fits of Table 5. A careful study of the overlaps so found doubtless would result in a slight modification of equation (10) and of the correction to M_1/M_0. Of course, all these representations, which follow form (1), are subject to systematic deviations described in sections 7 and 8.

Waldmeier's suggestions[12] related implicitly to a two-parameter representation of each outburst. A definitive decision as to the validity of such a representation and of the physical usefulness of formulae such as (21) and (22) must be postponed until an improved substitute for (1) has been found, and such a substitute is not presented here. In any event, with so few cycles available, the statisti-

[12] Waldmeier, *op. cit.*, Figs. 2 and 5.

cal situation may remain too indefinite to permit the decision for decades to come.

X. THE PROBLEM OF PREDICTING THE TIME OF START OF AN OUTBURST

A similar study relates to the possible correlation between the time of the start of an outburst and characteristics of that outburst or of the preceding one. *If such a correlation exists, then* s *ceases to be an independent parameter; and a one-parameter representation is possible.* Evidently, the new outburst never begins until the old one has faded rather low. For example, one finds evidence to support the *very tentative rule that the new outburst begins about a year after the old one has dropped to one-tenth of its maximum.* This problem could be readily given further study, employing data in the foregoing tables as a basis for computation.

XI. THE AREA AHEAD OF MAXIMUM

Waldmeier has stated the proposition that in every outburst the sum of all the monthly spot numbers between the preceding minimum monthly number and the maximum monthly number of the outburst is constant. Observed data which he presents[13] roughly bear out this suggestion, but in this part of his study he has omitted Cycles 1–6, inclusive—and Cycles 5 and 6, with the smallest maxima of all, if included, would definitely disprove his suggestion. There seems to be no adequate *statistical* reason for omitting the earlier cycles—as examination of the tables of the present paper shows. Of course there is no denying that the older data are uncertain, but their inclusion seems necessary.

From the standpoint of the present paper, a brief treatment of the area ahead of maximum is of some interest. The fraction α of the whole area M_0 of the outburst which is included ahead of the maximum may be found from tables for the incomplete gamma function. Equation (3) shows that the maximum is always at $\theta = a/b$. The fractional area included between $\theta = 0$ and $\theta = a/b$ is readily proved to be a function of a only, independent of b; and, referring to Pearson's tables[9] of $I(u, p)$, α is $I(a/\sqrt{a+1})$, and is independent of b. Values are presented in Table 11; α is nowhere as large as 0.500.

[13] *Ibid.*, p. 120.

For any given outburst, the computed area ahead of maximum would be αM_0. The observed values given by Waldmeier are subject to much uncertainty, in that a slight shift of the times of least and greatest monthly numbers obviously changes them relatively more than the intervals $v-u$ are changed.

XII. CORRELATIONS AMONG THE OBSERVATIONAL DATA

a) The very significant correlation between height of maximum, V, and the time of rise, $v-u$ (Table 3), of a cycle, has been rediscovered independently by several investigators, but even yet is

TABLE 11

FRACTIONAL AREA, α, AHEAD OF MAXIMUM

a	α	a	α
1.0	0.264	2.9	0.351
1.2	.281	3.2	.357
1.3	.289	3.5	.363
1.4	.294	3.9	.369
1.5	.300	4.3	.376
1.7	.308	4.7	.381
1.9	.316	5.0	.384
2.1	.326	6.0	.395
2.3	.335	7.0	.399
2.5	.341	49.0	0.462
2.7	0.345		

frequently ignored.[14] This relation is well satisfied by the methods of fit based on equation (1).

b) The relation between the time of rise and the time of fall often has been inadequately stated. The ratio of these depends upon the height of maximum. Similarly, an excellent correlation—to which explicit attention appears not to have been directed prior to the present study—*holds between* V *and* w–v: *that is, between height of maximum and interval between maximum and centroid.* This same phenomenon, however, previously has been implicitly recognized.[15]

c) A third, rougher, correlation probably exists, when annual spot numbers are studied, between the height of a minimum and

[14] A synthetic treatment of the spot cycle by the authors (*Pub. A.A.S.*, **9**, 21, 1936) adopted the outburst hypothesis but did not take this correlation into account.

[15] Waldmeier, *op. cit.*

the height of the following maximum. *Minima which are higher than average tend to be followed by especially high maxima.* To the extent to which equation (1) applies, this tendency is to be expected because a rapid initial increase in spot numbers at the beginning of an outburst is likely to result in a relatively high spot number for the year which includes that minimum and because such a rapid initial increase is associated with a high maximum.

d) Section X tentatively suggests an additional correlation relating to the time of start of an outburst.

e) Table 10 exposes an additional and remarkable correlation, which scarcely can be the result of chance: *the even-numbered cycles all have lower values of* a (*Case 2 solutions*) *than any odd-numbered cycle* (the only exception is Cycle 6). This result confirms the systematic difference in alternate cycles shown by Ludendorff[16] and gives a basis for the twenty-two-year "period" which sometimes has been suggested. The well-known reversal of polarization of the spots in alternate cycles is of great interest in this connection.

XIII. FAILURE OF THE SUPERPOSITION HYPOTHESIS

A Fourier analysis—and a fortiori periodogram analyses which do not restrict themselves to harmonic components—can account for any course of sunspot numbers whatsoever, once the sunspots have passed into history. *The improbability, obviously, is tremendous that such components would ever combine to give a succession of superficially dissimilar outbursts each of which nevertheless exhibits common family characteristics to the degree that the present study reveals.*

In addition to this argument, the failure of superposition treatments to predict successfully seems conclusive. The outburst hypothesis evades the test of long-time prediction because, until many more sunspot cycles have elapsed, data will be lacking for discussion of what weak statistical relations there may be between the parameters of successive outbursts. Short-range prediction ought to be fairly successful for the remaining course of an individual cycle which has reached or passed its maximum. The methods indicated in Section IX would apply to this problem—for example, to prediction of the remaining years of the present cycle (No. 17).

[16] *Zs. f. Ap.*, **2**, 370, 1931.

Further study along the lines which we have indicated may discover another direct analytic formula which retains the many advantages and avoids the defect of equation (1). If not, it should not be very difficult, retaining equation (1) as a first approximation, to modify the treatment empirically in such a way as to eliminate the discrepancies described by Tables 8 and 9. The definitive study doubtless ought to be made directly with the monthly, instead of with the annual, sunspot numbers. When either of these alternatives has been accomplished, it will be desirable to publish full tables for facilitating short-range prediction of the smoothed run of sunspot numbers.

PRINCETON UNIVERSITY OBSERVATORY
June 25, 1938

RADIAL VELOCITY-CURVE OF THE RR LYRAE VARIABLE W CANUM VENATICORUM*

ALFRED H. JOY

ABSTRACT

Twenty-four spectrograms of the short-period variable W Canum Venaticorum were obtained, mostly by the use of a 6-inch camera and a one-prism spectrograph giving a dispersion of 120 A/mm. The velocity-curve closely resembles the light-curve by Detre, but a lag of 6 per cent of the period is noted. The normal velocity is +26.0 km/sec, with a total range of 70 km/sec.

The spectroscopic absolute magnitude of −0.4 and a distance of 1400 parsecs were determined.

Of the short-period variables of the RR Lyrae type the velocity variations have thus far been published only for the type-star itself. The lack of observations may be attributed largely to the faintness of the stars, all of which fall well below the ninth magnitude in brightness at minimum light. Another difficulty is that the change in velocity is so rapid at certain times that exposures of an hour or more would involve doubtful corrections depending on both change in velocity and change in light.

Observations of W Canum Venaticorum were undertaken in order to test the applicability of low dispersion to this problem. A 6-inch camera giving a dispersion of 120 A/mm at $H\gamma$ was used with the one-prism spectrographs at the 60- and 100-inch telescopes. With this camera the exposure times varied from 8 to 50 minutes. Four additional plates, C2307, C2624, C7162, and γ21356, with a dispersion of 75 A/mm at $H\gamma$, are also available. The exposure times for the latter were 120, 165, 165, and 65 minutes, respectively.

In Table 1 are listed the data concerning 24 plates of W Canum Venaticorum. The elements,

$$\text{Max.} = \text{J.D. } 2421402.4206 + 0.55175981E\,,$$

by Detre[1] were used. The phases are expressed in decimal fractions of the period, and the estimated relative weights are given in the

* *Contributions from the Mount Wilson Observatory, Carnegie Institution of Washington*, No. 595.

[1] *A.N.*, **254**, 21, 1934.

last column. The velocities are plotted in Figure 1, and a rough curve is drawn to picture the course of the velocity variations. Detre's visual light-curve (range 9.9–10.7 mag.) is sketched above for comparison. A remarkable resemblance between the light- and velocity-curves is evident, but, as was found for variables of the δ Cephei type[2] and for RR Lyrae,[3] there is a distinct lag of the veloc-

TABLE 1

OBSERVATIONS OF W CANUM VENATICORUM

Plate	Date G.M.T.	J.D. 242+	Phase	Vel. (Km/Sec)	Wt.
C 2307	1923 June 23	3594.757	0.353	+24.9	1.5
2624	1924 Jan. 16	3801.981	.921	+24.9	1.0
γ21286	1938 Feb. 5	8935.899	.547	+42.2	1.0
21287	5	8935.928	.600	+52.8	0.3
21288	5	8935.958	.654	+43.3	0.6
21289	5	8935.988	.707	+37.6	1.0
21290	6	8936.021	.768	+41.4	1.0
21308	Apr. 9	8998.922	.768	+34.2	1.0
21309	9	8998.958	.833	+63.6	1.0
21310	9	8998.991	.894	+40.6	1.0
21311	10	8999.017	.940	+11.0	0.6
21312	10	8999.033	.970	+ 9.1	0.3
21313	10	8999.640	.070	−16.3	0.6
21314	10	8999.655	.097	−15.9	0.3
21315	10	8999.672	.127	−32.0	0.3
21316	10	8999.692	.164	− 6.9	0.6
21318	10	8999.751	.271	+26.1	1.0
21319	10	8999.774	.312	+18.9	1.0
C 7162	May 6	9025.908	.677	+48.0	1.5
7163	6	9025.990	.826	+38.0	0.6
γ21344	9	9028.791	.903	+63.1	0.6
21345	9	9028.822	.959	+ 9.0	1.0
21346	9	9028.831	.975	+ 7.9	1.0
21356	July 11	9091.755	0.017	+ 8.6	1.5

ity-curve as compared with the light-curve. The lag amounts to about 6 per cent of the period at both maximum and minimum phases and is closely the same as that found for RR Lyrae by Kiess and by Sanford. The normal velocity line is drawn so as to give equal areas of the velocity-curve above and below the line.

The normal velocity is found to be +26.0 km/sec, and the range

[2] *Mt. W. Contr.*, No. 578; *Ap. J.*, **86**, 435, 1937.

[3] Kiess, *Lick Obs. Bull.*, **7**, 148, 1913; Sanford, *Mt. W. Contr.*, No. 351; *Ap. J.*, **67**, 325, 1928.

is 70 km/sec (from −22 to +48 km/sec). In *Mt. W. Contr.* No. 578 the mean range for Cepheids was shown to be about 42 km/sec. If we may judge from RR Lyrae and W Canum Venaticorum, whose ranges are 61 and 70 km/sec, respectively, the velocity range of the short-period variables is at least 50 per cent greater than the mean of the δ Cepheids and double that found for stars with periods between one and two days.

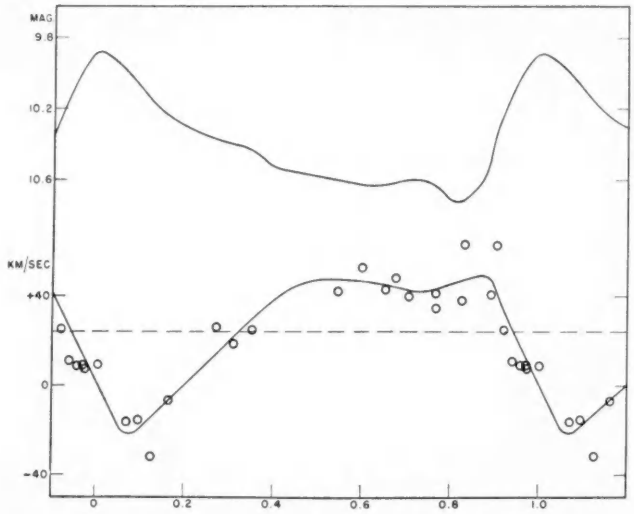

FIG. 1.—Light- and velocity-curves of W Canum Venaticorum. The visual light-curve (*above*) was observed by Detre with a wedge photometer. In the velocity-curve (*below*) the individual observations are plotted.

The spectral type of W Canum Venaticorum is found to be A6 at maximum and F6 at minimum. The spectroscopic absolute magnitude determined from the usual A- and F-curves is −0.4, which corresponds to a distance of 1400 parsecs. The galactic co-ordinates are $l = 36°$, $b = +70°$.

The results of this investigation indicate that much interesting and valuable information in this unexplored field may be obtained with a moderate expenditure of time and effort by the use of low-dispersion spectrographs.

CARNEGIE INSTITUTION OF WASHINGTON
MOUNT WILSON OBSERVATORY
July 1938

PHOTOGRAPHIC LIGHT-CURVES OF THE TWO SUPERNOVAE IN IC 4182 AND NGC 1003*

W. BAADE AND F. ZWICKY

ABSTRACT

Photographic light-curves of the two supernovae in IC 4182 and NGC 1003 have been derived from plates obtained at the Palomar and the Mount Wilson observatories. Since the distance moduli of the two nebulae are known, the absolute photographic magnitudes of the supernovae can be computed. At maximum their values were $M = -16.6$ and -14.0, respectively. An integration of the light-curve of the supernova in IC 4182 shows that during the outburst this star emitted radiation in the photographic region equivalent to $4 \cdot 10^7$ years of solar radiation within the same spectral range.

When we discussed some years ago the information then available about supernovae,[1] we realized that further advances in this field could be achieved only by a systematic search for these objects. Although fourteen supernovae had been discovered up to that time, the resulting data were so fragmentary that little more could be derived from them than the fact that supernovae as a class do exist. Since supernovae are very rare objects, even if large numbers of nebulae are kept under control, it was clear from the beginning that the time and effort necessary to carry through a systematic search program could be justified only if a proper search instrument were provided. As to the choice of instrument, there was no doubt that a Schmidt telescope of approximately 20 inches aperture would best meet the requirements of the proposed program. Sooner than expected, such an instrument became available; for early in 1935 the Observatory Council of the California Institute of Technology, whose members took an active interest in our plans, authorized the construction of an 18-inch Schmidt telescope[2] for the Palomar Observatory. The instrument, which has been constructed

* *Contributions from Mount Wilson Observatory, Carnegie Institution of Washington,* No. 601.

[1] *Mt. Wilson Comm.*, No. 114; *Proc. Nat. Acad. Sci.*, **20**, 254, 1934.

[2] The telescope, of the focal ratio $F/2$, has a correcting plate of 18 inches and a mirror of 26 inches aperture. The field covered by the photographic film has a diameter of $9^\circ.5$.

under the direction of Dr. J. A. Anderson, was ready in the fall of 1936. Since that time it has been used in an extensive search for supernovae by Zwicky. So far, three have been discovered by observations made on Palomar Mountain. Of these, the supernovae in IC 4182 and NGC 1003, discovered in the fall of 1937, have yielded valuable information because they were relatively bright objects which could be followed photometrically and spectroscopically over a long interval of time. Both are still under observation and can be followed probably through another season before they pass out of the reach of the 100-inch telescope. To avoid undue delay in the publication of the photometric results thus far obtained, we present in this paper the photographic light-curves[3] of the two supernovae from the time of their discovery up to the time of our latest observations.

THE SUPERNOVA IN IC 4182

The spiral nebula IC 4182.—This nebula (R.A. 13^h2^m9, Dec. $+37°$ 56′, 1938; gal. long. 67°.8, lat. +78°.9) is a late Sc spiral of 4′.1 diameter, oriented nearly perpendicular to the line of sight. It has a very low surface brightness, which necessitates long exposures to reveal its structure.[4] The integrated photographic brightness of the nebula is correspondingly low, being only of magnitude 13.5.[4] Nevertheless, it is easily resolved on plates obtained at the Mount Wilson reflectors from which the value $\bar{m}_s = 19.2$ has been derived for the mean apparent photographic magnitude of the five brightest stars in the system. Since for the average late-type system the corresponding value of the absolute magnitude is $\bar{M}_s = -6.3$,[5] we obtain the modulus $m - M = 25.5$, whence, for the distance of IC 4182, $D = 1.02 \cdot 10^6$ parsecs. The resulting values for the linear diameter (1200 parsecs) and the luminosity ($M = -12.0$) clearly indicate that IC 4182 is a dwarf system. For such systems, however, the absolute photographic magnitude of the brightest stars is decidedly fainter than −6.3, and rather of the order $\bar{M}_s = -5.6$. Substituting,

[3] Light-curves based on observations in the red region of the spectrum will be published after a sufficiently extended scale of red magnitudes has been established.

[4] For an illustration of IC 4182 see *Mt. W. Contr.*, No. 600; *Ap. J.*, **88**, 285, 1938.

[5] E. Hubble, *Mt. W. Contr.*, No. 548; *Ap. J.*, **84**, 158, 1936.

therefore, this smaller value as a second approximation, we obtain the following final data for IC 4182:

Modulus	24.8
Distance	912,000 parsecs
Diameter	1100 parsecs
Integrated absolute magnitude	−11.3 (photographic)

It was a very fortunate circumstance that these data were known to us when we compiled the observing list for our search program.[6] Since any supernovae appearing in IC 4182 should have, in the mean, the maximum apparent brightness $m_{pg} = 10.5$, we included the nebula in our observing list, although the chance for the discovery of a supernova did not seem to be very high, on account of the small stellar content of the system. Within less than a year, however, one of the brightest supernovae on record appeared in IC 4182. It offered an unusual opportunity for extensive photometric and spectroscopic observations. Because of its brightness and high declination, the nova could be followed through the conjunction with the sun, so that an uninterrupted record of its history has been obtained.

Photographic magnitudes of the comparison stars.—On account of the large observable range of the supernova, an extended sequence of comparisons had to be established, involving instruments of widely different apertures. To cover the interval from magnitude 8 to 11, polar comparisons were made with the 5-inch Ross lens (intrafocal) and the 10-inch Cooke refractor of the Mount Wilson Observatory. Magnitudes between 10 and 13 were derived from polar comparisons made with a schraffierkassette at the 60-inch reflector, which had been diaphragmed down to 40 inches. For stars fainter than 13, photographic magnitudes have been determined from focal exposures at the 60-inch reflector, using either the Polar Sequence or S.A. 57 as standard regions. The magnitudes of the comparison stars are therefore on the international system. Because of poor seeing conditions during the last spring season, a rather large number of comparisons had to be made to reduce sufficiently the influence of the systematic errors with which the individual plates may have been

[6] The nature of IC 4182 was discovered by Baade in 1936 during a search for near-by extragalactic systems of low luminosity.

affected. The final photographic magnitudes of the comparison stars, together with the residuals of the individual determinations, are given in Table 1. For identification of the stars see Plates XVII and XVIII. The sequence extends at present to photographic magnitude 17.0, which should be sufficient for observations of the supernova during this season. An extension of the sequence down to magnitude 21 is under way and will be published later.

TABLE 1

SEQUENCE FOR SUPERNOVA IN IC 4182

(Unit for Residuals, 0.01 Mag.)

Star	Mean m_{pg}	Residuals																BD
		5-Inch			10-Inch		Schraffier-kassette, 60-Inch			60-Inch								
A	8.37	−4	+ 2	+ 2														+38°2396
a	8.66	+3	+ 1	− 5														38 2403
b	8.93	+4	0	− 3														37 2371
c	9.11	+1	− 3	+ 3														37 2360
d	9.74	−1	−11	+ 8	+ 5	0												37 2367
e	9.79	+2	− 2	+ 8	+ 4	+ 2	− 5	0	− 9									38 2398
f	10.03	+4	− 5	+10	+ 3	0	− 5	0	− 7									38 2402
g	10.79		+ 5		−10	− 4	+ 5	+ 1	+ 3									38 2397
h	10.85	−3	−20		− 8	+14	+ 1	+ 4	+12									38 2405
i	10.78	+7	− 5		− 5	+ 4												+37 2368
k	11.46				−18	+ 5	− 1	+ 3	+ 5									
l	11.99						− 2	− 1	+ 3									
m	12.07						− 4	− 1	+ 5									
n	12.57						0	0	+ 1									
o	13.25						−11	+ 1	− 6	− 1	+ 5		+ 4	+12		− 3		
p	13.72						−25	−15	− 3	−19	+ 3	+ 8	+13	+19	+20	+ 2		
q	14.02										+ 2	+ 2	− 2	+ 2	− 2	0		
r	14.21										+12	− 1	− 4	+ 7	− 7	− 5		
s	14.73										+10	− 7	+ 1	+ 5	− 7	− 5		
t	15.22											−12	+ 4	+ 8	− 1	+ 1		
u	15.78												+ 1	+ 9	−15	+ 4		
v	16.07												− 3	+12	−11	+ 1		
w	16.34														−12	+11		
x	16.70														−10	+ 9		
y	17.04														− 5	+ 5		

Photographic light-curve of the supernova.—The observed photographic magnitudes of the supernova from August, 1937, until June, 1938, which have been obtained with the Palomar and the Mount Wilson instruments, are collected in Table 2.

The resulting light-curve is reproduced in Figure 1, in which the individual observations are marked by dots. It shows that the supernova was discovered when it was already past maximum. A pre-

PLATE XVII

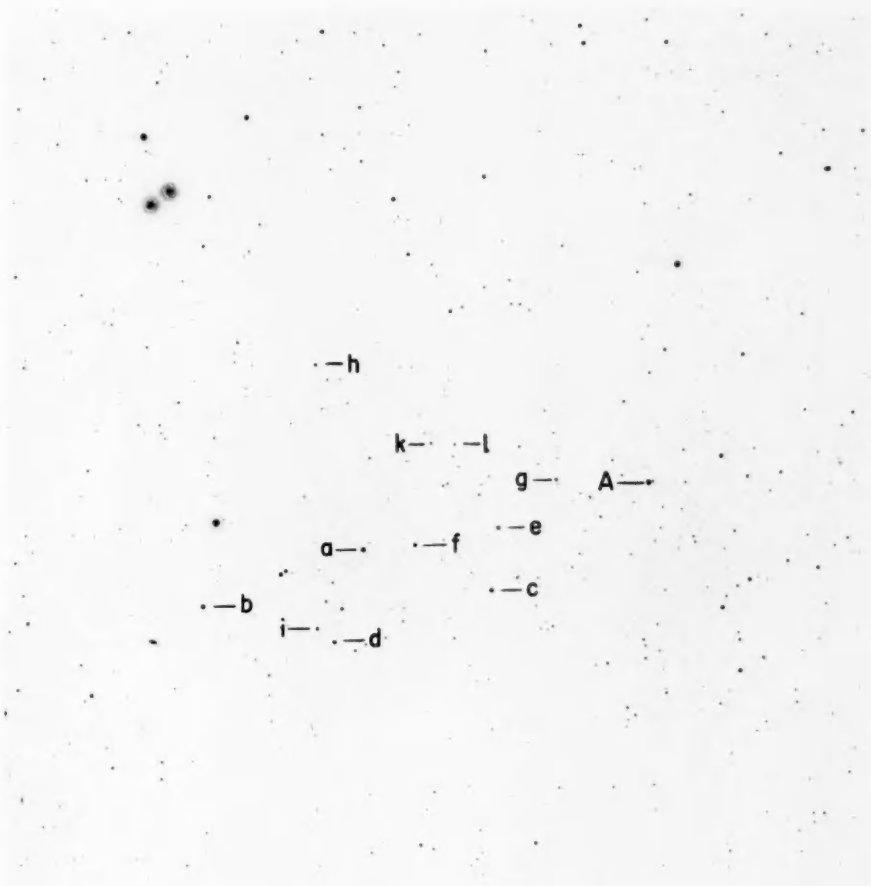

COMPARISON STARS FOR SUPERNOVA IN IC 4182

Scale, 1 mm = 92″.5. Enlarged 2.5 times from a film taken with 18-inch Schmidt telescope on Mount Palomar.

PLATE XVIII

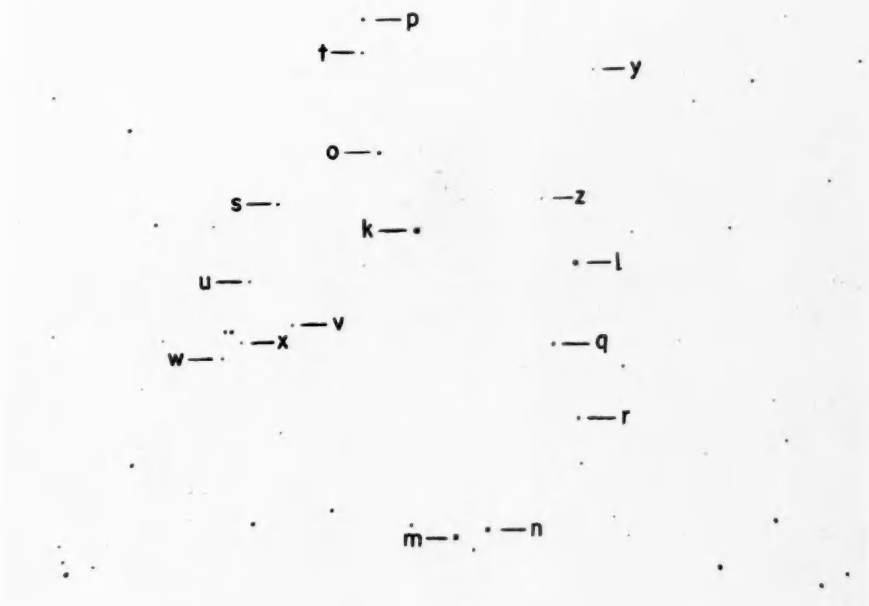

COMPARISON STARS FOR SUPERNOVA IN IC 4182
Scale, 1 mm = 13".2

TABLE 2

PHOTOGRAPHIC MAGNITUDES OF SUPERNOVA IN IC 4182

J.D. G.M.T.	m_{pg}	Instr.	J.D. G.M.T.	m_{pg}	Instr.
2428774.7	8.58	S*	2428808.6	11.36	S
775.7	8.63	S	808.6	11.35	S
776.7	8.62	S	810.6	11.52	S
777.7	8.64	S	813.6	11.46	S
778.7	8.74	S	815.6	11.62	S
779.6	8.83	S	818.6	11.72	S
779.7	8.98	S	820.6	11.86	S
780.6	9.25	S	831.0	11.94	S
780.7	9.14	5	833.0	12.03	S
781.7	9.13	5	837.0	12.02	S
781.7	9.09	S	842.0	12.05	S
781.7	9.24	S	862.9	12.38	S
782.7	9.50	S	865.0	12.40	10
783.7	9.54	S	865.0	12.46	10
783.7	9.55	S	865.0	12.42	10
784.6	9.58	S	865.0	12.43	10
784.6	9.55	S	866.0	12.49	60
785.6	9.78	S	866.0	12.43	60
785.6	9.77	S	871.9	12.47	S
786.6	9.81	S	873.9	12.47	S
786.6	9.89	S	880.9	12.64	S
787.6	9.93	S	895.9	13.13	60
787.6	9.93	S	896.0	13.15	60
788.6	10.08	S	896.0	13.15	60
788.6	10.30	S	896.0	13.11	60
788.7	9.92	5	897.0	13.03	S
789.6	10.11	S	899.0	13.13	S
789.6	10.45	S	904.9	13.13	S
789.7	10.24	5	906.9	13.05	S
790.6	10.22	S	907.9	13.17	S
790.6	10.37	S	908.9	13.39	S
790.7	10.32	5	910.0	13.23	S
791.6	10.37	S	910.9	13.30	S
791.6	10.54	S	921.9	13.48	S
792.6	10.56	S	947.8	13.65	S
792.6	10.41	S	949.8	13.71	S
793.6	10.52	S	950.8	13.72	S
793.6	10.56	S	951.8	13.71	S
794.6	10.79	S	952.8	14.13	S
794.6	10.68	S	953.8	14.13	S
799.6	11.12	S	954.8	13.92	100
799.6	11.31	S	955.8	13.94	100
800.6	11.25	S	963.9	14.10	S
800.6	11.19	S	981.8	14.32	S
801.6	11.30	S	985.7	14.35	S
801.6	11.16	S	988.7	14.34	60
802.6	11.27	S	988.7	14.44	60
802.6	11.25	S	989.7	14.21	S
803.6	11.31	S	990.8	14.57	60
803.6	11.26	S	992.8	14.66	S
804.6	11.33	S	2429010.8	14.68	S
804.6	11.26	S	012.7	14.90	S
806.6	11.29	S	024.6	15.07	100
806.6	11.31	S	040.8	15.28	S
807.6	11.42	S	048.8	15.57	60
807.6	11.39	S	049.8	15.57	60

* 18-inch Schmidt. Figures in this column indicate the apertures of the various telescopes used.

maximum observation by E. Leutenegger[7] makes it possible, however, to establish with sufficient accuracy the date and the brightness of the maximum. Leutenegger, who had photographed comet Finsler 1937 on August 16.9, U.T., found, upon a later examination of this plate, that it included IC 4182 and that the supernova was already present as a star of the ninth magnitude. At our request he

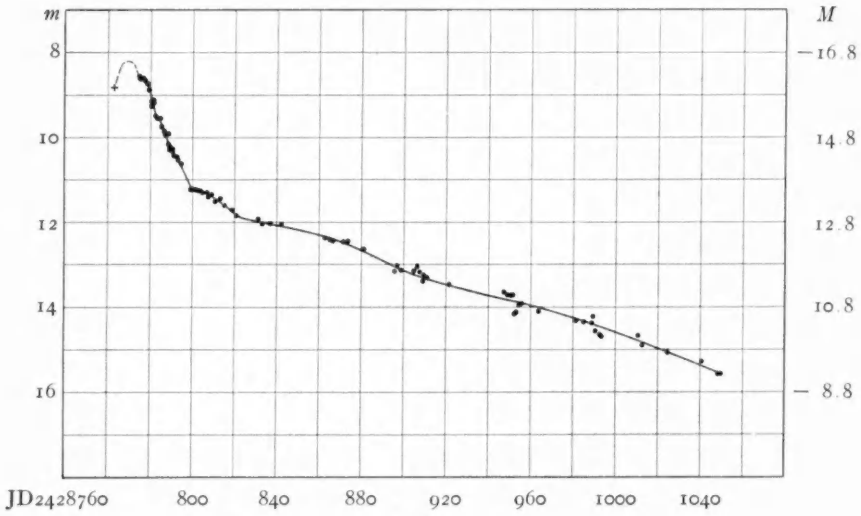

FIG. 1.—Photographic light-curve of supernova in IC 4182

kindly redetermined the magnitude of the supernova, using our system of magnitudes, with the following result:[8]

$$\text{JD } 2428762.4 \text{ G.M.T.} \quad m_{pg} = 8.85 .$$

The corresponding point is marked by a cross in Figure 1. There is hardly any doubt that the observation belongs to the ascending branch of the light-curve. We thus obtain for the date of the maximum August 22, 1937, and for the apparent maximum brightness, $m_{pg} = 8.2$. The light-curve itself resembles in many ways that of an ordinary nova. The decline is rather steep during the first 30

[7] *A.N.*, **263**, 446, 1937.

[8] We are much obliged to Dr. Leutenegger for his co-operation. An enlarged print of his plate which he kindly sent us leaves no doubt as to the correct identification of the supernova.

days following the maximum, with a gradient of 0.10 mag. per day. After that a gradient of 0.018 mag. per day represents the further decrease in brightness to the end of June, 1938.

Absolute photographic brightness of the supernova at maximum.— From $m_{pg} = 8.2$ for the apparent brightness of the supernova at maximum and the known modulus of IC 4182, $m - M = 24.8$, we obtain for the absolute magnitude of the supernova at maximum

$$M_{max} = -16.6 .$$

This is the highest value so far observed among supernovae, and 2.3 mag. brighter than the average supernova at maximum. Since the integrated absolute magnitude of IC 4182 is only -11.3, the supernova at its maximum surpassed in luminosity the nebula in which it originated by a factor of 100. The data already given fully explain the unusually large value $m_{max} - m_{neb} = +5.3$. It is due simply to the fact that a supernova of very high luminosity appeared in an extragalactic system of very low luminosity. Moreover, the difference is numerically well within the range allowed by the known dispersions in the luminosities of spiral nebulae and supernovae.

Finally, we compare the radiation of the supernova with that of the sun. Since the photographic absolute magnitude of the sun is $M = +5.3$, the supernova at its maximum surpassed the luminosity of the sun by a factor of $6 \cdot 10^8$. To obtain the total energy in the photographic region of the spectrum which the supernova radiated away during the outburst, we have integrated the light-curve over the first 225 days after the maximum. The total corresponds to $4 \cdot 10^7$ years of solar radiation within the same range of the spectrum. These two figures represent what may be said at the present time about the energy involved in a supernova outburst without invoking assumptions. Obviously, they are a mere fraction of the total energy emitted between $\lambda = 0$ and $\lambda = \infty$, which cannot even be guessed at because we do not know the intensity distribution in the spectrum. In the observed region from λ 7000 to λ 3300 the distribution is so peculiar that the assumption of black-body radiation for the supernova can be ruled out at once. In the photographic region a strong band at λ 4600, approximately 200 A wide, is the dominant feature. The fact that about half of the radiation emitted in the

photographic region between λ 5000 and λ 3300 originates in this relatively narrow band illustrates in a striking way the unusual features presented in supernovae.

THE SUPERNOVA IN NGC 1003

The spiral nebula NGC 1003.—The nebula (R.A. 2^h35^m3, Dec. $+40°36'$, 1938; gal. long. 112°.1, lat. $-16°.7$) is an Sc spiral of 4'.3 diameter, seen edgewise. The brightest stars of the system, which have the mean photographic magnitude $\bar{m}_s = 20.5$, are just above the limiting magnitude of 1-hour exposures with the 100-inch telescope. Adopting $\bar{M}_s = -6.3$ for the corresponding absolute magnitude, we find the modulus of NGC 1003 to be $m - M = 26.8$. The integrated apparent photographic magnitude of the nebula is $m_{\text{neb}} = 13.1$,[9] which gives $M_{\text{neb}} = -13.7$ for the absolute magnitude of the system, slightly below the mean value $\bar{M}_{0\,\text{neb}} = -14.2$ for the average extragalactic system. The distance and the linear diameter of NGC 1003, derived from the modulus $m - M = 26.8$, are $2.29 \cdot 10^6$ and 2980 parsecs, respectively. In view of the low latitude of the nebula, these figures should be corrected, however, for the general galactic absorption. The factor by which the uncorrected values of the distance are to be multiplied is, according to Hubble,[10]

$$\log f = -0.05\,|\operatorname{cosec} b|\,,$$

or, in the present case, $f = 0.67$. Thus, we have the following data for NGC 1003:

Modulus, 26.8,

Integrated absolute magnitude, −13.7 (photographic),

Distance $1.51 \cdot 10^6$ parsecs
Diameter 2000
} corrected for latitude effect.

We use intentionally the uncorrected value of the distance modulus. Since in the following discussions only magnitude differences are used, the latitude effect is unessential.

Photographic magnitudes of the comparison stars.—The sequence of our comparison stars is marked on Plate XIX. Their photographic

[9] *Mt. W. Contr.*, No. 600; *Ap. J.*, **88**, 285, 1938.

[10] *Mt. W. Contr.*, No. 485; *Ap. J.*, **79**, 8, 1934.

PLATE XIX

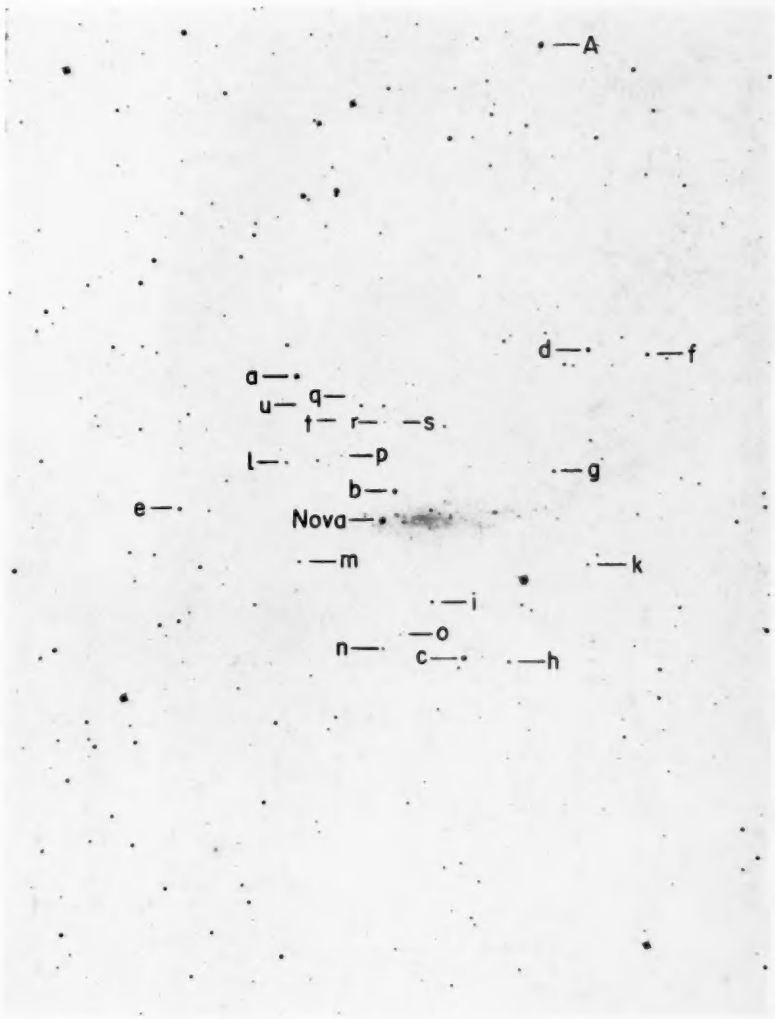

COMPARISON STARS FOR SUPERNOVA IN NGC 1003
Scale, 1 mm = 8″.0

magnitudes have been derived from comparisons with S.A. 22 and S.A. 68 made at the Mount Wilson reflectors. For stars fainter than 17.7 the scale is that of S.A. 68, for which photographic magnitudes down to $m_{pg} = 21.0$ are now available. Since careful checks have shown that the magnitude system of S.A. 68 agrees in zero point and

TABLE 3

SEQUENCE FOR SUPERNOVA IN NGC 1003

(Unit for Residuals, 0.01 Mag.)

Star	Mean m_{pg}	Residuals for Individual Plates						
		608	609	616	874	875	629	633
A	12.50	.....	.....		.....	.....	.....	.....
a	13.12	+12	.....	−10	− 1	.....	.....	.....
b	13.22	+18	.....	−13	− 4	.....	.....	.....
c	13.31	+23	.....	−15	− 9	.....	.....	.....
d	13.82	+ 9	.....	− 8	− 1	+ 2	.....	.....
e	14.46	+ 9	− 6	− 4	+ 3	− 2	.....	.....
f	14.74	+10	− 4	− 7	+ 4	− 4	.....	.....
g	15.46	+ 1	− 5	− 4	+10	− 1	.....	.....
h	15.55	0	+ 2	.....	+ 3	− 3	.....	.....
i	16.00	+ 5	− 1	.....	− 1	− 1	− 6	+ 1
k	16.22	+ 9	−11	.....	+ 7	− 6	.....	.....
l	16.56	.....	+ 7	.....	0	+ 7	−13	− 2
m	17.12	.....	+ 5	.....	.....	+ 2	− 9	0
n	17.50	.....	− 6	.....	.....	+ 3	−14	+17
o	17.80	.....	−23	.....	.....	+12	− 7	+18
p	18.22	.....	.....	.....	.....	.....	+ 4	− 4
q	18.54	.....	.....	.....	.....	.....	+ 7	− 7
r	18.81	.....	.....	.....	.....	.....	+ 5	− 5
s	19.25	.....	.....	.....	.....	.....	+ 4	− 3
t	19.82	.....	.....	.....	.....	.....	−12	+12
u	20.03	.....	.....	.....	.....	.....		.....

scale with that of the Polar Sequence and since there is no perceptible systematic difference between the magnitudes of S.A. 22 and S.A. 68, the magnitudes of our comparison stars should be on the international system. Their values are given in Table 3, together with the residuals for the individual determinations.

Photographic light-curve of the supernova.—Our measurements of the supernova, from the date of its discovery to the time when ap-

proaching conjunction with the sun prevented further observations, are given in Table 4.

TABLE 4

PHOTOGRAPHIC MAGNITUDES OF SUPERNOVA IN NGC 1003

J.D. G.M.T.	m_{pg}	Instr.	J.D. G.M.T.	m_{pg}	Instr.
2428787.8	12.98	S*	2428808.9	14.27	S
788.8	13.01	S	812.7	14.68	S
788.9	13.12	100	812.9	14.61	60
789.8	13.16	S	813.9	14.61	60
790.8	12.85	5	814.0	14.64	60
790.9	12.84	5	814.7	14.71	S
791.9	12.67	S	820.8	15.03	S
791.9	12.89	5	838.9	15.80	100
792.9	12.90	S	838.9	15.68	100
793.9	13.11	5	840.8	15.69	60
794.9	13.00	S	840.9	15.73	60
795.9	13.00	S	863.7	16.42	60
799.7	13.19:	S	865.7	16.47	60
799.7	12.93:	S	872.6	16.55	60
800.7	13.10	S	895.6	16.93	60
801.7	13.39	S	895.8	16.95	60
801.8	13.20	5	897.8	16.91	100
802.7	13.69	S	898.7	16.99	100
803.7	13.66	S	929.8	17.05	100
804.8	13.79	S	954.6	17.41	100
805.8	13.90	S	955.6	17.42	100
807.9	14.26	S	990.6	17.43	100
808.8	14.27	S			

* See note to Table 2.

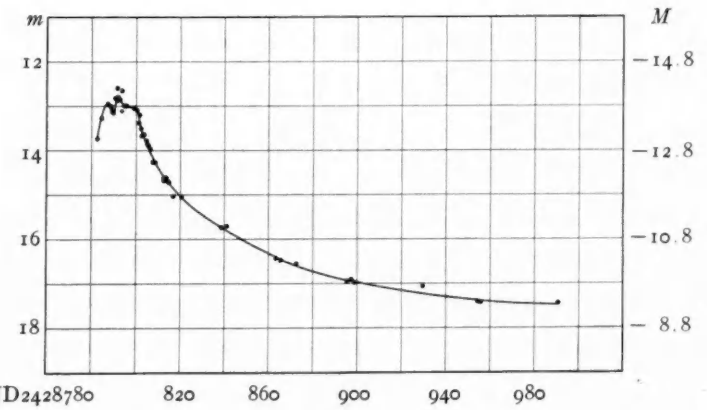

FIG. 2.—Photographic light-curve of supernova in NGC 1003

The resulting light-curve is reproduced in Figure 2. Included in this curve are the following two observations by A. A. Wachmann[11] which precede our earliest plates:

JD 2428782.6 G.M.T. 13.73
784.5 G.M.T. 13.28

Since Wachmann's magnitude system differs systematically from ours by +0.16 mag., his published magnitudes have been diminished by this amount. The light-curve shows the importance of Wachmann's early observations, which clearly belong, as he already pointed out himself, to the ascending branch. The supernova had a rather extended maximum lasting 10–12 days, during which minor fluctuations are indicated. The decline in brightness following the maximum is closely similar to that of the supernova in IC 4182. Since the apparent brightness of the maximum was $m_{max} = 12.8$, we obtain for the absolute photographic brightness of the supernova at maximum

$$M_{max} = -14.0,$$

a value practically identical with the mean, $\overline{M}_{max} = -14.3$, for supernovae.

Further discussion of the two light-curves is postponed until the observations of another season and the light-curves in the red region of the spectrum are available.

CARNEGIE INSTITUTION OF WASHINGTON
MOUNT WILSON OBSERVATORY
June 1938

[11] *Beob. Zirk.*, **19**, No. 42, 1937.

PHYSICAL PROCESSES IN GASEOUS NEBULAE

V. ELECTRON TEMPERATURES

JAMES G. BAKER,[1] DONALD H. MENZEL, AND
LAWRENCE H. ALLER

ABSTRACT

The relation between the electron temperature of a gaseous nebula and the temperature of the exciting star is derived and applied to an optically thin nebula. The b_n's have been recomputed both with the radiation field included and as a function of the temperature of the exciting star. The Balmer decrement proves to be steeper when the influence of Lyman line absorption is included.

The equations derived in papers I, II, and IV of this series may be applied to the problem of calculating the electron temperature of the nebular gas. We make the following assumptions: the electrons are produced by photo-ionization; radiationless encounters between the various components of the assembly are sufficiently frequent that the electrons attain a Maxwellian velocity distribution; the nebula is in a steady state with respect to the distribution of atoms in various levels; the energy emitted per unit time must equal the energy absorbed.

The calculations of paper III gave the values of the quantities $b_2, b_3, \ldots$ etc. The results are based on the equations for statistical equilibrium of quantum levels 2 and higher. These equations are sufficient to determine the absolute nebular emission and the Balmer decrement when N_e and T_e are given; we have still to predict the values of the two latter quantities from the physical parameters of the exciting radiation. In addition, there is the third parameter, b_1—which defines the number of atoms in the ground level—to be determined. We may suppose, for the sake of simplicity, that the radiation from the nuclear star is "black," at temperature T_1, with the dilution factor W specified. There are still two equations from paper I or paper IV that have not been employed, viz., the one defining the statistical equilibrium of level 1 and the one expressing conservation of emitted and absorbed radiation. A third relationship is ob-

[1] Society of Fellows, Harvard University.

tained when the density of the nebula is given, hence the problem is determinate. One may substitute the previously evaluated b_n's in the two remaining equations and calculate b_1, N_e, and T_e.

Fortunately, for the gaseous nebulae, where the radiation is very dilute one may determine T_e directly without first evaluating the intermediate b_n's. T_e proves to be independent either of the density or of the dilution factor, as long as the latter is small. The simplification is obtained by means of the mechanistic approach developed in paper IV. The numerical results are given for an optically thin nebula, by which term we mean a nebula of optical thickness small enough that the spectral energy curve of the star, beyond the Lyman limit, is not seriously depleted by absorption effects.

It now seems advisable to write out the necessary equations in the form in which they are to be used. We shall use the equations and the notation of papers I and II,[2] writing out first the explicit forms of the equations IV (3), IV (4), and IV (9). Adopting as before $b_\kappa = 1$, we find that IV (3) becomes, in view of the definitions of II and equations IV (14), I (25),

$$b_1 \int_{\nu_1}^{\infty} W_{1\kappa} \left(\frac{e^{h\nu_1/kT_e}}{e^{h\nu/kT_1} - 1} \right) \frac{d\nu}{\nu} = \sum_{1}^{\infty} \frac{S_n}{n^3} + \int_{\nu_1}^{\infty} W_{1\kappa} \left(\frac{e^{-h(\nu-\nu_1)/kT_e}}{e^{h\nu/kT_1} - 1} \right) \frac{d\nu}{\nu} . \quad (1)$$

It must be borne in mind that $W_{1\kappa}$ is a very small quantity of the order of 10^{-15}. The second term on the right of the foregoing equation represents the negative absorptions. It follows that

$$e^{+h\nu_1/kT_e} \int_{\nu_1}^{\infty} \frac{W_{1\kappa} e^{-h\nu/kT_e}}{e^{h\nu/kT_1} - 1} \frac{d\nu}{\nu} < \frac{e^{h\nu_1/kT_e}}{e^{h\nu_1/kT_1} - 1} \int_{\nu_1}^{\infty} W_{1\kappa} e^{-h\nu/kT_e} \frac{d\nu}{\nu}$$

$$< \frac{\dfrac{kT_e}{h\nu_1}}{e^{h\nu_1/kT_1} - 1} \overline{W}_{1\kappa} < \frac{\dfrac{kT_1}{h\nu_1}}{e^{h\nu_1/kT_1} - 1} \overline{W}_{1\kappa} \leq 3W_{1\kappa} .$$

Therefore, the effect of induced emissions, i.e., induced captures, is negligibly small. From (1) we see that b_1 is a very large quantity determined principally by the magnitude of $W_{1\kappa}$. Terms that con-

[2] D. H. Menzel, *Ap. J.*, **85**, 330, 1937; D. H. Menzel and J. G. Baker, *Ap. J.*, **86**, 70, 1937; J. G. Baker and D. H. Menzel, *Ap. J.*, **88**, 52, 1938; D. H. Menzel, L. H. Aller, and J. G. Baker, *Ap. J.*, **88**, 313, 1938.

tain both $W_{1\kappa}$ and b_1 as a product cannot be neglected, but the terms that contain $W_{1\kappa}$ without the b_1 factor can readily be neglected. This amounts to a formal proof of our previous statement that the negative absorptions from all levels and the positive absorptions from all levels but the first are negligible. Our equations may now be written

$$b_1 e^{X_1} \int_{y_1}^{\infty} W_{1\kappa} \frac{dy}{y(e^y - 1)} = \sum_1^{\infty} \frac{S_n}{n^3} = G_{T_e}, \tag{2}$$

which defines G_{T_e}. The equation of radiative equilibrium for the assembly is

$$\left.\begin{aligned} &T_e^2 \left(\frac{k^2}{2hRZ^2}\right) + akT_e + 2hrZ^2 \sum_{n=2}^{\infty} \sum_{n'=1}^{n-1} b_n \frac{1}{n'^3} \frac{1}{n^3} e^{X_n} \\ &- b_1 e^{X_1} \sum_2^{\infty} W_{1n''} \frac{2hRZ^2}{e^{h\nu/kT_1} - 1} \frac{1}{n''^3} - b_1 e^{X_1} kT_1 \int_{y_1}^{\infty} W_{1\kappa} \frac{dy}{e^y - 1} = 0, \end{aligned}\right\} \tag{3}$$

where

$$a = \sum_1^{\infty} \frac{1}{n^3}.$$

The equation of radiative equilibrium for the continuum becomes

$$\left.\begin{aligned} b_1 e^{X_1} \left(\frac{k}{2hRZ^2}\right) T_1 \int_{y_1}^{\infty} W_{1\kappa} \frac{dy}{e^y - 1} &= \left(\frac{k}{2hRZ^2}\right)^2 T_e^2 \\ &+ \left(\frac{k}{2hRZ^2}\right) aT_e + \tfrac{1}{2} G_{T_e} - \tfrac{1}{2} \sum_1^{\infty} \frac{S_n}{n^5}. \end{aligned}\right\} \tag{4}$$

Equations IV (1) and IV (2) may be discussed in a similar manner, and we shall treat the problem later in connection with the derivation of the formula for b_n. It is to be pointed out that all these equations contain b_1, T_e, and T_1. One might expect, therefore, that it would be possible to choose any two of them, eliminate b_1, and derive a relation between T_e and T_1. In particular, one might suppose that we could choose any two of equations (2), (3), or (4), solve each for b_1, and equate. Our choice is really somewhat more limited than

that. If we suppose, for example, the star to radiate as a black body with no absorption lines in the Lyman series, we do not know the b_n's and therefore cannot use equation (3). Our procedure in this case would be to solve (2) and (4) for b_1 and equate. In the problem where we supposed no radiation to leave the star in the Lyman lines but where the star is supposed to shine as a black body beyond the Lyman limit, we know the b_n's and can therefore apply any two of these three equations. Numerical calculations based on (2) and (3) gave exactly the same relation between T_e and T_1 as those based on (2) and (4). The agreement provides an excellent check on the formulas and computations. Note that the relation between T_e and T_1 does not depend on whether the central star has any line radiation or not. It is to be mentioned that the expressions for b_1 from (2) and (4) are equally good for a static or an expanding nebula because absorption in the continuum is not seriously affected by a Doppler shift. From (2) and (4) we have for the optically thin nebula, where $W_{1\kappa}$ does not depend on ν,

$$\left.\begin{aligned} &\frac{\left(\frac{k}{2hRZ^2}\right) T_1 \int_{y_1}^{\infty} \frac{dy}{e^y - 1}}{\int_{y_1}^{\infty} \frac{dy}{y(e^y - 1)}} \\ &\qquad = \frac{\left(\frac{k}{2hRZ^2}\right)^2 T_e^2 + a\left(\frac{k}{2hRZ^2}\right) T_e + \frac{1}{2} G_{T_e} - \frac{1}{2} \sum_1^{\infty} \frac{S_n}{n^5}}{G_{T_e}} \end{aligned}\right\} \tag{5}$$

or, symbolically,

$$f_1(T_1) = f_2(T_e) ,$$

since the left side of the equation depends only on T_1 and the right side only on T_e. For any assigned T_1 the corresponding T_e may be readily found. Each side of the equation is plotted as a function of its appropriate temperature. A specified value of T_1 determines $f_1(T_1)$, which must equal $f_2(T_e)$. From the graph of $f_2(T_e)$ the appropriate T_e may then be ascertained. It is to be mentioned that the quadratic $f_2 - f_1$ gives but one real positive root.

The relation between T_e and T_1 is given in the following table for the optically thin nebula. The Gaunt g factor was taken equal to unity in the calculations.

T_1	T_e
5,000	5,000
10,000	9,500
20,000	18,000
40,000	34,000
80,000	57,000
160,000	92,000
320,000	132,000

Note that for the higher temperatures the electron temperature departs farther and farther from the temperature of the source. For very high temperatures the effect of the neglect of the g factor produces an error of at most 5 per cent in the foregoing results. At low temperatures the error is negligible.

From equation (2) or (4) we can determine b_1. The fact that its order of magnitude must be determined by the dilution factor follows at once from elementary considerations. Comparing the gaseous nebula with an assembly in thermodynamic equilibrium at temperature T_e, we see that the captures must go at essentially the same rate but that the photo-ionizations are fewer by a factor of about W_{1K}. As a result, there appears an enormous excess of atoms in the ground state as compared with the assembly in thermodynamic equilibrium.

The ionization equation for hydrogen follows at once. We shall defer discussion, however, because ionization is unimportant so far as the present investigation is concerned.

We now write equation IV (2) in terms of the physical quantities involved. In view of I (7), and using the notation of II (3), we find, neglecting the terms multiplied by W and not by $b_1 W$,

$$\frac{N_i N_e K Z^4}{n^3 T_e^{3/2}} \left\{ \sum_{n''=n+1}^{\infty} b_{n''} e^{X_{n''}} g_{n''n} u_{n''n} + \bar{g} S_n + \left[W_{1n} \frac{b_1 e^{h\nu/kT_e}}{e^{h\nu/kT_1} - 1} \right] \frac{2n^2 e^{X_n}}{n^2 - 1} - e^{X_n} b_n t_n \right\} = 0 . \tag{6}$$

TABLE 1

STELLAR TEMPERATURE, ELECTRON TEMPERATURE, AND ASSOCIATED VALUES OF b_n

n	$T_\star$ 5,000°	10,000°	20,000°	40,000°	80,000°	160,000°
	T_e 5,000°	9,500°	18,000°	34,000°	57,000°	92,000°
	b_n (Neglecting Radiation Field)					
2	0.00003	0.0029	0.027	0.090	0.220	0.388
3	.0033	.025	.089	.195	.324	.471
4	.018	.068	.151	.270	.392	.526
5	.043	.109	.210	.324	.444	.560
6	.072	.150	.251	.366	.482	.585
7	.099	.182	.290	.400	.511	.605
8	.126	.213	.319	.425	.531	.621
9	.150	.237	.341	.449	.549	.639
10	.171	.261	.363	.469	.563	.650
11	.191	.281	.381	.481	.576	.659
12	.209	.299	.396	.492	.588	.666
13	.223	.313	.409	.503	.598	.673
14	.238	.328	.420	.511	.604	.679
15	0.251	0.339	0.430	0.520	0.610	0.685
	b_n (Including Radiation Field)					
2	2.98	2.567	2.369	2.281	2.181	2.393
3	1.72	1.608	1.603	1.561	1.429	1.551
4	1.48	1.414	1.411	1.367	1.258	1.356
5	1.40	1.33	1.33	1.29	1.19	1.27
6	1.37	1.29	1.27	1.25	1.16	1.22
7	1.36	1.25	1.25	1.22	1.14	1.19
8	1.34	1.22	1.22	1.20	1.12	1.17
9	1.32	1.20	1.20	1.19	1.11	1.16
10	1.31	1.18	1.18	1.18	1.10	1.15
11	1.28	1.17	1.17	1.17	1.09	1.14
12	1.26	1.15	1.16	1.16	1.09	1.13
13	1.23	1.14	1.15	1.15	1.08	1.13
14	1.20	1.13	1.14	1.14	1.08	1.12
15	1.19	1.12	1.13	1.14	1.07	1.11

This equation may be solved in a manner similar to the method explained in paper II, once the W_{1n} factors are known. We have

$$b_n = \frac{S_{nr} + V_{nr}}{e^{X_n} t_n}, \tag{7}$$

where

$$\left.\begin{aligned} S_{nr} &= \left[S_n + W_{1n} \left(\frac{b_1 e^{h\nu/kT_e}}{e^{h\nu/kT_1} - 1} \right) \frac{2n^2 e^{X_n}}{n^2 - 1} \right] \\ &= \left[S_n + \frac{W_{1n}}{W_{1\kappa}} \frac{G_{T_e}}{\int_{y_1}^{\infty} \frac{dy}{y(e^y - 1)}} \frac{\frac{2n^2}{n^2 - 1}}{(e^{h\nu/kT_1} - 1)} \right]. \end{aligned}\right\} \tag{8}$$

For an optically thin nebula surrounding a star radiating as a black body, $W_{1n} = W_{1\kappa}$. When we consider the transfer problem, this relation will no longer hold. V_{nr} is defined in terms of S_{nr} in the same manner that V_n was defined in terms of S_n.

The mathematical grouping of these terms must not be interpreted as due to their physical similarity. S_n arises from captures on the level in question; the W_{1n} term originates from transitions from the ground level to the nth level.

If the star is assumed to radiate as a black body, the b_n's are considerably different from the b_n's discussed in paper III. For small values of n they are larger than unity and gradually approach 1 as $n \to \infty$, as indeed they must. For purposes of comparison, b_n is tabulated as a function of the temperature of the central star for the two cases considered.

Computation (Table 1) shows the Balmer decrement to be very insensitive to the excitation temperature. It should be pointed out that the optically thin nebula here considered will have a brilliance much less than that of the nuclear star, so that the present results are not directly applicable to planetary nebulae. But the enormous effect of the nuclear radiation suggests that even in an optically thick nebula the nuclear radiation might show some influence on the Balmer decrement, which would tend to be steeper in consequence.

In the next paper the theory of radiative transfer for the Lyman levels and continuum will be discussed.

HARVARD OBSERVATORY

THE MAGNITUDE OF THE SUN, THE STELLAR TEMPERATURE SCALE, AND BOLOMETRIC CORRECTIONS

G. P. KUIPER

ABSTRACT

Three connected subjects are treated in this paper. The first section deals with the effective temperature, the absolute photovisual and bolometric magnitudes, and the spectral type of the sun. The quantities adopted are: $T_e = 5713°$ (Unsöld); $M_{pv} = 4.73$; $M_{bol} = 4.62$; spectrum dG2.

The second section contains a discussion of T_e of the O, B, and A stars. The result is given in Table 3 and shown in Figure 1.

In the third section, tables of bolometric correction are constructed, as far as possible independently of assumptions about the shape of the spectral energy-curves. For spectral types earlier than Fo, theoretical spectral energy-curves are used; the results are found in Tables 6 and 3. For later types, empirical bolometric corrections are derived from Pettit and Nicholson's radiometric observations. The discussion is based on Table 7 and Figures 2 and 3; the result is given in Tables 9 and 10.

In the fourth section, effective temperatures are derived for late-type stars with suitable data: Castor C and the giants for which diameters were measured interferometrically. Limb darkening has been taken into account. The result for Castor C is $3550 \pm 110°$; for the giants, the values in Table 11.

In the last section, color temperatures are collected and reduced to the system of effective temperatures. Particular attention is paid to the observations of the dwarfs (Tables 12 and 14), on which the reduction to effective temperatures depends to a large extent (sun). Table 13, last column, gives the derived effective temperatures for classes A–M; they are shown graphically in Figure 4. Directions are given for the calibration of temperatures derived from W. Becker's *Catalogue* of color indices and Pettit and Nicholson's water-cell absorptions, to effective temperatures (p. 469). Two applications are given. The result on ϵ Aurigae reduces a difficulty previously encountered by B. Strömgren.

INTRODUCTION

The purpose of this article is the selection or derivation of the most probable set of effective temperatures and of bolometric corrections that can now be obtained. These data are required in the discussion of the mass-luminosity relation given in the following paper. Only a few new results are derived here, but the main object is to select and relate the most reliable observations and results thus far obtained.

Among the recent investigations of the temperature scale, those by Pannekoek[1] and Pilowski[2] are of special interest. The results of Pannekoek's paper are extensively used in our article. Pilowski's pa-

[1] *Ap. J.*, **84**, 481, 1936. [2] *Zs. f. Ap.*, **11**, 265, 1936.

per is an attempt to use, for main-sequence stars only, the statistical relation between radius and spectral type, and between spectral type and absolute magnitude, from which the relation between spectral type and surface brightness is derived. The first relation is found from spectroscopic binaries; the last, from stars in general. But as Pannekoek has pointed out,[3] the relation between spectral type and temperature is much closer than the statistical relations from which this relation is derived by Pilowski, so that it seems preferable to restrict the discussion to those stars for which all the data are well determined. Furthermore, Pilowski derived "radiation temperatures," as defined by Brill, and not effective temperatures ("radiation temperatures" are formal temperatures related to the visual surface brightnesses by Planck's formula; since the stars do not exactly radiate as black bodies, the "radiation temperatures" depend on the wave length used in measuring the surface brightness). It will be our aim to obtain the more fundamental[4] effective temperatures, defined by

$$L = 4\pi R^2 \cdot \sigma T_e^4 , \tag{1}$$

in which L is the luminosity and R the radius of a star, and σ the radiation constant. If L and R are expressed in terms of the sun, we have

$$L = R^2 \left(\frac{T_e}{T_{e\odot}} \right)^4 . \tag{2}$$

If L and R are known, T_e may be found from equation (2). But since L is never known directly from observation, but usually only the absolute visual (or photovisual) magnitude, equation (2) can be used in practice only if a table of bolometric corrections is available. The bolometric correction is defined by

$$\text{B.C.} = M_{\text{bol}} - M_{\text{pv}} = m_{\text{bol}} - m_{\text{pv}} , \tag{3}$$

if

$$M_{\text{bol}} = M_{\text{bol}}\,(\text{sun}) - 2.5 \log L . \tag{4}$$

[3] *Op. cit.*, p. 505.

[4] E.g. Pannekoek, *op. cit.*, p. 483.

The definition of the quantity M_{bol} (sun) is given in the course of this paper. It involves the zero point of the table of bolometric corrections. The photovisual magnitudes (m_{pv}) used in this paper are international photovisual magnitudes (IPv) on the system of the North Polar Sequence of 1922. Other visual magnitudes are reduced to this system before they are used as is explained on p. 477.

In the following sections it will appear that a satisfactory table of bolometric corrections can be constructed *without recourse to the assumption of black-body radiation*, and that also the scale of stellar effective temperatures can be brought into a fairly satisfactory state.

THE TEMPERATURE AND THE LUMINOSITY OF THE SUN

1. The effective temperature of the sun is one of the very few absolute determinations of stellar temperatures which may be obtained. The luminosity, expressed in stellar magnitudes, is of importance in fixing the unit of stellar luminosities.

The solar effective temperature is derived from the solar constant; since the atmospheric extension depends on the wave length, the determination of this constant involves a spectrophotometric study of the whole accessible solar spectrum. Unsöld has just published[5] a careful rediscussion of the available data, and we adopt his result:

$$T_e = 5713 \pm 30^\circ \text{ K (estimated mean error)},$$

or

$$\log T_e = 3.757 \pm 0.002 \text{ (m.e.)}. \qquad (5)$$

2. The stellar magnitude of the sun is usually taken from Russell's discussion,[6] which gave $m_v = -26.72$ and $M_v = +4.85$. In the present paper, as in the next one, an attempt is made to reduce all magnitudes to the IPv system. Accordingly, in the comparisons tabulated by Russell IPv magnitudes will be used:

a) Zöllner found the sun 26.87 ± 0.05 mag. brighter than Capella, or −26.68 IPv.

b) Fabry found it to be 26.94 mag. brighter than Vega, or −26.85 IPv.

[5] *Physik der Sternatmosphären*, chap. ii, 1938.

[6] *Ap. J.*, **43**, 103, 1916.

c) Ceraski found it to be

22.93—0.66 + 4.86 mag. brighter than Procyon,
22.93—0.66 + 6.30 mag. brighter than Polaris, and
22.93−0.66 + 3.22 mag. brighter than Sirius.

With weights 4, 4, and 1, as used by Russell, Ceraski's value is −26.64 IPv.

d) W. H. Pickering made 10 determinations using different stars, which give the average −26.93 IPv.

The straight mean of these *four visual determinations* is *−26.77 IPv.*

No direct visual determinations of the magnitude of the sun have been published since Russell's discussion.

3. Two photographic determinations are available, already mentioned in Russell's paper. Since the dwarf F and G stars have colors almost uniquely determined by their spectral type,[7] it appears safe to adopt the color index corresponding to the spectral type. This type, as determined by Morgan and by the writer, is G2. The corresponding color index is[8] + 0.53.

E. S. King, from 10 determinations, found $m_{pg} = -25.83$. Six of these depend on comparisons with Polaris, for which King used his value $m_{pg} = 2.69$, as compared with 2.55 IPg. Applying the same correction, −0.14 mag., to the other 4 comparisons (since the magnitudes of the comparison stars were determined from direct comparisons with Polaris), King's determination becomes −25.97 IPg, or −26.50 IPv.

The second photographic determination is by Birck. The result, as reduced by Russell to King's photographic system, is −26.12, to which the correction −0.14 mag. should apply as mentioned above. Accordingly, we have $m_{pg} = -26.26$ IPg or −26.79 IPv. Giving double weight to King's determination, we obtain *−26.60 IPv* from the *two photographic determinations.*

The preceding values may be supplemented by two other determinations, one which uses the moon as an intermediate step, and the other depending on Pettit and Nicholson's radiometric work.

The use of the moon as an intermediate step involves, first, the determination of the magnitude difference between the sun and

[7] Cf. Morgan, *ibid.*, **87**, 460, 1938.

[8] *Ibid.*, **86**, 180, 1937.

moon, and second, the determination of the stellar magnitude of the moon.

4. A very fine determination of the magnitude difference between sun and moon has recently been published by Rougier.[9] He used for these measurements a photoelectric (potassium) cell. He observed the sun through an optical device which reduced the brightness by 14.87 mag., and observed the moon without that device. This made the intensities to be measured of the same order of magnitude. The reduction was obtained by placing two microscope objectives and some diaphragms at proper distances. The reduction constant followed from geometrical optics and from an empirical determination of the absorption by the objectives. The uncertainty in the reduction constant was estimated to be ± 0.01 mag. Both the sun and the moon were compared with a standard lamp, which provided a provisional zero point of the magnitude scale. With this zero point, the magnitude of the sun was found to be -17.33 ± 0.03; of the full moon, -3.04; and of the moon at other phases, the values given in Rougier's Table 30.[10]

Since the relative magnitudes in Rougier's system seem to be very well established, the calibration to stellar magnitudes by means of the moon can be made from magnitude determinations at any lunar phase covered by Rougier.

Rougier's magnitude difference may be combined with 5 magnitude determinations of the moon.

a) King's photographic measures,[11] 83 in all, were made by individual comparisons with Polaris. In principle, therefore, one observation should suffice to fix Rougier's zero point, and the whole of King's work should give a good determination if no serious systematic errors are present.

If all of King's observations are used, it is found[12] that the magnitude of the full moon is -11.64 on King's scale. If only the part between the first and last quarter is used, when the observations by both authors could be made at greater altitudes (63 observations), we find -11.58 ± 0.05 (p.e.) on King's scale. Adopting the latter

[9] *Ann. Strasbourg*, **2**, Part 3, 1933; **3**, Part 5, 1937.

[10] *Ibid.*, **2**, 319.

[11] *Harvard Ann.*, **59**, 63–94, 1912.

[12] Rougier, *op. cit.*, p. 323.

value, and the IPg magnitude for Polaris (2.55 instead of King's value 2.62), we obtain

$$m(\text{full moon}) = -11.65 \text{ IPg}.$$

b) Two visual determinations of the stellar magnitude of the moon are available, the first of which is by Zöllner. (Two still older determinations will not be used here.) Zöllner found[13] the full moon to be 12.31 mag. brighter than Capella. Reducing his observations to full moon with the aid of Rougier's light-curve instead of Zöllner's own curve, we find 12.48 mag. for the difference. Hence, we have

$$m(\text{full moon}) = -12.29 \text{ IPv (Zöllner)}.$$

c) The second visual determination is by W. H. Pickering.[14] He compared both the moon and Arcturus with a pentane lamp, the color of which was made equal to these objects by means of a blue solution acting as a filter. The scale was exclusively based on the inverse-square law. Reducing the observations[15] to full moon with the aid of Rougier's light-curve, and using only the observations made between first and last quarter,[16] we find for the full moon −12.63 on Pickering's scale (with Arcturus 0.24 mag.). For the IPv magnitude of Arcturus we find +0.04, so that

$$m(\text{full moon}) = -12.83 \text{ IPv (Pickering)}.$$

This result is based on 18 observations of the moon but on only 4 of Arcturus. The internal probable error of the mean of the observations of Arcturus alone is ±0.11 mag. But Pickering's observations are of interest because of their extreme simplicity.

The agreement between the two visual determinations is rather poor. Giving Pickering's result double the weight of Zöllner's, the combined visual result is

$$m(\text{full moon}) = -12.65 \text{ IPv}.$$

[13] *Photometrische Untersuchungen*, pp. 109 and 124, 1865.

[14] *Harvard Ann.*, **62**, 62–69, 1908. [15] *Ibid.*, Table XI, p. 65.

[16] Two observations, Nos. 9 and 10, were omitted because of Pickering's comments on them.

d) Pettit's radiometric work on the moon as a whole[17] gives incidentally a determination of its visual magnitude.[18]

Unfortunately, Rougier's light-curve and Pettit's curve of the reflected light are not in very good agreement.[19] It seems probable that at least part of the discrepancy can be attributed to the extrapolation of the light-curve to full moon, which is necessarily somewhat arbitrary, particularly when few observations are made very near full moon. Although color determinations of the moon show no change during the lunation, only a small variation could appreciably affect the difference between the photoelectric and the radiometric observations, in view of the yellow color of reflected moonlight.

On account of this difference, Pettit's determination will give a lower limit to the brightness of the full moon as compared with Rougier's system, which we have used in the reductions. (It is clear that this fact arises only because we use the magnitude of the full moon as derived by Pettit from his own curve. In our previous discussion we use Rougier's definition of the full moon only as a constant connecting the solar magnitude with all the lunar observations between first and last quarter. Hence, it does not concern us whether or not Rougier's definition is exactly correct.)

Pettit's computed value for the brightness of the full moon is -12.63 mag., which is on the Harvard scale. Since this value is a lower limit in the system used here, we shall adopt -12.75 IPv as a probable value.

e) Calder[20] compared the moon photoelectrically with Capella, Vega, and Deneb, with a standard lamp as intermediary. In order to obtain the photoelectric magnitude of the lamp on the international scale, we apply 0.8[21] of the color index (IPg − IPv) to the IPv magnitudes. With the directions of page 478 we find for the IPv magnitudes of Capella, Vega, and Deneb, + 0.19, + 0.09, and +1.34, respectively; and hence, with the color indices given elsewhere[22] we find the photoelectric magnitudes to be +0.75, + 0.09, and + 1.39. These values, in connection with the differences found by Calder,

[17] *Ap. J.*, **81**, 17, 1935; *Contr. Mt. W. Obs.*, No. 504.

[18] *Ap. J.*, **81**, 33–34.

[19] *Ibid.*, Fig. 4, p. 28. [20] *Harvard Ann.*, **105**, 445, 1937.

[21] E.g., Stebbins and Whitford, *Ap. J.*, **87**, 252, 1938. [22] *Ibid.*, **86**, 180, 1937.

lead to −4.33, −4.35, and −4.33 mag. for the lamp, or −4.34 mag. in the mean.

Calder measured the moon on two nights, one of which led to final results. The phase angle during these observations was $+5^{\circ}50'$, so that the correction to full moon[23] is −0.12 mag. (Calder, with a somewhat different definition of full moon, obtained −0.18 mag.). Calder's data then make the full moon 7.75 mag. brighter than the standard lamp, or −12.09 IPe.

We must now reduce the five different values for the magnitude of the moon to one system, for which we adopt the IPv system. To that end the color index of the moon is needed. The color index of the sun has been assumed to be + 0.53 mag.[24] The difference between the color indices of sun and moon is found from the following measures (the moon is the redder):

Wilsing, Scheiner, Russell*	0.25 mag.
Pettit†	.20
Danjon‡	.33
Calder§	0.17
Weighted mean	0.22 mag. (6)

* *Ap. J.*, **43**, 126, 1916.
† *Pub. A.S.P.*, **38**, 243, 1926.
‡ *Ann. Strasbourg*, **3**, 146, 274, 1936–37.
§ *Harvard Ann.*, **105**, 452, 1937. The color index was found to be equal to that of Capella, and hence 0.17 mag. larger than for the sun.

Pettit's determination has been given double weight and Danjon's visual determination half-weight.

Accordingly, the color index of the moon is + 0.75 mag., corresponding to dKo, in agreement with Pettit's result.

The five magnitude determinations of the full moon are, therefore,

−11.65 IPg	= − 12.40 IPv	(King)
	12.65	(Zöllner, W. H. Pickering)
	12.75	(Pettit)
−12.09 IPe	= − 12.69 IPv	(Calder)
Mean	= − 12.66 IPv	(7)

In forming the mean, double weight was given to the two modern determinations. It should be remarked that Pettit's own reduction,

[23] Rougier, *op. cit.*, Table 30. [24] Cf. p. 432.

-12.63 HS, is very close to the average; but we felt that a small correction was needed to allow for the difference between Rougier's and Pettit's light-curve.

The value -12.66 IPv here obtained does not appreciably modify Russell's result -12.55 HS; the difference is about equal to the somewhat greater relative brightness of the full moon as defined by Rougier's light-curve.

This result for the brightness of the full moon, together with Rougier's photoelectric difference, 14.29 mag., gives

$$m(\text{sun}) = -12.66 - (14.29 - 0.8 \times 0.22) = -26.77 \text{ IPv}.$$

5. Pettit and Nicholson's paper on "Stellar Radiation Measurements"[25] contains a calibration of radiometric magnitudes in terms of energy, from which the authors obtained the radiometric magnitude of the sun, -27.18 mag. From this figure the bolometric magnitude is found to be $-27.18 - \Delta m_r + 0.62 = -27.01$ mag. The constant 0.62 mag. is explained on page 451; it reduces the quantity $(m_r - \Delta m_r)$ to the zero point of bolometric magnitudes used in this paper.[26] The average bolometric correction for a G2 dwarf is, then, 0.07, as found below (Table 9). Hence, the resulting visual magnitude of the sun is -26.94 IPv.

The uncertainty of the bolometric magnitude of the sun derived from Pettit and Nicholson's measures is probably less than 0.05 mag. But, as we shall see later, there may be some scatter in the heat indices for main-sequence stars, which also enters in the empirically determined bolometric corrections. Hence, the quantity 0.07 may be in error by a small amount.

The four groups of determinations of the IPv magnitude of the sun thus far discussed are:

Four visual determinations	-26.77 IPv,	weight 1
Two photographic determinations	26.60	$\frac{1}{2}$
Sun-moon, plus 5 determinations of moon	26.77	2
Radiometric determination	-26.94	3
Weighted mean	-26.84 ± 0.04 (p.e) IPv	

[25] *Ap. J.*, **68**, 279, 1928; *Contr. Mt. W. Obs.*, No. 369.

[26] The quantity Δm_r includes the zenith absorption of the atmosphere as well as the loss in the telescope (Pettit and Nicholson).

One observation of the magnitude of the sun remains to be discussed. Calder[20] compared the sun on three days with his standard lamp, which, as we have seen, was in turn compared with three stars. The photoelectric magnitude of the sun was found to be 21.46 mag. brighter than the standard lamp, for which we obtained −4.34 IPe. Hence $m(\text{sun}) = -25.80$ IPe $= -26.22$ IPv.

This value deviates 0.6 mag. from the mean value obtained above. The photoelectric method used by Calder is, of course, capable of yielding very accurate results. The difference cannot, therefore, be ascribed to an accidental error in Calder's work, nor can our mean value be in error by an amount much larger than 0.1 or 0.2 mag. We conclude that Calder's observation may be affected by a systematic error and that it seems best to omit it at the present time.

In order to obtain the most probable value of the bolometric magnitude of the sun, we combine the result obtained from Pettit and Nicholson's radiometric work, −27.01 mag., with the weighted mean, −26.75 IPv, of the first three groups of observations given above. This mean leads to $m_{\text{bol}} = -26.82$. On account of the uncertainty in the bolometric correction, the relative weights have to be different from those assigned in forming the mean IPv value. We raise the weight of the radiometric determination from 3 to 5 and lower the total weight of the other determinations from $3\frac{1}{2}$ to $2\frac{1}{2}$. The weighted mean then becomes

$$m_{\text{bol}} = -26.95, M_{\text{bol}} = +4.62, \tag{8}$$

whereas

$$m_{\text{pv}} = -26.84, M_{\text{pv}} = +4.73\,. \tag{9}$$

The third quantity needed for the sun is its spectral class. From low-dispersion slit spectra Dr. Morgan and the writer independently found G2 on the conventional scale.

SUNSPOTS

As mentioned below, only for three stars in addition to the sun have radii and luminosities been determined with such accuracy as is needed for furnishing reliable determinations of effective temperature. For that reason it is fortunate that the sun provides a second

determination for a type much later than G2. Since Minnaert and Wanders have shown that the umbra of sunspots is in radiative equilibrium,[27] it follows that the relation between surface brightness and spectral type will be the same as for ordinary stars in radiative equilibrium. Since, further, the value of the surface gravity is very nearly the same for G and K dwarfs, the relation found will be valid for dwarfs.

The effective temperature of the umbra of medium to large-sized spots is $5713\sqrt[4]{0.42} = 4600°$ as determined from the total radiation,[28] 4450° from the surface brightness,[29] and 4700° from the degree of ionization.[30] We adopt 4600°.

The spectral type of these spots is usually given as K0. We assume that this means that the type is within the limits G8 and K2. With the limits indicated, the value has been plotted in Figure 4. An accurate comparison with dwarf K-type spectra would be of great interest.

TEMPERATURES OF EARLY-TYPE STARS

1. Partly on the basis of theoretical work by Unsöld[31] and Pannekoek[32] and from Pannekoek's recent review of the methods of temperature determination,[33] we derive the following conclusions.

Effective temperatures depend in a somewhat irregular way on stellar colors; the relation is not yet fully accounted for by the theory of the continuous absorption coefficient. The relation is further complicated for the late-type stars by the presence in the spectrum of numerous lines and bands and for the early-type stars by space reddening. Nevertheless, colors will be useful for giving interpolatory values between certain points in the spectral sequence for which effective temperatures may be derived.

Temperature determinations based on the Boltzmann function show certain anomalies which make this method uncertain at the present time.

2. For the O and B stars the best determination may be made

[27] *Physik der Sternatmosphären*, p. 363, 1938.

[28] *Ibid.*, p. 361.

[29] *Ibid.*, p. 363.

[30] *Ibid.*, p. 366.

[31] *Zs. f. Ap.*, **8**, 32, 1933; p. 225, 1934.

[32] *M.N.*, **95**, 529, 1935.

[33] *Ap. J.*, **84**, 481, 1936.

from a study of the maxima of certain spectral series, rediscussed on the basis of the theory of the continuous absorption coefficient, as Pannekoek has done. His Table IV[34] contains the necessary information, which seems particularly valuable since each element gives an independent temperature determination in which possible variations of abundance with spectral type enter as accidental errors. Of course,

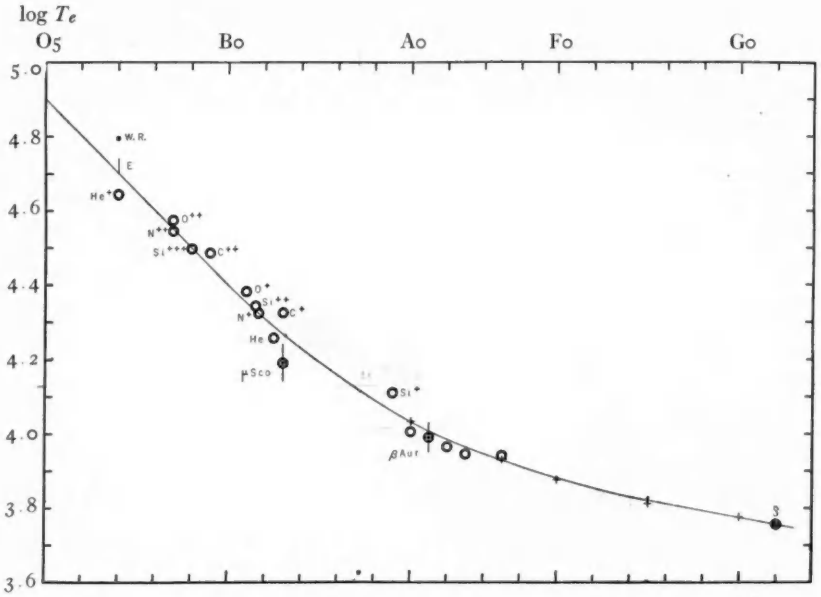

FIG. 1.—The stellar temperature scale for types O–G

the method is independent of space absorption, which affects most of the early-type stars.

Pannekoek's values for $\log g = 4.4$ (main-sequence stars) are plotted in our Figure 1. The accordance between the different elements is very satisfactory. Even if in the future it should be necessary to revise the theory of the continuous absorption coefficient, it seems unlikely that the variations with temperature of the corrections could be so large as to affect appreciably the positions of the

[34] *Ibid.*, p. 496. Double weight was given to the column headed "E. G. Williams." In addition Dr. Morgan has informed the writer that the maximum of Si^+ should be placed at B9 rather than at Ao if the classification near Ao is based on the strength of the K line and *He* 4471. Cf. Morgan, *Pub. Yerkes Obs.*, **7**, Part 3, 1935.

maxima. The influence on the observed maxima of a gradual transition with increasing temperature of absorption lines to emission lines should be considered, but it is probably small because of the great differences between the ionization and excitation potentials of the series used between types Bo and O8. If the effect is present, the temperatures found are somewhat too high.

Pannekoek's temperatures for log $g = 2.4$ (giant B and O stars) are systematically 3000° lower.

In Figure 1 are also plotted four temperature determinations of A stars by Pannekoek, based on the intensity of the K line. According to Pannekoek, there is a possibility of a small systematic error common to all four points.

TABLE 1

Star	Spec.	1000π
μ_1 Sco	B_3, B_3	$7''.4 \pm 0''.8$
β Aur	A_1, A_1	37 ± 4
RS CVn	F_4, G8	48 ± 12
44 Boo B	dG2p	79 ± 5
α Gem C	dK6+, dK6+	73 ± 3

3. Five eclipsing binaries are known which show two spectra and have a measurable parallax. They are collected in Table 1.

For 44 Bootis B no spectroscopic orbit has been determined as yet, and the light-curve is still somewhat provisional, owing to the proximity of A. The parallax of RS CVn is still very uncertain. The other three systems are discussed below, Castor C on pages 455–458.

Pannekoek has already discussed the system of β Aurigae,[35] but our rediscussion leads to a somewhat lower value of the temperature and a somewhat greater uncertainty of the result obtained.

Stebbins found β Aurigae at maximum 0.35 mag. fainter than β Tauri. According to Zinner's compilation, the magnitude of β Tauri is 1.98 ± 0.04 (m.e.) P.D. and that of β Aurigae 2.26 ± 0.06 P.D. From these data, and from Table 2, page 478, we find for β Aurigae at maximum on the IPv scale, 2.10 ± 0.04 and a value

[35] *Ap. J.*, **84**, 506, 1936.

slightly brighter than 2.04±0.06, respectively. We shall adopt 2.07 IPv, which happens to be identical with the HD magnitude used by Pannekoek. The trigonometric parallax being 0".037±0".004 (p.e.), the absolute magnitude of the average component is +0.66± 0.24 (p.e.).

There are two main sources of uncertainty in the derived temperature: (1) the unknown value of the limb darkening; (2) the uncertainty in the absolute magnitude, owing to the parallax.

Shapley has given two photometric solutions of Stebbins' data, U (uniform) and D (fully darkened). Considering these extremes, as well as an intermediate case, we have for $\pi = 0''.037$:

	U	$\frac{1}{2}(U+D)$	D
a_1	0.147	0.153	0.159
cos i	0.218	0.223	0.228
log $R/R\odot$	0.414	0.431	0.448
T_e	10150	9800	9500

The last line follows from equation (2), page 430, in connection with the table of bolometric corrections (Table 6).

The intermediate solution will be adopted on the basis of Pannekoek's theoretical work on limb darkening,[36] which indicates a value of $u = 0.5$ for 10,000° in the visual region of the spectrum (selenium cell). A slightly different value of u would not change the result appreciably.

The second source of uncertainty is of more importance. With the intermediate solution a probable error of ±960° in T_e is found, or ±0.04 in log T_e. (Obviously, the uncertainty in log T_e is larger than ±0.24/10, since for this temperature the visual brightness increases more slowly with increasing T_e than the bolometric brightness.)

According to Baker, the spectral type is more advanced than that of Sirius (A0) and is nearly equal to that of α_2 Geminorum (A1).

We have, accordingly, for A1:

$$\log T_e = 3.99 \pm 0.04 \text{ (p.e.)}. \qquad (10)$$

This value is plotted in Figure 1.

[36] *M.N.*, **95**, 733, 1935.

4. The system of μ_1 Scorpii has recently been discussed by Rudnick and Elvey.[37] At maximum, μ_1 Scorpii was found to be 0.60 mag. brighter than μ_2. The magnitude of the latter star is 3.92 PD (Zinner), or 3.68 IPv, so that at maximum μ_1 is 3.08 IPv. The cluster parallax is 0".0074 (Kapteyn). The probable error of this parallax depends largely upon the probable error of the PCG proper motion, which is 11 per cent of the proper motion itself in each co-ordinate. The probable error of the parallax is, therefore, at least 11 per cent of its value, and the average absolute magnitude of the components, -1.82 IPv, has a probable error of at least ± 0.24 mag.

Miss Maury found the photographic intensity of B to be about 0.6 or 0.7 of A. Since $J_f/J_b = 0.613$ (Rudnick and Elvey), we may assume that the components have equal radii. In that case $a_b/a = a_f/a = 0.380$ and $b_i/a = 0.336$. From these data we find by the method used in the next article[38] that $R/a = 0.346$, and the adjusted value of $a_i/a = 0.370$. With this value of R and Miss Maury's value of $a \sin i = 9{,}534{,}000$ km, together with $i = 62°.0$, we find $R_b = R_f = 5.37\odot$.

Adopting the bolometric corrections of Table 6 below, which are uncertain by probably not more than 0.1 mag., we find 16,000° as the average effective temperature of the components. The minimum value of the probable error of this result (owing to the uncertainty of the parallax alone) is $\pm 1900°$. In logarithms:

$$\log T_e = 4.20 \pm 0.05 \text{ (minimum p.e.)}. \qquad (11)$$

This value is shown in Figure 1 at B3, the average spectral type according to Miss Maury.

5. An eclipsing system of still earlier type (Bo±), which will become of great interest when the spectroscopic orbit and the mass ratio have been determined, is SZ Camelopardalis, for which Wesselink published[39] an exceptionally accurate light-curve. The system being a member of the cluster NGC 1502, a fairly accurate determination of the absolute magnitude will be possible. With a distance modulus of 12.0,[40] the absolute IPv magnitude of the primary is -4.8, if $\Delta m = 1.0$ is assumed.

[37] *Ap. J.*, **87**, 553, 1938.

[38] Cf. the treatment of V Puppis, p. 500.

[39] Dissertation, Leiden, 1938.

[40] Trumpler, *Lick Obs. Bull.*, **14**, 156, 1930. See also *Ap. J.*, **86**, 187, 1937.

Since, in general, the parallax is the main source of error in an absolute T_e determination, it is of interest to know the effect of a certain error in the parallax. In Table 2, for six different values of T_e the probable error of T_e and of log T_e has been computed under the assumption that the probable error of the parallax is 10 per cent of its value. This corresponds to ± 0.22 mag. in the distance modulus, which for distant objects is really the quantity desired (space absorption). It may be hoped that for galactic clusters the probable error may be reduced below this value. The probable error of log T_e for very high temperatures follows simply from the Rayleigh-Jeans law:

$$M_{pv} = C - 2.5 \log T_e \quad (T_e \to \infty) .$$

It follows from Table 2 that for the range 10,000°–40,000° (A0–O8) the percentage error in T_e is about the same as that in the parallax.

TABLE 2

PROBABLE ERROR, IF P.E. OF π IS 10 PER CENT

T_e	In T_e	In log T_e
10,000°	± 930°	±0.040
15,000	1650	.047
20,000	2150	.046
25,000	2600	.046
30,000	3400	.049
40,000	±4500	.048
∞		±0.088

For much higher temperatures the error in T_e would be double that of the parallax, whereas for temperatures of G and K stars the percentage error will be less than half that of the parallax.

6. Stars earlier than O8 are not covered by the maxima discussed by Pannekoek. From the publication by E. G. Williams,[41] which was extensively used by Pannekoek, we may tentatively derive one more maximum, that for He^+. A plot of Williams' measured intensities shows a steady increase in strength of He^+ toward the earlier types up to O7, while for the only O6 star the strength is considerably less again. The maximum is probably near O7. According to

[41] *Ap. J.*, **83**, 296, Table VI, 1936.

Pannekoek, the temperature corresponding to this maximum is 44,000° for log $g = 4.4$.

Another source of information is Beals's study of the Wolf-Rayet stars.[42] Two stars are mentioned which have not only a Wolf-Rayet spectrum but also an absorption O7 spectrum. These stars, HD 193793 and HD 211856, have mimimum temperatures (determined by Beals using the Zanstra method) of about 59,000°[43] and 65,000°.[44]

The Zanstra method as applied to stars having relatively small shells (Wolf-Rayet stars, Be stars, etc., contrary to planetary nebulae), was discussed theoretically by Gordeladse,[45] who pointed out that the observed emissions in such objects are only partly due to absorptions from the ground state and that absorptions from higher levels contribute appreciably. As Dr. Wurm mentioned to the writer, this fact will be of importance when the observed emissions are strong, which will cause many atoms to fall into intermediate levels. As Gordeladse states, the temperatures derived by the strict application of the Zanstra method will in this case lead to too-high temperatures. The average of the two minimum temperatures found by the Zanstra method, 62,000°, may therefore be somewhat too high.

Another estimate may easily be made, as Dr. Wurm suggested, from the circumstance that certain emissions are present (He^{+}, C^{++}, and C^{+++} in HD 193793, W VI; and He^{+}, N^{++}, and N^{+++} in HD 211856, W6 or W7). This would lead to temperatures of the order of 50,000°–55,000°, found by comparison with Pannekoek's temperatures for the absorption lines. More definite results could only be obtained by a detailed treatment of the behavior of different atoms in diluted radiation.

Gordeladse's remarks also apply to the emission B stars. Temperatures derived for Be stars by the unmodified Zanstra method, as given by O. Mohler,[46] may be in error. In addition, a selection effect enters; only stars having emissions above a certain strength are discussed, whatever the cause of these emissions may be. This probably accounts for the small scatter in the temperatures found

[42] *Pub. Dom. Ap. Obs. Victoria*, **6**, 95, 1934.

[43] *Op. cit.*, Table 8, p. 139.

[44] *Op. cit.*, Table 8 and p. 143.

[45] *Zs. f. Ap.*, **13**, 48, 1936.

[46] *Pub. U. Mich. Obs.*, **5**, 43, 1933.

by Mohler (which average 18,000°) and the absence of a notable dependence on spectral type (Bo–B8).

7. From Figure 1, which shows all the temperature data collected for the O, B, and A stars, mean values may be read, which are found in Table 3. The values for O6 and O5, given in parentheses, are mere extrapolations. The bolometric corrections for these temperatures, derived in the next section, are added.

TABLE 3

Spec.	log T_e	B.C.	Spec.	log T_e	B.C.
O5	(4.9)	−5.6	B3	4.27	−2.01
O6	(4.8)	4.9	B4	4.23	1.79
O7	4.7	4.3	B5	4.19	1.58
O8	4.60	3.8	B6	4.16	1.42
O9	4.50	3.24	B8	4.09	1.04
Bo	4.40	2.70	Ao	4.03	0.72
B1	4.36	2.48	A2	3.986	0.52
B2	4.31	−2.22	A5	3.93	−0.31

BOLOMETRIC CORRECTIONS

1. Before attempting to fix the temperature scale of the later spectral classes it is advantageous to consider the bolometric corrections, B.C. $= m_{\text{bol}} - m_{\text{pv}}$. Three computations of this quantity as a function of T_e have been made, all assuming black-body radiation. Hertzsprung[47] made the computation for the lower temperatures, using the sensitivity curve of the eye; Pike[48] did the same for the higher temperatures. Finally Hertzsprung has computed the bolometric correction for photovisual instead of visual magnitudes.[49] From his data we derive the bolometric corrections given in Table 4; we denote with Δm, bolometric corrections computed on the assumption of black-body radiation. It is seen that these corrections to photovisual magnitudes are very similar to those for visual magnitudes, although photovisual magnitudes are more nearly monochromatic.

[47] *Zs. f. Wiss. Phot.*, **4**, 49, 1906; Eddington, *The Internal Constitution of the Stars*, p. 139.

[48] *M.N.*, **89**, 539, 1929.

[49] *Zs. f. Wiss. Phot.*, **30**, 173, 1931.

It is well known that the stars do not radiate as black bodies. The values Δm can therefore not be used; they need a correction which we denote by δm. This correction can be evaluated only if the whole spectral energy-curve is known. Two approximations are available to this ideal case: (1) theoretical spectral energy-curves, computed on the basis of a certain assumed composition of stellar atmospheres, and (2) radiometric observations of low-temperature stars (for high temperatures too much of the energy is radiated in the inaccessible ultraviolet).

2. Spectral energy-curves have been computed by Unsöld[50] and Pannekoek.[51] Unsöld adopted for the stellar atmospheres the same

TABLE 4

T	Δm	T	Δm
2,000°	−4.69	6,000°	−0.02
2,500	2.84	8,000	0.06
3,000	1.74	10,000	0.28
3,500	1.07	12,000	0.55
4,000	0.64	15,000	0.97
4,500	0.36	20,000	−1.61
5,000	−0.18		

abundance of hydrogen, one-third by weight, as had been found in stellar interiors (B. Strömgren, Eddington). This ratio corresponds to 14 hydrogen atoms for each metal atom. Burkhardt, in discussing the intensity jump at the head of the Balmer series, later[52] considered 50:1 for this ratio, whereas Pannekoek adopted 1000:1. We have used Pannekoek's computations in preference to Unsöld's because for $T = 10{,}080°$ Unsöld predicts the intensity jump at 3647 A to be 0.62 mag., against Pannekoek's 1.20 mag. The observations[53] give about 1.2 mag. (Although this agreement with Pannekoek's predictions does not necessarily confirm the high abundance of hydrogen used by Pannekoek, in view of numerical uncertainties[54] in the theory

[50] *Zs. f. Ap.*, **8**, 241 ff., 1934; *Physik der Sternatmosphären*, pp. 131–138, 1938.

[51] *Ap. J.*, **84**, 484, 1936. [52] *Zs. f. Ap.*, **13**, 56, 1936.

[53] *Handb. d. Ap.*, **7**, 460. See also Kienle, *Erg. d. exakt. Naturwiss.*, **16**, 462, 1937; Unsöld, *Physik der Sternatmosphären*, p. 134, Fig. 53*b*.

[54] Unsöld, *op. cit.*, pp. 135–136.

of the continuous absorption coefficient the agreement is important for the derivation of the bolometric corrections).

In spite of this agreement on the strength of the Balmer continuum, the corrections δm obtained from Pannekoek's data cannot be considered as final. It is true that for temperatures higher than 6500°–7000° the theoretical relation between color temperature (defined by the slope of the spectral energy-curve) and effective temperature is in fair agreement with observation for such widely different compositions as have been adopted by Unsöld and Pannekoek; but for the solar temperature the difference between the two temperatures is predicted with the wrong sign by both authors, a difficulty which has not been cleared up.[55, 56]

For three effective temperatures—10,080°, 5040°, and 3150°—Pannekoek has computed spectral intensities for most of the spectrum; for other temperatures, only at three wave lengths, 4000, 5000, and 6000 A. A complication arises from the fact that the relation between surface and effective temperatures, $T_e^4 = 2\,T_0^4$, no longer exactly holds. Pannekoek gives the necessary corrections, from integrations over the computed spectra, for the three temperatures stated. In the absence of detailed computations we adopt interpolatory corrections for the other temperatures. The result of these corrections is to increase the total bolometric correction by values varying between 0.08 mag. ($T_e = 5040°$) and 0.25 mag. ($T_e = 25{,}200°$, the highest temperature considered by Pannekoek).

Applying these small corrections to the computed spectral intensities of Table 1,[57] we find, for $\lambda = 5500$ A, the δm values given in Table 5. The true bolometric correction to photovisual magnitudes is, then, B.C. $= \Delta m + \delta m$.

It so happens that δm reaches the maximum value of +0.10 mag. for $T_e = 6600°$ when Δm is zero. In order to avoid bolometric corrections with different signs, we subtract +0.10 mag. from all the δm values before adding them to Δm. The bolometric corrections thus obtained are given in Table 6 for temperatures up to 50,000°.

[55] Cf. also Minnaert, *Zs. f. Ap.*, **12**, 260, 1936.

[56] During a symposium at the Yerkes Observatory (June, 1938) Dr. Wildt announced a mechanism of continuous absorption that may remove the difficulty.

[57] *Op. cit.*, p. 486.

The correction δm has been extrapolated for temperatures higher than 25,000°, assuming that it slowly decreases.

For low temperatures, δm is not well determined by Table 5. Furthermore, the values given are based on a smoothing process for

TABLE 5

T_e	δm	T_e	δm
3150°	−1.26	8400°	−0.10
5040	−0.06	10080	.21
5600	+0.01	12600	.37
6300	+0.09	16800	.46
7200	+0.06	25200	−0.44

TABLE 6

THEORETICAL VALUES OF BOLOMETRIC CORRECTIONS

(Temperatures in 1000°)

T_e	B.C.	T_e	B.C.
3.0	$-3^m.2$:	13	$-1^m.18$
3.5	2.1:	14	1.35
4.0	1.3:	15	1.51
4.5	0.63	16	1.66
5.0	0.34	17	1.80
5.5	0.17	18	1.94
6.0	0.06	19	2.06
6.5	0.00	20	2.18
7.0	0.01	22	2.40
7.5	0.12	25	2.69
8.0	0.22	30	3.12
9.0	0.40	35	3.5
10	0.57	40	3.8
11	0.78	45	4.1
12	−0.98	50	−4.3

absorption bands and lines that can be only roughly correct; also, as we have seen, for the solar temperature an incorrect value of the color index is predicted. Fortunately, it is for the low temperatures that the second source of information regarding bolometric corrections is important.

3. The radiometric observations by Pettit and Nicholson[58] provide extremely valuable information about both the bolometric cor-

[58] *Ap. J.*, **68**, 279, 1928; *Contr. Mt. W. Obs.*, No. 369.

rections and the temperature scale. The theoretical work discussed above indicates that the observed energy-curves of low-temperature stars are displaced toward the red with respect to the Planck curves, that correspond to their effective temperatures. The displacement may be about 10 or 15 per cent. If this result is correct, the temperatures derived from water-cell transmissions and heat indices, being essentially color temperatures, should, of course, be too low; but the bolometric magnitudes obtained would still be correct, since the reductions to "no atmosphere," Δm_r, were computed with a Planck curve corresponding to the observed energy distribution. Furthermore, the corrections Δm_r (which include instrumental losses) vary between 0.4 and 0.6 mag. for spectral types between F5 and M6, indicating, first, that nearly all the energy reached the instrument (so that deviations from a Planck curve cannot have entered seriously) and, second, that a small error in the assumed temperature hardly affects the derived bolometric magnitude.

From Pettit and Nicholson's data, bolometric corrections were derived for all stars of classes A0–M6. For F0–M the results are given in Table 7. The radiometric magnitudes, m_r, were corrected by $-\Delta m_r$; then magnitudes on the IPv scale were obtained[59] from Zinner's compilation or *Potsdam Publications*, Volume 17; for Groombridge 34 my own measures were used, and for B 4342 the value was taken from Mrs. Gaposchkin's compilation. Variable stars with ranges not less than 0.2 mag. are indicated by parentheses.

The differences, $(m_r - \Delta m_r) - m_{pv}$, give the bolometric corrections apart from the zero point. The latter was made equal to that of Table 6 by a comparison of the corrections derived by the two methods for stars of types dF0–G0. This is the only interval where both the theoretical computation and the radiometric determination should be approximately correct. The comparison is shown in Table 8; the temperature scale of Figure 1 was adopted. The difference F2 − G0 is nearly the same as that found by both methods. There is a small discrepancy for the A stars, probably because the deviations from the Planck curve were accounted for in the first computation but not in the second; the difference is in the right direction.

[59] The corrections are given in Table 2, p. 478.

We shall adopt Table 6 for stars earlier than Fo and Table 7 for stars later than Fo.

With the zero point just defined (which makes the theoretically determined bolometric correction zero at 6600°) the constant correc-

TABLE 7

Star	IPv	Sp.	M	B.C.	Star	IPv	Sp.	M_{pv}	B.C.
β Cas	2.37	dF2	+1.6	−0.02	δ And	3.42	gK3	+ 0.5	−0.87
α Tri	3.47	dF4	+2.0	− .07	53 Eri AB	3.94	gK1	+ 1.3	0.50
α CMi	0.45	dF3	+2.8	− .07	β Cnc	3.67	gK4	− 0.4	1.21
α Per	1.90	cF4	−4.4	− .12	α Hya	2.18	gK4	− 1+	1.12
ξ Peg	4.13	dF6	+2.6	− .02	ζ Cep	3.55	cK1	− 4+	1.13
η Boo	2.82	F9	+3.1	− .16	α Tau	1.02	gK5	− 0.7	1.46
ϵ Leo	3.09	G1	−2.	− .23	γ Dra	2.41	gK5	− 0.6	1.31
β CVn	4.26	dG0	+4.4	− .18	ξ Cyg	3.82	cK4	− 4.	1.50
λ Ser	4.40	dG1	+4.3	− .09	61 Cyg A	5.43	dK5	+ 7.8	0.94
γ Cyg	2.29	cF7	−5.	− .13	61 Cyg B	6.09	dK6	+ 8.5	1.06
α Aqu	3.18	cF9	−3.	− .47	β And	2.22	gK5+	+ 0.3	1.63
ι Per	4.08	dG0	+3.7	− .01	Ci 1218	6.52	dK6	+ 8.2	1.04
α Aur $\frac{AB}{2}$	0.94	gG1	−0.1	− .35	B 4342	7.57±	*dK4+	+ 7.3	0.94±
β Com	4.27	dF9	+4.9	+ .03	α Sco	1.30	cM0	− 3.9	2.54
η Peg	3.09	gG2	−1+	− .48	Gr. 34	8.09	*dM1+	+10.4	2.08
η Psc	3.78	gG6	0.	− .36	α Cet	2.81	gM0	− 1.	1.96
β Her	2.80	gG6	−0.7	− .51	α Ori	(0.96)	cM1+	− 4+	(2.55)
β Cet	2.18	gG6	+0.8	− .48	π Leo	4.78	gM1	0.	1.66
ϵ Vir	2.90	gG6	+0.7	− .35	B 2935	7.50	*dM2+	+10.4	1.98
τ Cet	3.53	dG6	+5.9	− .10	m Vir	5.13	gM2	0.	1.98
o Tau	3.75	gG6	−0.4	− .36	λ Aqu	3.83	*gM2	− 0.5	1.89
γ Tau	3.80	gG8	+0.9	− .38	β Peg	(2.62)	gM3	− 1+	(2.25)
α UMa AB	1.96	gG9	−0.5	− .64	55 Peg	4.60	*gM1	+ 0+	1.48
ϵ Boo A	2.66	G9	−2.	− .61	15 Tri	5.58	*gM2+	0	2.06
β Aql	3.72	G9	+3.2	− .18	μ Gem	3.10	gM3	− 1	2.36
δ Eri	3.57	dG9	+3.8	− .32	δ Vir	3.62	gM3	0	2.31
β Gem	1.23	gG9	+1.2	− .48	30 Psc	4.62	*gM3+	+ 1:	2.53
o_2 Eri A	4.38	dK2	+5.9	− .15	ρ Per	(3.65)	*gM4	0	(2.92)
ψ UMa	3.12	gK1	+0.8	− .65	51 Gem	(5.18)	gM4+	− 0+	(2.79)
α Boo	0.04	gK2	−0.3	− .84	B 3100	5.39	gM4+	0	2.95
τ Psc	4.55	gK2	+1+	− .37	13 Sge	(5.52)	*gM4	0	(2.68)
α Ari	2.03	gK2	+0.4	− .59	62 Sgr	4.57	*gM4	0	2.83
ϵ Eri	3.69	dK2	+6.1	− .15	56 Leo	(5.88)	*gM5	− 1	(2.99)
70 Oph A	4.20	dK1	+5.7	− .05	α Her A	(3.52)	M5	− 2	(4.27)
B	5.90	dK4	+7.4	− .53	R Lyr	(4.3±)	*gM4+	− 1+	(3.7±)
γ And A	2.33	gK3	−1.4	− .95	45 Ari	(6.02)	*gM5+	0	(−4.28)
α Ser	2.76	gK2	+1.0	−0.62					

tion to the Mount Wilson values of $m_r - \Delta m_r$ is +0.62 mag. This same zero point has been adopted in Table 7.

The spectral types in Table 7 are mostly due to Dr. Morgan, who has recently obtained a very homogeneous and accurate set of spec-

tral types for the brighter stars.[60] A small systematic deviation for the G stars with respect to the Mount Wilson system has been removed, but for the K and M dwarfs the types are left unchanged. The system for the giants is practically identical with that used at Mount Wilson. A few determinations, indicated by an asterisk, are my own. For α Orionis, Morgan obtained cM3; but since it is possi-

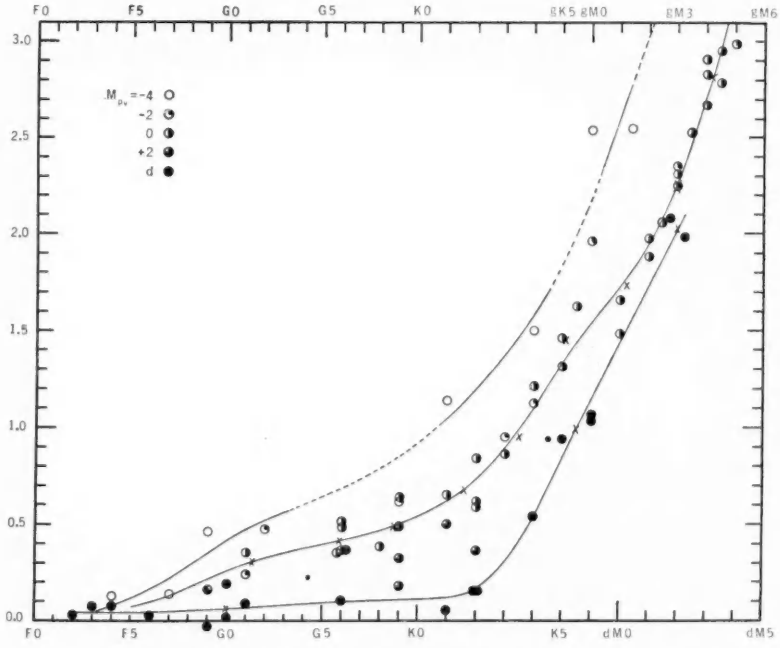

FIG. 2.—Empirical bolometric corrections for types F–M. The three curves represent the dwarfs, giants ($M_v = 0.0$), and supergiants ($M_v = -4.0$), respectively.

ble that the spectral type varies slightly, as well as the magnitude, the average, M1+, of all determinations available has been adopted.

The absolute magnitudes are based partly on up-to-date trigonometric determinations and partly on spectroscopic data, some of which were kindly supplied by Dr. Morgan.

Figure 2 shows the relation between bolometric correction and spectral type, taking into account the absolute magnitude. Three lines are drawn in the diagram, indicating the mean positions for

[60] Mostly unpublished.

main-sequence stars, stars with $M_{pv} = 0.0$ (giants), and stars with $M_{pv} = -4.0$ (supergiants), respectively. The curve for M = 0.0 is well determined; the normal points, indicated by crosses and independent from each other, are seen to fit the curve very well indeed.

The absolute-magnitude effect is very clearly shown, more so than in Pettit and Nicholson's original diagram. This result justified the rediscussion of the accurate radiometric observations with other im-

TABLE 8

Spec.	No.	Theoretical	Radiometric
dA2	11	−0.53	−0.42
dF2	4	.01	.04
dG0	5	−0.10	−0.06

TABLE 9

EMPIRICAL BOLOMETRIC CORRECTIONS FOR DIFFERENT M_{pv}

Sp.	Main Sequence	$M = 0.0$	$M = -4.0$	Sp.	Main Sequence	$M = 0.0$	$M = -4.0$
F2	−0.04	−0.04	−0.04	K4	−0.55	−1.11	−1.56
F5	.04	.08	0.12	K5	0.85	1.35	1.86:
F8	.05	.17	0.28	K6	1.14	.....	.....
G0	.06	.25	0.42	M0	1.43	1.55	2.2
G2	.07	.31	0.52	M1	1.70	1.72	2.6
G5	.10	.39	0.65:	M2	2.03	1.95	3.0:
G8	.10	.47	0.80:	M3	(2.35)	2.26	−3.6:
K0	.11	.54	0.93:	M4	(2.7)	2.72	.....
K2	.15	.72	1.20	M5	−(3.1:)	−3.4:	.....
K3	−0.31	−0.89	−1.35				

proved data. The absolute-magnitude effect is in agreement with that shown by colors; it disappears in the early F stars.

Table 9 gives the bolometric corrections for the three absolute magnitude groups, read from the curves of Figure 2. This table may be used for stars for which no radiometric data are available. For the M stars the increase in bolometric correction is so rapid, however, that a direct determination of the radiometric magnitude should be made for all stars where the bolometric magnitude is needed. This, of course, is also true for the K supergiants, particularly

when the absolute magnitude is uncertain. But for earlier types Table 9 should be useful if a good spectral type, as well as an approximate value of the absolute magnitude, is known. The uncertainty in the bolometric correction should then not exceed about 0.1 mag., which is good enough for most purposes.

No radiometric observations are available beyond dM2. The color index increases continuously for the later dwarfs to 2.0 mag. for

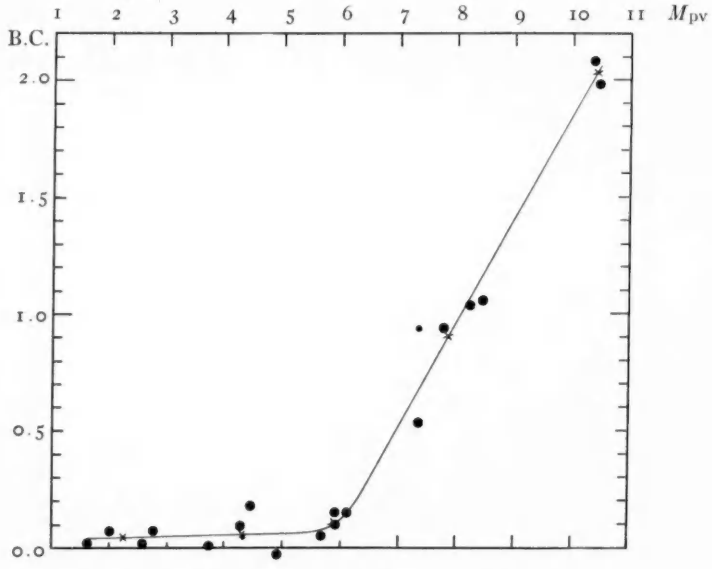

FIG. 3.—Empirical bolometric corrections for main-sequence stars

Wolf 359 (M8), and there can be no doubt that the bolometric correction will also increase. We shall extrapolate the bolometric correction values for types later than dM2; we shall see on page 487 that the values obtained are not inconsistent with observations of colors and spectra.

Because of the very small scatter on the lower part of the main sequence,[61] the bolometric correction may be plotted directly against M_{pv}. Figure 3 shows the result, which is also tabulated in Table 10. Unfortunately, the relation is not yet very strongly determined.

[61] Morgan, *Ap. J.*, **87**, 589, 1938; Kuiper, *ibid.*, p. 592.

Table 10 will be useful when the spectral type is uncertain. Unresolved binaries will, of course, affect Table 10 but not Table 9.

TEMPERATURES OF K AND M STARS

1. For low-temperature stars, the spectral energy-curve is far better determined by radiometric observations (heat indices and water-cell absorptions) than by color indices. The latter define only a small part of the short-wave slope of the spectral energy-curve, which, moreover, is crowded with absorption lines and bands.

Yet there are indications that temperatures derived from the observed spectral energy-curve (uncorrected for absorption lines) may

TABLE 10

EMPIRICAL BOLOMETRIC CORRECTIONS FOR MAIN SEQUENCE

M_{pv}	B.C.	M_{pv}	B.C.
3.0	−0.05	7.0	−0.51
4.0	.05	8.0	0.95
5.0	.06	9.0	1.40
6.0	−0.12	10.0	−1.85

be systematically too low, by perhaps 10 or 15 per cent (Pannekoek). We could determine this percentage empirically if for some late-type stars absolute temperature determinations were available.

This, fortunately, is the case. For the dwarfs the eclipsing binary Castor C may be used; for the giants, the measurements of angular diameter.

2. *Castor C.*—This important star was discovered by Adams and Joy[62] to be a spectroscopic binary, showing two spectra. Van Gent[63] found that the system is an eclipsing variable with two equal minima. The orbital elements were derived by Joy and Sanford,[64] and an improved light-curve was subsequently published by van Gent.[65] Van Gent also rediscussed the dimensions of the system. Later a few visual observations made in 1923 were published by Haas.[66]

Van Gent in his second paper used 1166 exposures made on twen-

[62] *Pub. A.S.P.*, **32**, 158, 1920.

[63] *B.A.N.*, **3**, 121, 1926.

[64] *Ap. J.*, **64**, 250, 1926.

[65] *B.A.N.*, **6**, 97, 1931.

[66] *A.N.*, **242**, 119, 1931.

ty-one nights. The probable error of one exposure is ± 0.046 mag., so that the light-curve has considerable weight. The two minima have equal depth, which agrees with the equality of the two spectral types as observed at Mount Wilson. In his photometric solution van Gent assumed two identical spherical stars.

The assumption of sphericity is very nearly correct. We may use Roche's model in computing the ellipticity of the components, for two reasons: (1) for stars of not too large a mass the concentration of matter toward the center will not be very different from Eddington's standard model ($\rho_c/\bar{\rho} = 54$); (2) the value of r/a is small (0.16). Taking the periods of rotation to be equal to the period of revolution, we find,[67] with $r/a = 0.16$, that the ratio between the two equatorial axes is 1.0063. Hence the coefficient of the ellipticity correction is 0.0068 mag. Only 0.23 of this value, or 0.0016 mag., enters in the part of the light-curve near the minimum that has actually been used.

The assumption of equality in size is not quite correct, since the Mount Wilson observers found the ratio of the intensities of the spectra to be about 5:4. The surface brightnesses being the same, the radii are about in the ratio $\sqrt{5} : \sqrt{4}$.

Van Gent obtained r/a and sin i from a least-squares solution in which the weights of the equations of condition were carefully determined. We shall examine whether his solution may be retained for the average component even if the two radii are slightly unequal. The results will have also a more general interest.[68]

For two circular disks of equal and uniform surface brightness, each with radius r, the fraction of light lost is

$$\frac{1}{\pi}\left(\arccos D - D\sqrt{1 - D^2}\right), \tag{12}$$

where D is the projected distance between the centers, expressed in terms of $2r$. D varies, therefore, between $D = 0$ (eclipse central) and $D = 1$ (first or last contact).

[67] Cf. p. 496 of the next paper.

[68] Since along the main sequence the radius varies very slowly with absolute magnitude, the case of nearly equal radii is of special importance. The conclusions reached here explicitly are in agreement with Russell's statements, *Ap. J.*, **35**, 330, 1912.

Suppose, now, that the radii are slightly different but with their sum unchanged: $r_1 = r(1+\epsilon)$ and $r_2 = r(1-\epsilon)$. Then the fraction of light lost, neglecting higher than second powers of ϵ, is

$$\frac{1}{\pi}\left(\arccos D - D\sqrt{1-D^2} - \epsilon^2 \frac{[1-D^2]^{3/2}}{D}\right). \qquad (13)$$

This expression is valid for all values of D except very small ones ($D^2 >> \epsilon^2$). Hence, (13) and (12) should be compared only for partial eclipses.

The first power of ϵ is lacking in (13), as might have been expected from the symmetry of the problem. That means that the solutions (12) and (13) differ only in ϵ^2, $\frac{(13)-(12)}{(12)} \sim \epsilon^2$. It is not at once evident from the equations that this also holds for D values close to unity (beginning and end of eclipse). Series development gives

$$\frac{(13)-(12)}{(12)} = -\tfrac{3}{2}\epsilon^2[1 + a(1-D) + \ldots.], \qquad (14)$$

in which $a = \frac{11}{128} - \frac{7\sqrt{2}}{384} = 0.06$.

For Castor C, r_1^2/r_2^2 is about 5/4; hence $\epsilon = 0.056$ and $\epsilon^2 = 0.003$. The small correction (14) is approximately equivalent to a small error in the grating constant used, amounting to 0.005 mag. per magnitude. This grating constant has a slight uncertainty. Van Gent adopts 0.923 mag. and Oosterhoff, more recently,[69] 0.95 mag. I have therefore examined what change is caused in the solution if the larger value of the grating constant is used. It appears that r/a is not seriously changed but that i increases by 0°.2 or 0°.3.

It is permissible, therefore, to use van Gent's solution for the mean component, except that the inclination should be increased by about 0°.2. This solution, made for uniform disks, is $r/a = 0.16005$; $i = 86°.5$.

The amount of darkening, and its dependence on wave length, has not yet been studied empirically; this would be particularly

[69] *B.A.N.*, **7**, 115, 1933.

promising in view of the fact that Pannekoek's theoretical work[70, 71] predicts a strong dependence on wave length. For the average component of Castor C, log $g = 4.61$ (c.g.s. units); from Pannekoek's Table 26*a*[71] we find

λ	7000	6000	5000	4000	3500	3000 A
C	2.75	1.97	1.05	0.33	0.13	0.035
u	0.73	0.66	0.51	0.25	0.115	0.034

Verification of this theoretical result will be most interesting. In the meantime we may adopt the theoretical value for 4200 A, $u = 0.3$. A fully darkened solution, kindly made by Dr. A. J. Wesselink, gave $r/a = 0.169$ and $i = 85°.2$. For $u = 0.3$ we may therefore adopt $r/a = 0.163$ and $i = 86°.0$.

The apparent magnitude of Castor C at maximum was measured by the writer on two nights and found to be 8.93 IPv. The probable error is estimated to be ± 0.05 mag. The parallax being $0''.073 \pm 3$, the absolute magnitude of the average component is $M_{pv} = 9.00$.

The spectral type, as determined by Dr. Morgan as well as by the writer, is K6+; the star does not show the *TiO* bands in the visual region (<Mo) but is later than 61 Cygni B (K6). According to Table 9, the bolometric correction is -1.28 mag. Table 10 gives for $M_{pv} = 9.00$, B.C. $= -1.40$ mag. We adopt -1.32; hence $M_{bol} = 7.68$. The probable error of this quantity is estimated at ± 0.14 mag. (of this, ± 0.05 is due to the apparent magnitude, ± 0.09 to the parallax, and ± 0.10 to the bolometric correction).

The luminosity of the average component is, therefore, 3.06 ± 0.14 mag. fainter than the sun, or log $L = -1.22 \pm 0.056$.

The value of $a \sin i$ found by Joy and Sanford[64] is 2,695,000 km. With $i = 86°.0$ and $r/a = 0.163$, we have log $R/\odot = -0.198$ ($R = 0.633\odot$). From equation (2), page 430, we now obtain

$$\log T_e/\odot = -0.306 \pm 0.014 + \tfrac{1}{2}(0.198) = -0.207 \pm 0.014 .$$

Or

$$\log T_e = 3.550 \pm 0.014, \text{ and } T_e = 3550 \pm 110° . \qquad (15)$$

[70] *M.N.*, **95**, 733, 1935.

[71] *Pub. Amsterdam*, No. 4, Tables 26 and 26*a* (Addendum), 1935.

3. Using Michelson's interferometer method, Pease has obtained angular diameters for several stars. A full account of the methods and results was published by Pease in 1931.[72] Measured diameters were given for 7 stars, obtained with the 20-foot interferometer on the 100-inch telescope. The result for the faintest star, α Herculis (3.5 mag.) was preliminary[73] and was omitted in a subsequent unpublished paper by Dr. Pease, which was kindly communicated to the writer. The star will also be omitted here. For α Orionis the mean of all 9 determinations listed by Sanford,[74] $0''.0411 \pm 0''.0016$ (p.e.), will be adopted (when mirror separations were given only, $\lambda = 5650$ A was used to find the diameters). The data for the 6 stars are

TABLE 11

Star	d''(Obs.)	IPv	m_{bol}	log T_e	Sp.
α Boo	$0''.020$	0.04	−0.80	3.61	gK2
α Tau	.020	1.02	−0.44	3.58	gK5
α Ori	.041	(0.96)	−1.59	3.54	cM1+
β Peg	.021	(2.62)	+0.37	3.49	gM3
o Cet (M)	.047	var.	−0.14±	3.38	gM6±
α Sco	0.040	1.30	−1.24	3.51	cMo

found in Table 11; for α Orionis the diameter should be better known than for any of the other stars.

A particularly important feature of the 20-foot interferometer is the auxiliary apparatus for measuring the influence of seeing on the visibility of the fringes; it is probable, therefore, that the diameters obtained with it have no serious systematic errors.

The computation of effective temperatures from diameters, nearly free from assumptions about the spectral energy-curve, is made by using the radiometric observations of Pettit and Nicholson. These authors have already indicated the method;[75] for our purpose we write the formula in the form

$$\log T_e = 2.703 - \tfrac{1}{2} \log d'' - \tfrac{1}{10} m_{bol} . \qquad (16)$$

[72] *Erg. d. exakt. Naturwiss.*, **10**, 84–96, 1931.

[73] *Ann. Rept., Mt. W. Obs.*, 1925.

[74] *Contr. Mt. W. Obs.*, **20**, 270; *Ap. J.*, **77**, 117, 1933.

[75] *Contr. Mt. W. Obs.*, **16**, 480; *Ap. J.*, **68**, 300, formula (4), 1928.

The constant 2.703 follows at once by inserting the values for the sun.

The quantities d'' (obs.) of Table 11 have been derived from the interferometer measures by assuming uniform disks for the stars. In the original paper by Michelson and Pease[76] the influence of darkening toward the limb was examined and the results were tabulated. But a recent paper by Dünnweber[77] considers darkening in the customary analytical form; the effect is tabulated against the ordinary darkening coefficient. We shall, therefore, use Dünnweber's results.

The order of magnitude of the correction factor to d'' is found as follows: for the stars in Table 11, $\log g = 2$ approximately (c.g.s. units). For this value of g, $T_e = 3350°$ ($5040/T_e = 1.5$), and $\lambda = 5650$ A, Pannekoek's Table 26*a*[71] gives $C = 1.1$ ($u = 0.53$). With this value of C (or β in Dünnweber's notation) the factor with which the diameters should be multiplied is 1.07. After preliminary temperatures were found by using this factor, a second approximation was obtained for each star separately; the factor is 1.09 for α Boo; 1.08 for α Tau; 1.07 for α Ori, α Sco, and β Peg., and 1.025 for o Ceti (Max.).

The theoretical question whether the darkening toward the limb could be quite different from that computed by Pannekoek, on account of the possible presence of very large atmospheres (VV Cephei, ζ Aurigae) has not been examined. If the effect would correspond to a diminished effective surface gravity, Pannekoek's tables show that then only a small decrease in darkening would result.

The data on magnitudes and spectra are taken from Table 7. The effective temperatures computed by (16), after correcting d'' as indicated above, are given in the fifth column. The probable error of the result for α Orionis, which corresponds to the internal probable error of d'' (obs.) found above, is ± 0.008 in $\log T_e$ ($T_e = 3470° \pm 70°$).

The six temperature values of Table 11 are shown graphically in Figure 4. A discussion of the results is given in the next section.

[76] *Contr. Mt. W. Obs.*, **10**, 86 ff.; *Ap. J.*, **53**, 254, 1921.

[77] *Zs. f. Ap.*, **13**, 104, 1936.

COLOR TEMPERATURES; THE STELLAR TEMPERATURE SCALE

No attempt will be made here to discuss all the many papers in which original measures of color or gradient are given or in which such measures are rediscussed. Our present interest is limited to finding a set of color temperatures that may be calibrated to effective temperatures by means of the results of the preceding sections. The

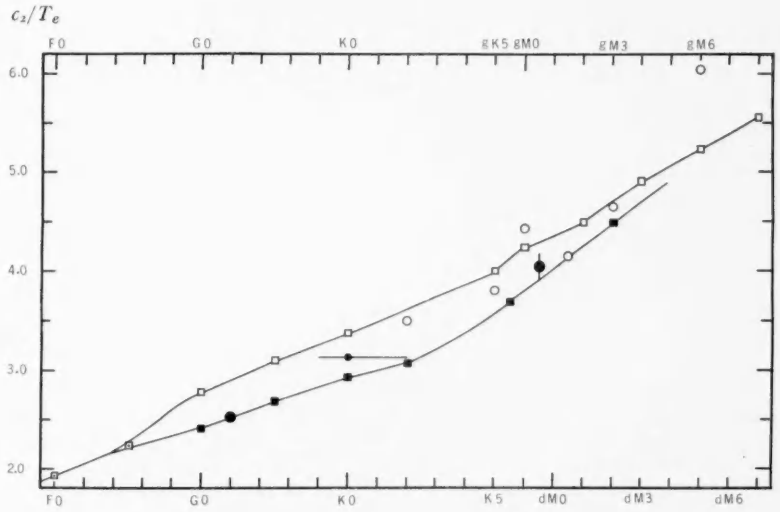

FIG. 4.—The stellar temperature scale for types F–M. Black dots: dwarfs; open dots: giants. Circles are absolute determinations; squares are based on reduced color data.

necessity of such a calibration has perhaps not always been apparent, in view of the fact that, for instance, the temperature scale given in Russell, Dugan, and Stewart's textbook *Astronomy*, which is based on colors, shows values consistent with other information. But it should not be overlooked that the zero point of that scale was adjusted to the effective temperature, not to the color temperature of the sun. If the color temperature (6700°±) is used, and if the color index adopted for the sun (0.57 mag.) is left unchanged, the color temperature of A0 stars is raised from 11,200° to 14,500° (the gradient $\phi_0 = 1.14$). This value is in good agreement with the four re-

cent determinations for Ao stars made in the same general region of the spectrum; three of these are spectrophotometric:

Greenwich 1932*.....	$\phi_0 = 1.07 \pm 0.05$ (p.e)
Greenwich 1933†.....	0.91 ± 0.05
Kienle‡.....	1.15 ± 0.05
Mean.....	$\phi_0 = 1.04$, or $T_c = 17{,}000°$

* *M.N.*, **94**, 488, 1934.
† *Ibid.*, p. 505. ‡ *Erg. d. Exakt. Naturwiss.* **16**, 446, 1937.

The fourth is the photoelectric determination by W. Becker.[78] His value is 16,400°. The spectrophotometric values may be expected to be somewhat higher than those based on colors, since the absorption lines, which crowd toward the violet, are avoided in the spectrophotometry.

That the high color temperatures for Ao stars are, in fact, to be expected theoretically was shown by Unsöld[79] and, more explicitly, by Pannekoek.[80]

For the classes earlier than M1 we shall base our further discussion on two sources of color temperatures: (1) W. Becker's recent derivation,[78] which is of considerable weight for two reasons: (*a*) the photoelectric colors are accurate and homogeneous, and (*b*) a large number of stars (738) is included; (2) Brill's temperature scale,[81] which is based on most of the important series of determinations of color temperature published previous to 1932.

The two scales of color temperature, expressed as c_2/T, are given in the second and third columns of Table 13. The spectral types in the first column are on the same system as those in Table 7: the giants are on the Mount Wilson scale, and also the dwarfs of type earlier than K2. For the later dwarfs the scale adopted by Dr. Morgan and the writer[61] is used because of its applicability to very faint stars.[82] In this system the M stars (giants and dwarfs) are

[78] *Veröff. Berlin-Babelsberg*, **10**, Heft 6, p. 8 (Table 5), 1935.

[79] *Zs. f. Ap.*, **8**, 246, Fig. 4, 1934.

[80] *M.N.*, **95**, 532, 1935.

[81] *Handb. d. Ap.*, **5**, 193 and 199, 1932.

[82] An M star of photographic magnitude 15.0 can be obtained in less than one hour with the spectrograph used by the writer on the 40-inch telescope.

classified by the strength of the *TiO* bands in the red and orange.[83] Whereas the classes thus obtained for the giants appear to be in excellent systematic agreement with the Mount Wilson classes, the dwarfs differ systematically by −0.1 class at Mo. At M4 there is agreement again.

The spectral types used by Becker and Brill seem, on the average, to be nearly on the Mount Wilson system. We may therefore, according to the preceding paragraph, adopt their temperatures as

TABLE 12

BECKER'S COLOR INDICES FOR G AND K DWARFS

Star	Spec.	C_{pe}	Star	Spec.	C_{pe}
η Cas	Go	0.105	61 UMa	G4	0.217
μ Cas	G6	.183	8 CVn	Go	.115
HR 483	G1	.143	43 Com	F9	.114
107 Psc	Ko	.304	59 Vir	Go+	(.158)
HR 511	Ko	.300	ξ Boo	G8+	.226
δ Tri	G1	.124	η CrB	Go	.120
HR 753	K3	.381	λ Ser	G1	.156
ι Per	Go	.130	26 Dra	G1	.105
κ Cet	G5	.197	70 Oph	K1+	.325
39 Tau	G2	.124	HR 7162	Go	.081
λ Aur	Go	.157	σ Dra	G8+	.254
χ^1 Ori	Go	.115	61 Cyg	K5(+)	.541
ψ^5 Aur	Go	.074	51 Peg	G4	(.179)
11 LMi	G8+	.276	HR 8832	K3	.402
15 LMi	Go+	.112	85 Peg	G2	0.160
47 UMa	G2	0.162			

they stand, except for dwarfs later than Ko. Since Becker gives the color indices for the individual stars, we shall make a new reduction for the G and K dwarfs, using spectral types in the system adopted here. The data are collected in Table 12; as we shall see later, they are of great importance in a comparison to be made with the sun. For binaries observed as one star (70 Oph., 61 Cyg. etc.) the weighted mean spectral type of the components is given. The writer is again indebted to Dr. Morgan for the spectral types used here. Particular care was taken to omit all subgiants from Table 12, since the colors of these objects are decidedly redder than those of ordinary dwarf stars.

[83] Theoretically, these bands have the advantage over those in the blue because they are more fundamental.

A plot was made of the data in Table 12, and normal points were read off at Go, G2, etc. The plot shows the small scatter to which Morgan has drawn attention.[84] For this reason the averages should be of value in spite of the limited material on which they are based.

From the mean color indices, temperatures in Becker's system were found by means of Table 4 in Becker's paper. The results are

TABLE 13

THE STELLAR TEMPERATURE SCALE (LAST COLUMN)*

Sp.	c_2/T_c (Becker)	c_2/T_c (Brill)	Becker Corr.	Brill Corr.	Aver.	W.C.	c_2/T_e (Prov.)	c_2/T_e (Adop.)	T_e
Ao	0.88	1.06	1.44	1.22	1.33	.....	1.33	1.34	10,700
A5	1.27	1.37	1.83	1.53	1.68	.....	1.68	1.68	8,530
Fo	1.43	1.68	1.99	1.84	1.92	.....	1.92	1.92	7,500
F5	1.67	2.05	2.23	2.21	2.22	.....	2.22	2.22	6,470
dGo	1.84	2.23	2.40	2.39	2.40	.....	2.40	2.40	6,000
dG2	1.95	(2.35)	2.51	2.51	2.51	.....	2.51	2.51	5,710
dG5	2.10	2.53	2.66	2.69	2.68	.....	2.68	2.68	5,360
dKo	2.42	2.64	2.98	2.80	2.92	.....	2.92	2.92	4,910
dK2	2.60	.....	3.16	.....	3.16	3.34	3.10	3.08	4,650
dK5+	3.28	.....	3.84	.....	3.84	4.28	3.92	3.69	3,900
dM2	.....	.....	.....	.....	.....	5.16	4.87	4.49	3,200
gGo	2.31	2.48	2.87	2.64	2.76	.....	2.76	2.76	5,200
gG5	2.52	2.95	3.08	3.11	3.10	3.46	3.14	3.10	4,620
gKo	2.99	3.28	3.55	3.44	3.50	3.83	3.52	3.39	4,230
gK5	3.83	4.15	4.39	4.31	4.35	4.58	4.32	4.00	3,580
gMo	4.04	4.43	4.60	4.59	4.60	4.81	4.56	4.22	3,400
gM2	.....	.....	.....	.....	.....	5.16	4.87	4.49	3,200
gM4	.....	.....	.....	.....	.....	5.63	5.34	4.90	2,930
gM6	.....	.....	.....	.....	.....	6.00	5.71	5.22	2,750
gM8e	.....	.....	.....	.....	.....	6.38	6.09	5.54	2,590

* Interpolations should preferably be made between the recipocal temperatures ($c_2 = 14{,}320$) of the preceding column. The spectral types are on the Mount Wilson system, except for the K and M dwarfs (cf. pp. 462–463).

entered in the second column of Table 13 of this paper (dGo–dK5+).

The data in the third column are based on Brill's investigation. Brill derived first the temperature scale for the giants and then averaged the differences (giants-dwarfs), expressed in reciprocal temperature, taken from 5 determinations.[81] Fearing a systematic error with respect to the other determinations, we have omitted the second

[84] *Ap. J.*, **87**, 460, 1938.

source quoted by Brill and have recomputed the differences between giants and dwarfs.

The transformation of color temperatures to effective temperatures may, to a first approximation, be made by adding a constant to all reciprocal temperatures, as is suggested by our remarks on the temperature formula in Russell, Dugan, and Stewart's *Astronomy*. It remains to be seen whether this simple reduction, which involves only one constant for the whole temperature scale, is sufficient or whether additional corrections are required.

We reduce the two temperature scales to the sun by adding 0.56 and 0.16, respectively, to the reciprocal temperatures; this leads to $c_2/T = 2.51$ (or $T = 5713$) for dG2.[85] The corrected scales are given in the fourth and fifth columns, respectively. Except for the A stars, where the interagreement is only fair, the two corrected scales agree quite well. (The accuracy is most readily judged by remembering that the scale of reciprocal temperatures is almost exactly double that of ordinary color indices.) The average scale is given in the sixth column.

Before discussing possible further corrections to the temperatures in the sixth column, it is preferable to consider the data for spectral class M, which is not properly covered by the color data. (Becker found even a decrease in color index for the later M giants, undoubtedly due to the increasing strength of the *TiO* absorption in the visual region.) The *TiO* absorption also vitiates temperature determinations from heat indices for the later M stars, as was pointed out by Pettit and Nicholson.[86] Least of all affected are the water-cell absorptions obtained by Pettit and Nicholson, which are particularly significant since they analyze the spectral energy-curves of the late-type stars near the maximum. For temperatures much higher than 4000°, however, the water-cell absorptions lose their value, as is shown by Table IV of Pettit and Nicholson's paper.

Accordingly, the color temperatures derived from water-cell absorptions, not exceeding 4300°, are added in Table 13, seventh column. The data for the giants are simply taken from Pettit and Nicholson's Table V, whereas the dwarfs (K–M) are again listed separately (Table 14). The weighted mean spectral class for 70 Ophiuchi is

[85] Cf. pp. 431 and 438.

[86] *Ap. J.*, **68**, 295, 1928.

slightly later for radiometric than for photoelectric observations, of course. The number of observations made by Pettit and Nicholson is given in the last column.

Three groups are indicated, with mean spectral types dK2, dK5+, and dM2. In the first group equal weight will be given to all three stars; in the second group the components of 61 Cygni should obviously have more weight than the other stars, not only because they have been more frequently observed but also because they are brighter. We shall give them three times the weight of the other stars of

TABLE 14

Star	Spec.	W.C.	n
o_2 Eri A	dK2	$0^{M}50$	6
ϵ Eri	K2	0.58	5
70 Oph AB	K2	0.63	5
61 Cyg A	K5	0.70	7
61 Cyg B	K6	0.82	7
Ci 1218	K6	1.06	2
B 4342	K4+	1.03	2
B 2935	M2	1.04	2

that group. The last star is as faint as 5.4 mag. radiometrically, and the water-cell absorption is probably only approximate. We shall follow Pettit and Nicholson, who adopt W.C. = 1.14 for dM2,[87] probably on the basis that the heat indices for dM2 and gM2 are equal and that W.C. = 1.14 for gM2.

With the three average water-cell absorptions, color temperatures in Pettit and Nicholson's system are found from their Table IV (or V); the results have been entered in Table 13.

The six lines in common between columns 6 and 7 of Table 13 indicate a systematic correction of −0.29 to column 7 if it is to be reduced to column 6. With this correction applied, column 8 is obtained; equal weights are given to columns 6 and 7.

The temperature scale of the eighth column has, therefore, the following properties: (1) it embodies most of the essential data on color temperatures existing; (2) it is homogeneous with respect to

[87] *Op. cit.*, Table 5.

the zero point of the color equivalent (this has been obtained by adding a constant to the three basic systems); and (3) the constants make the temperature for dG2 equal to the effective temperature of the sun.

We shall now examine whether this provisional system needs further corrections. The test is obviously twofold: (1) the representation of the A stars; (2) the representation of the K and M stars for which effective temperatures were derived.

TABLE 15

Star	Spec.	M_{pv}	c_2/T (Prov.)	c_2/T_e (Obs.)	Obs.−Prov.
α Gem C	dK6+	+9.0	4.19	4.04	−0.15
α Boo	gK2	−0.3	3.84	3.50	−0.34
α Tau	gK5	0.7	4.32	3.79	− .53
α Sco	cMo	3.9	4.56	4.43	− .13
α Ori	cM1+	4+	4.79	4.14	− .65
β Peg	gM3	1.0	5.10	4.65	− .45
o Cet (M)	gM6±	−2:	5.71±	6.06	+0.35±

It appears that the A stars are very well represented. The provisional temperatures are plotted in Figure 1 as crosses; no essential improvement can be made.

The comparison with the late-type stars with known diameters is given in Table 15. The fourth column contains the "provisional" reciprocal temperatures from Table 13, and the fifth the reciprocal effective temperatures found on page 458 and in Table 11. The probable error of the observed reciprocal temperature of Castor C is ±0.13.

Table 15 shows that for the lower temperatures our provisional scale needs correction. The correction given by Castor C is −0.15± 0.13 (p.e.) at $c_2/T = 4.2$; the correction given by the other stars is −0.40±0.08 (p.e.) at $c_2/T = 4.66$. In forming this average, double weight was given to α Orionis and half-weight to o Ceti (max.), for which the data are, of course, somewhat indefinite. The weight for α Orionis would have been increased but for the possible variability of the quantities involved. The probable error ±0.08 follows from the internal agreement of the six objects, with the weights assigned

as indicated. If *o* Ceti is omitted from the average, we obtain the correction -0.46 ± 0.06 (p.e.) at $c_2/T = 4.57$. The absolute amount of correction derived from the giants may be somewhat too small, because two supergiants are present for which the temperatures may be expected to be somewhat lower than for ordinary giants of the same spectral type.

We shall adopt the correction -0.30 for $c_2/T = 4.2$, and -0.40 for $c_2/T = 5.0$. These corrections leave a residual of $+0.15\pm0.13$ for Castor C, and -0.04 ± 0.08 or -0.11 ± 0.06 for the giants, depending on which average is used. Since a correction of -0.29 had already been applied to the system of reciprocal color temperatures derived from water-cell absorptions, we find that the total correction, both for $c_2/T = 4.2$ and 5.0 (T in the provisional scale), amounts to 15 per cent of the original temperature. This solves the problem given on page 455: the color temperatures derived from water-cell absorptions have to be increased by about 15 per cent in order to represent effective temperatures. This result confirms Pannekoek's theoretical conclusions for low-temperature stars.[88]

The data available are, of course, insufficient for showing whether this percentage, 15, is constant for the late K and M stars. It is reasonable to assume that this is the case to a first approximation. For the provisional reciprocal temperatures of Table 13 smaller than 4.2, we shall adopt smaller corrections and make them vanish at $c_2/T = 3.0$. For the spectral types later than Mo, for which the temperatures depend on water-cell absorptions only, we shall adopt the original color temperatures published by Pettit and Nicholson, increased by 15 per cent. This discussion completes the formation of the last two columns of Table 13.

The temperature scale of Table 13 is shown graphically in Figure 4. The lines representing the giants and the dwarfs show a striking similarity to the corresponding lines in Figure 2; this is gratifying since the observational data used in the two diagrams are, with one exception (dM2), independent. Even details such as the bend in the dwarf curve at K2 and in the giant curve at Mo are common to the two figures.

One point of importance has not been fully analyzed: the mean

[88] *Ap. J.*, **84**, 490 ff., 1936.

absolute magnitude of the giants for which Table 13 gives the temperature scale. Becker states that in the formation of the averages for giants the c stars and red supergiants were excluded. The evaluation of the precise mean absolute magnitude would require an analysis similar to that given for the bolometric corrections (Table 7). But the advantage would not be great; it seems far better to use the original color measures catalogued by Becker for spectral types A–K (provided space reddening may be neglected) and the original measures of water-cell absorption by Pettit and Nicholson for temperatures lower than 4000°. From these measures, effective temperatures in the system of Table 13 may be derived. This automatically takes account of the absolute-magnitude effect (which is large, and difficult to evaluate accurately) and avoids uncertainties of spectral type and absolute magnitude.

The process of obtaining effective temperatures as outlined in the preceding paragraph follows immediately from the way in which Table 13 was constructed.

1. If the spectral type is between Ao and Mo, and the star is contained in Becker's *Catalogue*,[89] take the value of the column headed "F.I." With this value enter a table by Becker[90] for conversion into color temperature (the value then obtained is equivalent to the second column in Table 13). Add 0.56 to c_2/T (fourth or eighth column of Table 13); if the result is smaller than 3.0, the reciprocal effective temperature has already been found. If the result is larger than 3.0, subtract a correction that is 0.00 at $c_2/T = 3.0$, 0.30 at 4.2, and 0.40 at $c_2/T = 5.0$. The final value is the reciprocal effective temperature.

2. If the star has been measured radiometrically by Pettit and Nicholson,[91] and is of type later than gG5 or dK2, take the water-cell absorption from the ninth column,[91] obtain the color temperature from Table IV (or V),[92] and increase this value by 15 per cent if the color temperature is less than 3200°; increase it by 480° between 3200° and 3600°; add 450° at 4000°, and 420° at 4400°.

[89] *Veröff. Berlin Babelsberg*, **10**, Heft 3, pp. 25–41, 1933.

[90] *Ibid.*, Heft 6, p. 8, Table 4, 1935.

[91] *Ap. J.*, **68**, Table III (pp. 286–291), 1928; *Contr. Mt. W.*, No. 369.

[92] *Op. cit.*

We shall give two applications of the procedure just described. One relates to the giants of Table 15; the temperatures computed directly from the color data are found in Table 16. The differences between these temperatures and those computed from the measured diameters are more irregular than those shown in Table 15, but the values in Table 16 should be preferred, since the absolute-magnitude effect is now taken into account and uncertainties in spectral class are eliminated. If weights are assigned as before (α Orionis double weight, *o* Ceti half-weight), the average of the last column is -0.16 ± 0.13 (p.e.). The absolute amount of this deviation is now approximately identical to that for Castor C, $+0.15 \pm 0.13$ (p.e.).

TABLE 16

Star	c_2/T_e (Becker)	c_2/T_e (W.C.)	Av.	c_2/T_e (Diam.)	Diam.−Av.
α Boo	3.62	3.67	3.64	3.50	−0.14
α Tau	4.24	4.06	4.15	3.79	−0.36
α Sco	.....	4.67	4.67	4.43	−0.24
α Ori	.....	4.62	4.62	4.14	−0.48
β Peg	.....	4.59	4.59	4.65	+0.06
o Cet	.....	4.90±	4.90±	6.06	+1.16±

The second application is the derivation of the effective temperature of ε Aurigae. From Becker's color index we find $T_e = 6870°$. This figure is somewhat higher than the value 6300° adopted in the discussion of this system,[93] which was made before the present paper was completed. The temperature difference corresponds to 0.37 mag. bolometric if the dimensions of the star are left unchanged. Hence, if the F2 star lies 0.37 mag. above the average empirical mass-luminosity relation (which is not very much less probable than that the deviation is 0.0 mag.), our dimensions and masses may be retained, but the computed luminosities of both components must be increased by 0.37 mag. or by 0.15 in log L. The higher temperature now found diminishes by a considerable factor the discrepancy found by Strömgren[94] for the ultraviolet intensity. The factor is

[93] *Ap. J.*, **86**, 572 and 612, 1937; also **87**, 213, 1938.

[94] *Ibid.*, **86**, 604, 1937.

6.6 at 1000 A and 48 at 500 A. If the star is slightly reddened because of its distance (about 1000 parsecs), the factor will be larger.

In conclusion, some desiderata may be mentioned in connection with the results of this paper:

1. An accurate photometric study of Castor C and β Aurigae in two or three very different wave lengths.

2. The discovery and study (photometric and spectrographic) of eclipsing binaries showing two spectra, in galactic clusters.

3. Further determinations of trigonometric parallax for the stars in Table 1.

4. Radiometric observations of Barnard's star (dM6) for settling the question of the temperature scale and of the bolometric corrections for the late M dwarfs.

YERKES OBSERVATORY
June 1938

THE EMPIRICAL MASS-LUMINOSITY RELATION

G. P. KUIPER

ABSTRACT

After a brief historical introduction the problem is subdivided into two main parts. The first, on the temperature scale and bolometric corrections, is treated in the preceding article. The second problem, the derivation of the empirical mass-luminosity relation, is treated in three sections in this article: (1) the visual binaries, (2) some selected spectroscopic binaries, and (3) Trumpler's massive stars in clusters. An attempt has been made to obtain the most accurate observational data for all quantities entering into the discussion, including magnitudes and spectral types.

Tables 1 and 7 give the visual binaries used at present. Table 5 shows the derived quantities for the stars of Table 1, and Table 6 shows the quantities of theoretical interest for the stars of Table 5 for which the accuracy is sufficiently great. Visual binaries in the same class as those of Table 1, but for which the data are still incomplete, are collected in Table 8.

The problem of the spectroscopic binaries is only partly treated in this paper. Only some representative objects are discussed; they are found in Table 12. Theoretical values of the ellipticity and reflection constants are used in the discussion of the observations. Trumpler's massive stars are discussed in Table 13.

In all three sections the results of the preceding article have been used. The data are shown graphically in Figures 1 and 2.

INTRODUCTION

The discovery of the mass-luminosity relation has been of great importance to the progress of astronomy. The relation has been used in statistical astronomy and in double-star astronomy and has been a central problem of theoretical astrophysics. Since for most stars no direct determination of the mass can be made, the use of the mass-luminosity relation is the only method of estimating the total mass of the known stars per volume of space—an important dynamical quantity.[1] In binary-star statistics the observable Δm and a rough knowledge of the absolute magnitude can now be used in obtaining a statistically useful determination of the mass ratio, which is of great cosmogenetic interest.[2] Investigations, such as a recent one on ϵ Aurigae[3] show the need of having the relation well established. But particularly the theoretical importance, both in ab-

[1] E.g., Oort, *B.A.N.*, **6**, 285, Table 34, 1932.

[2] *Pub. A.S.P.*, **47**, 17 ff., 143 ff., 1935.

[3] *Ap. J.*, **86**, 574, 1937.

stract form and in numerical form for particular stars, is clear from Eddington's work and from more recent developments.[4, 5]

1. *Historical.*—The idea that the mass and the luminosity are correlated seems to have developed gradually as the knowledge of parallaxes increased. Even today the knowledge of masses is to a large extent limited by the knowledge of accurate parallaxes. The fact that one of the best-known stars, Sirius B, does not follow the general mass-luminosity relation must have delayed the discovery of that relation.

Halm was probably the first to state explicitly the existence of a statistical relation between intrinsic brightness and mass.[6] His conclusion was essentially based on the correlation of mass with spectral type and of spectral type with luminosity. The first relation was established mainly from double-line spectroscopic binaries. The result was therefore partly accidental, because double-line spectroscopic binaries are very rare among giants, so that Halm was essentially dealing with main-sequence stars only. In fact, the relation was not recognized in Russell's paper of 1913,[7] although in 1914 Russell found evidence[8] for a definite correlation, which was obtained by comparing absolute magnitudes derived from hypothetical parallaxes with absolute magnitudes derived by methods of stellar statistics.

Hertzsprung, in 1918, gave the relation[9]

$$\log m = -0.06(M_v - 5),$$

in fair agreement with modern data. He also gave the corresponding formula for the mass ratio of a binary derived from Δm, and the first formula for dynamical (not hypothetical) parallaxes. Van Maanen shortly afterward emphasized that the mass-luminosity relation is independent of spectral type.[10]

[4] B. Strömgren, *Erg. d. exact. Naturwiss.*, **16**, 497, 513, 1937.

[5] S. Chandrasekhar, *Introduction to the Study of Stellar Structures*, "Astrophysical Monograph," chaps. vii and viii, 1938. (In press.)

[6] *M.N.*, **71**, 638, 1911. [7] *Observatory*, **36**, 327, 1913. [8] *Pop. Astr.*, **23**, 340, 1914.

[9] *A.N.*, **208**, 96, 1919. Already in 1915 Hertzsprung had given the same relation in a less explicit form (*Ap. J.*, **42**, 115, n. 2).

[10] *Pub. A.S.P.*, **31**, 231, 1919.

Many other investigations followed, most of which have been reviewed by Lundmark.[11] Of all these, Eddington's results are undoubtedly the best known, particularly because Eddington used the relation in connection with his well-known theoretical investigations.

The most recent study of the subject is that by P. P. Parenago,[12] which was received after most of the present investigation was completed. In some ways the two investigations run parallel: for instance, in the use of bolometric corrections derived from radiometric observations and the estimation of weights of the individual mass determinations. But the present study uses several improved orbits, mass ratios, and Δm values and does not use spectroscopic parallaxes. Minor discrepancies will be found by comparing Parenago's Table 2 with our Tables 1 and 5. The treatment of the spectroscopic binaries is entirely different in the two papers: Parenago uses spectroscopic absolute magnitudes whereas we use the stellar temperature scale. A number of objects are used here which are not considered by Parenago; among these are Trumpler's stars.

2. *The present investigation* is limited to those individual stars for which the three fundamental quantities—the mass $\boldsymbol{m}$, the radius R, and the luminosity L—may be obtained from the observations with fair precision. The derivation of the radius, in addition to the other two quantities, does not require any extra information, since radius and luminosity are simply related by the effective temperature, which is needed in any case before the eclipsing binaries can be used. In view of the fact that all three parameters are required in theoretical work, we shall give them explicitly as the final result of the investigation.

Since all the emphasis is laid on accurate data for individual stars (as required in theoretical work), no attempt is made here to supplement the results by a statistical treatment of other data of smaller individual accuracy. Such a statistical treatment would be useful for determining the trend of the mass-luminosity relation for the giants and the O stars, where few data of high individual accuracy are available.

A close co-operation between theory and observation will certainly

[11] *Handbuch der Astrophysik*, **5**, Part II, 1933.

[12] *A.J. Sov. Union*, **14**, 33, 1937.

be the quickest and least wasteful method of solving the fundamental problems of stellar structure and evolution.[5] In this connection it would seem that the visual binaries of Tables 1, 7, and 8 deserve preference in double-star observations and in determinations of parallax and mass ratio. At least four to six determinations for each object will be needed in order to make the mass determinations sufficiently accurate. Photometric and spectroscopic measures of double-line spectroscopic binaries that are also eclipsing variables are obviously the second group of observations especially needed. Finally, investigations on the stellar temperature scale are required for the computation of luminosities from radii and vice versa.

Many important direct or indirect contributions to the knowledge of stellar masses have recently become available: Schlesinger's *Catalogue of Parallaxes;* Boss's *General Catalogue of 33342 Stars*, containing many mass ratios for visual binaries, based on all the available meridian positions; many new orbits, of which we want to mention especially those derived with the help of photographic measures (Strand, van den Bos, Hertzsprung); and several new mass ratios by van de Kamp. For the discussion of the eclipsing binaries, of special importance is Pannekoek's rediscussion of the temperatures of O and B stars, derived from maxima of spectral series. Data for very interesting systems, such as ζ Aurigae and VV Cephei, have recently been published. Last, but not least, Trumpler's discovery of very massive stars in galactic clusters should be mentioned. These many advances make it promising to assemble and discuss the data now available.

We have already referred to the stellar temperature scale as an integral part of the subject under discussion, being needed in the conversion of radii into luminosities and vice versa, according to the formula

$$\frac{L}{L_\odot} = \left(\frac{R}{R_\odot}\right)^2 \cdot \left(\frac{T_e}{T_{e\odot}}\right)^4. \qquad (1)$$

Before this formula can be used, the relation between M_{vis} and L has to be known. This relation is given by the bolometric correction.

Hence, the subject falls into two parts: (1) the discussion of the stellar T_e scale and the derivation of the bolometric corrections; and

(2) the discussion of the binary systems, with suitable observational data, and of Trumpler's stars. The first problem is treated in the preceding article; the second naturally falls into three parts: the visual binaries, the eclipsing binaries, and Trumpler's massive stars.

THE VISUAL BINARIES

If the orbital elements and the parallax of a visual binary are known, Kepler's third law

$$3 \log a'' - 2 \log P - 3 \log \pi'' = \log \Sigma m \qquad (2)$$

will give the total mass, Σm, of the system. If the orbit is well determined, and hence the error in $(3 \log a'' - 2 \log P)$ is small, the error in Σm will depend mainly on the error in the parallax; we then have $3\Delta(\log \pi'') = -\Delta(\log \Sigma m)$. If the probable error of the parallax equals one-tenth of the parallax itself, the probable error in $\log \Sigma m$ will be ± 0.13. This value corresponds to about ± 1.4 absolute magnitude in the region of the mass-luminosity relation covered by the visual binaries of our list. The computed absolute magnitude is also affected by an error in the parallax, and a certain compensation of errors occurs when the data are used in a diagram correlating mass and luminosity; the value ± 1.4 mag. is then reduced to ± 1.2 mag. As true deviations from the mean mass-luminosity curve larger than 2 mag. are very rare indeed, it is obvious that data with probable errors larger than ± 1.2 mag. are of no individual value. Hence, all systems for which the probable error of the parallax exceeds 10 per cent are excluded from our discussion.[13]

The remaining binaries are collected in Table 1. It would be of great importance for the knowledge of stellar masses if parallax observers would pay special attention to these objects, particularly to those for which the probable error of the parallax still exceeds $\pm 0''.004$. Of not much less importance are the stars in Table 8, which may be used in the near future.

The first three columns of Table 1 need no explanation. The fourth column gives, on the international photovisual system, the

[13] We have, furthermore, excluded stars with parallaxes smaller than $0''.045$. No attempt is made here to use averages for binaries of different spectral types—a problem considered recently by Professor Russell.

apparent magnitude of the combined light of the binary. Most of these data are based on Zinner's catalogue (which is on the Potsdam

TABLE 1

VISUAL BINARIES FOR THE MASS-LUMINOSITY RELATION

Name	α 1900	δ 1900	m_{AB}	Spec.	Δm	P	a''	Ref., Q	π'' (Trig.)
HR 159	0^h32^m2	$-25°19'$	5.61	G7	0.3	25.00	0".670	2, A	0".072±6
η Cas	0 43.0	+57 17	3.57	Go, K5+	3.74	526.0	12.534	3, B	.182±5
p Eri	1 36.0	−56 42	5.21	G5	0.06	251	8.31	4, C	.161±7
o_2 Eri BC	4 10.7	− 7 49	9.37	B9, M5e	1.48	247.9	6.894	1, AB	.202±3
α Aur	5 09.3	+45 54	0.19	G4, F4	0.15	104.02d	0.0536	1, A	.0632
α CMa	6 40.7	−16 35	−1.52	A0, A5	10.06	49.94	7.62	1, A	.376±2.6
α Gem	7 28.2	+32 06	1.59	A0, A1	0.86	340	5.84	1, B	.073±3
α CMi	7 34.1	+ 5 29	0.45	F3, ...	10.3	40.23	4.26	1, A	.291±4
9 Pup	7 47.1	−13 38	5.27	G2	0.7	23.34	0.69	1, A	.061±4
ξ UMa	11 12.9	+32 06	3.77	F9, F9	0.43	59.86	2.5355	1, A	.138±6
γ Vir	12 36.6	− 0 54	2.98	F0, F0	0.03	171.37	3.746	3, A	.089±7
ζ UMa A	13 19.9	+55 27	2.43	A2, A2	0.0±	20.54d	0.0115	1, A	.045
α Cen	14 32.8	−60 25	−0.20	G4, K1	1.37	80.09	17.593	5, A	.756±7
ξ Boo	14 46.8	+19 31	4.51	G8, K5	1.96	149.95	4.884	3, A	.147±6
44 Boo	15 00.5	+48 03	4.79	G1, G5	(0.82)	219.5	3.609	3, B	.079±5
ADS 10075	16 24.5	+18 37	6.82	K2	0.01	217.1	2.198	1, AB	.059±6
ζ Her	16 37.5	+31 47	2.93	G1, ...	2.80	34.42	1.349	1, A	.110±5
$-8°4352$	16 50.1	− 8 09	9.20	M4	0.1	1.72	0.19	6, AB	.148±4
HR 6416	17 11.5	−46 32	5.54	Ko, ...	2.6	242	4.94	7, BC	.132±6
HR 6426	17 12.2	−34 53	5.82	K5, ...	1.2	42.2	1.83	1, A	.147±6
HR 6516	17 25.2	− 0 59	5.22	G6	0.14	46.0	1.06	1, A	.050±4
26 Dra	17 34.0	+61 57	5.22	G1, ...	2.61	76.06	1.55	8, B	.066±5
μ Her BC	17 42.5	+27 47	9.80	M4	0.1	43.02	1.287	1, A	.109±6
70 Oph	18 00.4	+ 2 31	3.97	K1, K4	1.68	87.85	4.558	3, A	.196±4
99 Her	18 03.2	+30 33	5.13	F5, ...	3.40	54.7	1.13	9, A	.049±5
HR 7162	18 53.3	+32 46	5.17	Go, ...	1.78	61.8	1.24	10, A	.058±5
δ Equ	21 09.6	+ 9 36	4.50	F6	0.0	5.70	0.26	4, A	.060±4
τ Cyg	21 10.8	+37 37	3.73	F0, ...	2.82	49.8	0.94	11, A	.046±4
Kr. 60	22 24.4	+57 12	9.64	M4+, M6	1.5	44.52	2.362	1, A	.256±4
85 Peg	23 56.9	+26 33	5.80	G2, ...	3.5:	26.46	0.82	4, AB	0.090±6

EXPLANATION OF NINTH COLUMN (REF.)

1. W. S. Finsen, "Catalogue of Visual Binary Star Orbits," *Circ. Union Obs.*, **91**, 24, 1934. In most cases the same orbit is given in R. G. Aitken's recent book, *The Binary Stars*, p. 284, Table 1. This last table is complete to September, 1933. Baize's catalogue (*Bull. Astr.*, **10**, 273, 1937) was received after this section was written.

2. W. H. van den Bos, *Circ. Union Obs.*, No. 98, 1938.

3. K. A. Strand, *Annals Leiden Obs.*, **18**, Part II, 1937.

4. W. J. Luyten, "Investigations of Binary Stars," *Pub. Minnesota*, **2**, Part I, 1934.

5. E. Hertzsprung, *B.A.N.*, **7**, 330, 1936.

6. G. P. Kuiper, unpublished. The orbit is nearly circular in appearance; $i = 0°$, $e = 0.04$.

7. H. N. Russell, *A.J.*, **45**, 95, 1936; also W. S. Finsen, *Circ. Union Obs.*, No. **95**, 230, 1936. Finsen's orbit is a parabola: $n = 0.0707$; $q = 2''.175$. Russell's orbit represents the measures better than does Finsen's. In computing the mass, Russell's orbit has been given double weight.

8. P. Rudnick, *A.J.*, **43**, 164, 1934.

9. W. J Luyten and E. Ebbighausen, *ibid.*, **45**, 54, 1936.

10. R. C. Huffer, *Ap. J.*, **80**, 270, 1934.

11. W. J. Luyten and E. Ebbighausen, *A.J.*, **44**, 119, 1935.

system),[14] corrected by the amount $-0^m.22 + 0.11C$.[15] Other magnitude data were first reduced to the PD system with the aid of Zin-

[14] *Veröff. Bamberg*, **2**, 1926.

[15] F. W. Seares, *Trans. I.A.U.*, **4**, 142, 1932; C. Payne Gaposchkin, *Harvard Ann.*, **89**, 105–107, 1935.

ner's tables, and then to the IPv system.[16] The magnitudes of o_2 Eridani BC, BD $-8°4352$, and Krüger 60 are my own determinations. For μ Herculis BC, the reduced Harvard magnitude is 9.79 mag., and my own measures give 9.82 mag.

For convenience, the correction IPv $-$ PD $= -0.22 + 0.11C$, which seems to be well established, is tabulated against spectral type in Table 2. The color index C is defined as IPg $-$ IPv, which makes $C = 1.08$ for gKo if $C = 0$ for Ao.

TABLE 2

Spec.	IPv−PD	Spec.	IPv−PD	Spec.	IPv−PD
O	−0.24	dGo	−0.17	gGo	−0.15
Bo	.24	G5	.16	G5	.13
B8	.23	Ko	.14	Ko	.10
Ao	.22	K2	.12	K2	.09
A2	.21	K5	.09	K5	.05
A5	.20	dMo	−0.05	gMo	−0.03
Fo	.20				
F5	−0.18				

The fifth column of Table 1 gives the spectral type either of the two components separately or of the combined light. For A stars the HD classes were used, and for most of the other stars spectral types were obtained by Dr. Morgan or the writer.[17] In particular, the writer wishes to acknowledge Dr. Morgan's classification of the spectra of the components of Capella. Three-prism spectrograms were used which were compared with similar spectrograms of other F and G giants. Dr. Morgan estimates Δm(pg) = 0.0, which is in good agreement with the small visual difference found interferometrically.

For α Centauri B the published spectral type is K5; but since this value led to an abnormally large radius for this star, the writer has asked Dr. Shapley's permission to compare the Harvard spectra of this star with those of 61 Cygni (dK5), ϵ and 40 Eridani (dK2),

[16] The valuable compilation by C. Payne Gaposchkin (*Harvard Obs. Mimeograms*, 3, 1938), was received after this paper was practically completed. It was used for Table 8 (except γ CrA, which seems to be in error).

[17] Cf. pp. 451 and 463 of the preceding article.

and τ Ceti and ξ Bootis (dG8). The result, K1, is quite well determined and makes the star a normal dwarf.[18] The writer wishes to thank Dr. Shapley and Miss Hoffleit for their kind co-operation.

The sixth column of Table 1 contains the magnitude differences between the components. The majority of the determinations are my own, but ten Harvard values were available and these were included.

The seventh, eighth, and ninth columns give the relevant orbital data, including the references explained at the bottom of the table, and the quality Q of the orbit. $Q = A$ indicates an orbit as good or nearly as good as may be obtained for the pair in question; B means a more uncertain orbit, usually due to the fact that the measures cover the orbit only partly; and C means that the orbit is quite uncertain.

The list of references illustrates the activity in orbital determinations since the appearance of the "Catalogue of Orbits," by Finsen in 1934. Of particular interest is Strand's publication on six classical binaries (five of which are used here), in which many photographic measures are incorporated.

The last column gives the trigonometric parallax, in all but a few cases the same as in Schlesinger's *Catalogue* of 1935. The few more recent determinations available were included.

The data on mass ratios for the binaries of Table 1 are collected in Table 3. A most important source of information is the new *Boss General Catalogue*, which contains the mass ratios that can be derived from meridian observations. In addition, van de Kamp has recently determined several mass ratios photographically, each based on at least fifty plates.

One word should be said about mass ratios determined for binaries that are not separated on the plates used, or, if observed visually, are not resolved in the meridian circle. These binaries are ζ Herculis, 99 Herculis, HR 7162, τ Cygni, and 85 Pegasi. The result of the finite size of the image (caused by imperfect seeing and optical effects) will be that in such cases not the brighter star is observed but the center of light. The position of this center may be computed if

[18] The result is in agreement with that just published by Miss Hoffleit (*Harvard Ann.*, **105**, 57, 1937).

TABLE 3

Star	$\frac{m_2}{m_1+m_2}$	Authority	Ref.	Star	$\frac{m_2}{m_1+m_2}$	Authority	Ref.
η Cas...	0.405	Boss GC	1	ζ Her...	0.372	Boss GC	1
	.385	Strand	2		.382	Van de Kamp	7
o_2 Eri BC	.31	Van den Bos	3	26 Dra...	.38	Boss GC	1
α Aur...	.443±	Reese, Sanford	4	70 Oph..	.478	Boss GC	1
α CMa..	.282	Boss GC	1		.416	Comstock	8
	.326	Van de Kamp	5		.427	Strand	9
α Gem..	.64	Boss GC	1	99 Her...	.265:	Boss GC	1
α CMi..	.235	Boss GC	1	HR 7162..	.45	Van de Kamp	10
γ Vir...	.508	Boss GC	1	τ Cyg..	.328	Van de Kamp	11
ζ UMa .	.501	Hadley	6	Kr. 60...	.359	Van de Kamp	12
α Cen...	.446	Boss GC	1	85 Peg...	.52	Boss GC	1
ξ Boo...	.461	Boss GC	1		0.51	Van de Kamp	13
44 Boo ..	.791	Boss GC	1				

EXPLANATION OF FOURTH COLUMN (REF.)

1. B. Boss, *General Catalogue of 33342 Stars*, **1**, Appen. II, 1937. ζ Her: B (observed) = 0.313; Δm = 3.00; B (corrected) = 0.372. 26 Dra: since the separation reaches 1".7, the meridian positions must refer to the primary, and B needs no correction. 99 Her: B (obs.) = 0.223:; Δm = 3.40; B (corr.) = 0.265:. According to a personal communication by Dr. Jenkins, the weight of this determination is small. 85 Peg: B (obs.) = 0.48; Δm = 3.5; B (corr.) = 0.52.

2. *Ann. Leiden Obs.*, **18**, Part II, 75, 1937; the probable error is ±0.019.

3. *B.A.N.*, **3**, 132, 1926.

4. *Lick Obs. Bull.*, **1**, 35, 1901; *Pub. A.S.P.*, **34**, 179, 1922. Value is approximate.

5. *A.J.*, **45**, 124, 1936; 59 plates were used, dating from 1920 to 1933.

6. *Pub. Michigan Obs.*, **2**, 101, 1915.

7. *A.J.*, **44**, 83, 1935. From 50 plates between 1919 and 1934, B = 0.323± 0.015 was found, which, corrected for Δm = 3.00, gives 0.382.

8. *Ibid.*, **32**, 157, 1920. Based on relative micrometer positions of three field stars, separated by the present writer from Comstock's values obtained from meridian positions. The probable error is ±0.025.

9. *Ann. Leiden Obs.*, **18**, Part II, 135, 1937. Value derived from radial-velocity observations published by Berman. The probable error is ±0.028.

10. *A.J.*, **46**, 36, 1937. From 54 plates between 1919 and 1936, B (obs.) = 0.288 ± 0.045 was found, which, corrected for Δm = 1.78, gives B = 0.45.

11. *Ibid.*, **45**, 121, 1936. From 53 plates between 1916 and 1935, B (obs.) = 0.257 ± 0.024. Corrected for Δm = 2.82, B = 0.328.

12. *Ibid.*, **47**, 1, 1938. From 57 plates between 1916 and 1936, B = 0.359 ± 0.007. (The difference between the x- and y-solutions suggests a somewhat larger uncertainty.)

13. Personal communication. From measures in the x-direction B (obs.) = 0.476 ± 0.012; from the y-direction B (obs.) = 0.419 ± 0.034, weighted mean B (obs.) = 0.470 ± 0.012; Δm = 3.5; B (corr.) = 0.51.

the magnitude difference, Δm, is known. The center will be on the line connecting the components, at a distance $[L_2/(L_1 + L_2)]s$ from the brighter star, where L_1 and L_2 are the luminosities of the components, measured in the wave length considered, and s is their separation. It follows that the observed (or apparent) values of $B = m_2/(m_1 + m_2)$ will have to be increased by $L_2/(L_1 + L_2)$, in order to give the true values of B.[19] This correction has been applied in Table 3, with the details given in the footnotes. In Table 4 the correction $(B - B_{obs})$ is tabulated against Δm. It appears that Δm, except if larger than 3 mag., must be known quite accurately in order that significant mass ratios may be obtained. If Δm is well

TABLE 4

Δm	$B-B_{obs}$	Δm	$B-B_{obs}$
0.0	0.500	2.5	0.091
0.5	.387	3.0	.059
1.0	.285	3.5	.038
1.5	.201	4.0	.025
2.0	0.137	5.0	0.010

determined, there is no difficulty in obtaining mass ratios even for close pairs with small Δm.

We have not attempted to include in Table 3 all mass ratios that have been published, but only those that seemed most reliable. Several extensive investigations based on meridian positions have now been replaced by the GC mass ratios. Particularly when the whole orbit has not yet been observed, as in the case of η Cassiopeiae, α Geminorum, γ Virginis, and ξ Bootis, the meridian observations should give a more reliable determination of the mass ratio than even the best photographic measures extended over a period of less than twenty years. This is obvious from the fact that in such cases the accuracy involves the square of the time interval used.

The binaries for which the mass ratios are known yield *two* absolute mass determinations each, free from assumptions. The determination of mass ratios is therefore most important.

[19] Cf. E. Silbernagel, *A.N.*, **233**, 168, 1928; P. van de Kamp, *A.J.*, **46**, 37, 1937.

If the mass ratio is not known, and the components have nearly equal magnitudes, we shall assign half the total mass to the average of the two magnitudes. This has been done for nine pairs in Table 1. In these cases each binary yields only one absolute mass determination.

Only two pairs, HR 6416 and 6426, are left for which Δm is not small, and no mass ratio is available from observations. Here we shall use the mass ratio corresponding to the observed Δm, adopting the slope of the mass-luminosity relation found in this paper. We shall use the primaries of these two systems only.

For the systems in Table 3 with more than one determination of the mass ratio, relative weights must be assigned to these determinations. The weights of the two values of η Cassiopeiae are probably in ratio about 1:2; hence, $B = 0.392$ has been adopted. For Sirius, van de Kamp's photographic determination extends over thirteen years near apastron, where the curvature of the relative orbit is slightly over 1″. The size of the whole orbit, 14″, is covered by the meridian observations (for simplicity, the comparison is made in the *relative* orbit). The value $B = 0.295$ has been adopted, which gives weight 0.7 to the GC determination.

For ζ Herculis the agreement is better than could be expected. In time the photographic determination will be very accurate.

Three determinations are available for 70 Ophiuchi, with approximate weights 2:1:1, making the average 0.450; this value is very well established.

Table 3 contains two anomalous values: for 44 Bootis and 85 Pegasi. Taking the duplicity of the companion into account, the slope of the mass-luminosity relation would give $B = 0.61$ for 44 Bootis. In view of the relatively small part of the orbit covered by the observations, the observed value of B can probably not be considered contradictory to the value $B = 0.61$.

The case of 85 Pegasi is perhaps more puzzling. The GC value of the mass ratio is based on 0.400 from the x-direction (weight 0.71) and 0.669 from the y-direction (weight 0.29). Van de Kamp's determination was described in note 13 of Table 3, and is of high weight. The observations as they stand would indicate that the primary is of abnormally low mass and the secondary of abnormally

high mass; but if the parallax of the system should be too large by twice its probable error, the primary would be nearly normal and the large mass of the secondary might be explained by assuming it to be double.

The data of interest in connection with the mass-luminosity relation are found in Table 5. Explanation of the columns is given beneath the table.

We have not attempted to give numerical estimates of the uncertainties of the mass ratios used. Qualitative data are given of pages 480 and 482. The weights in column 8 will be upper limits for the masses in the tenth column; the secondaries will be of lower relative accuracy than the primaries unless the components are nearly equal. For the nine objects where the average component is used in column 10, the weight remains identically the same as given in column 8, of course.

Table 6 gives the quantities of theoretical interest for the stars of Table 5 having weight 3 or more; α Geminorum and ξ Ursae Majoris are omitted because the components are spectroscopic binaries, and HR 6426 is omitted because the spectral type refers to a blend of the two components. Furthermore, faint and close companions, such as that of Procyon, cannot be used because no spectral type is known, whereas for Krüger 60 B no reliable estimate of T_e can be made. 70 Ophiuchi has occasionally been suspected to be a triple system, but the evidence has never been entirely convincing, and Strand's discussion of accurate photographic measures gives no indication of the presence of a third body.

The masses of Table 6 are taken directly from Table 5; the luminosities follow from the bolometric magnitudes of Table 5, in connection with the bolometric magnitude of the sun, 4.62.[20] The value $\Delta \log T_e = \log T_e/\odot$ follows from the temperature scale of the preceding article,[21] except for dwarfs later than M2, for which no radiometric measures are available. For these stars we shall adopt the temperature scale for the giants, on the basis of the following considerations.

As we have seen, the heat indices (or bolometric corrections) are nearly the same for gM2 and dM2; the color indices are also nearly

[20] Cf. p. 438 of the preceding paper.

[21] Table 13, p. 464.

TABLE 5

VISUAL BINARIES FOR THE MASS-LUMINOSITY RELATION

(1) Star	(2) M_{pv}		(3) M_{bol}		(4) log Σm	(5) p.e. (π)	(6) p.e. (Orb.)	(7) p.e.	(8) Wt.	(9) $\frac{m_2}{m_1+m_2}$	(10) log m	
HR 159	5^M65		5^M55		+0.11	±0.09	±0.03	±0.10	1	av.	−0.19	
η Cas	4.90	8.64	4.84	7.52	+ .07	.03	.015	.03	9	0.392	−0.14	−0.33
p Eri	6.99		6.89		+ .34	.05	.08	.09	1	av.	+ .04	
o_2 Eri BC	11.14	12.62	10.26	9.5:	− .19	.018	.015	.02	18	.31	− .35	− .70
α Aur	− 0.13	+ 0.02	− 0.58	− 0.13	+ .88	.....	.01	.01	100	.443	+ .62	+ .52
α CMa	1.36	11.42	0.64	11.10	+ .523	.008	.005	.009	120	.295	+ .37	− .01
α Gem	1.32	2.18	1.08		+ .65	.04	.04	.06	3	.64	+ .35	
α CMi	2.77	13.1	2.71	<13.1	+ .29	.016	.015	.02	21	.235	+ .17	− .34
9 Pup	4.95		4.88		+ .42	.06	.04	.08	2	av.	+ .12	
ξ UMa	5.24		5.18		+ .24	.05	.002	.05	4	av.	− .06	
γ Vir	3.47	3.50	3.37	3.40	+ .40	.09	.005	.09	1	.508	+ .10	+ .11
ζ UMa A	1.45	1.45	0.93	0.93	+ .72	.....	.04:	.04:	.6:	.501	+ .41	+ .41
α Cen	4.46	5.83	4.37	5.70	+ .29	.010	.002	.01	100	.446	+ .04	− .06
ξ Boo	5.52	7.48	5.42	6.70	+ .21	.04	.005	.04	5	.461	− .06	− .12
44 Boo	5.21	6.0±	5.14	....	+ .30	.07	.03	.08	2	.7	− .2	.....
ADS 10075	6.42		6.27		+ .04	.11	.03	.12	1	av.	− .26	
ζ Her	3.22	6.02	3.15	....	+ .19	.05	.01	.05	4	.38	− .02	− .23
$-8°4352$	10.80		8.1		− .15	.03	.04	.05	4	av.	− .45	
HR 6416	6.23	8.8	6.12	....	− .01	.05	.04	.06	2	(.366)	− .21	.....
HR 6426	6.97	8.2	6.44	....	+ .04	.04	.03	.05	3	(.438)	− .22	.....
HR 6516	4.46		4.36		+ .65	.09	.03	.09	1	av.	+ .35	
26 Dra	4.41	7.02	4.34	....	+ .35	.08	.05	.10	1	.38	+ .14	.....
μ Her BC	10.74		8.0		− .05	.06	.015	.06	3	av.	− .35	
70 Oph	5.64	7.32	5.56	6.78	+ .21	.024	.002	.02	17	.450	− .05	− .13
99 Her	3.63	7.03	3.59	....	+ .61	.11	.03	.12	1	.264:	+ .48	.....
HR 7162	4.18	5.96	4.12	....	+ .41	.10	.02	.10	1	.45	+ .15	+ .06
δ Equ	4.14		4.10		+ .40	.07	.02	.08	2	av.	+0.10	
τ Cyg	2.12	4.94	2.02	....	+ .54	.10	.015	.10	1	.328	+ .36	+ .05
Kr. 60	11.94	13.44	9.0	9.9::	− .40	.016	.012	.02	25	.359	− .60	− .85
85 Peg	5.61	9.1±	5.54	....	+0.03	±0.07	±0.03	±0.08	2	0.51	−0.28	−0.26

EXPLANATION OF TABLE 5

1. The name of the star.

2. The absolute visual magnitude, on the IPv scale. Either both components are given or the average, depending on the data in the last column.

3. The bolometric magnitude, computed from column 2, Tables 6, 9, and 10 of the preceding paper, and the spectral type from Table 1. If radiometric observations were available, they were also used; they received double weight, compared with the values derived from the visual magnitudes.

4. The logarithm (base is 10) of the sum of the masses, computed from P, a'', and π'' of Table 1; the unit of m is the solar mass.

5. The probable error in log Σm, resulting only from the probable error of π''. For this purpose the probable error of π'' was computed to one more decimal.

6. The probable error in log Σm, resulting only from the uncertainty of the orbital elements used. This value is an estimate, of course; but considerable time was spent in making the estimate as close as possible. For Capella and Mizar, the uncertainty in the masses depends mainly on the uncertainty in i, which was determined from interferometer observations. The estimated probable errors correspond to a probable error of $\pm 0^{\circ}.4$ in i for Capella and of $\pm 3^{\circ}$ for Mizar.

7. The probable error, resulting from the combination of the probable errors in the two preceding columns. This combination can be made in the usual manner, since the two sources of error are independent and since the small compensation of errors mentioned on page 476 of this paper was removed before the values in column 5 were computed. Hence, columns 5, 6, and 7 all refer to the uncertainty parallel to the (log m) axis of a mass-luminosity diagram, the uncertainty in the other co-ordinate having been eliminated.

8. The weight of the determination of log m, corresponding to the probable error in column 7. The unit corresponds to a probable error of ± 0.10 in log m.

9. The adopted value of the mass ratio, based on Table 3 and subsequent discussion in the text.

10. The logarithm of the masses of the components or the average component based on columns 4 and 9.

the same.[22] Hence, the effective temperatures are probably nearly the same, as we have assumed in the preceding paper.

When a spectrum (extending from 4000 A to 6600 A) of BD $-8°4352$ (dM4) was compared with spectra of M4 giants, it was found that although the red *TiO* bands correspond (as they should, since the classification is based on them), the *TiO* bands in the yellow, green, and blue are considerably weaker. Dr. Morgan has found the

TABLE 6

Star		log *m*	log *L*	Δ log T_e	log *R*	log ρ	log *g*	*E* km/sec
η Cas	A	−0.14	−0.09	+0.021	−0.09	+0.27	4.47	0.56
	B	− .33	−1.16	− .166	−0.25	+0.56	4.60	0.53
o_2 Eri	B	− .35	−2.26	+ .303	−1.74	+5.01	7.56	15.5
	C	− .70	−1.96:	− .305	−0.37	+0.56	4.48	0.30
α Aur	A	+ .62	+2.08	− .082	+1.20	−2.84	2.65	0.17
	B	+ .52	+1.90	+ .066	+0.82	−1.79	3.32	0.32
α CMa	A	+ .37	+1.59	+ .273	+0.25	−0.23	4.31	0.84
	B	− .01	−2.59	+ .175	−1.65	+5.08	7.72	27.5
α CMi	A	+ .17	+0.76	+ .077	+0.23	−0.36	4.16	0.56
ζ UMa	$\overline{A}$	+ .41	+1.48	+ .229	+0.28	−0.28	4.29	0.86
α Cen	A	+ .04	+0.10	− .018	+0.09	−0.07	4.30	0.57
	B	− .06	−0.43	− .078	−0.06	+0.27	4.50	0.64
ξ Boo	A	− .06	−0.32	− .051	−0.06	+0.25	4.49	0.63
	B	− .12	−0.83	− .157	−0.10	+0.34	4.52	0.61
ζ Her	A	− .02	+0.59	+ .010	+0.29	−0.74	3.84	0.31
$-8°4352$	$\overline{AB}$	− .45	−1.40	− .290	−0.12	+0.06	4.23	0.30
μ Her	$\overline{BC}$	− .35	−1.37	− .290	−0.10	+0.12	4.30	0.36
70 Oph	A	− .05	−0.38	− .078	−0.03	+0.20	4.46	0.61
	B	− .13	−0.86	− .136	−0.16	+0.49	4.62	0.68
Kr. 60	A	−0.60	−1.77	−0.298	−0.29	+0.42	4.42	0.31
Sun		0.00	0.00	0.000	0.00	+0.15	4.44	0.64

same phenomenon even more strikingly in Barnard's star (dM6), as compared with M5–M6 giants. Another difference between the spectra of giants and dwarfs of type M is, of course, the broad absorption feature near *Ca* 4227, present in dwarfs but absent in giants. If the effective temperatures of M giants and M dwarfs were about the same, the spectral differences mentioned would tend to give the dwarfs the larger color index (for two reasons) but the smaller bolometric correction. The bolometric corrections are not known for the later M dwarfs, but the color indices are, approxi-

[22] Seares, *Pub. Nat. Acad. Sci.*, **5**, 232, 1919.

mately, from Seares's determination for Barnard's star[23] (dM6, $C = 1.76$) and from the approximate value for Wolf 359 (dM8, $C = 2.0$).[24] The M giants are known to become slightly bluer (as measured by the ordinary color index) with advancing type.[22] The color difference is, therefore, in the direction to be expected from the appearance of the spectra.[25] Whether or not the full difference would be accounted for (which would mean that the effective temperatures of giants and dwarfs are equal) would be difficult to determine. Another approach to the temperatures of the M dwarfs would be to estimate the distortion of the color index of Barnard's star by the *TiO* absorption. Dr. Morgan estimates that the corrected value may be about 2.0 mag., with a considerable uncertainty.

With this (uncertain) value, the effective temperature in our system may be computed if color indices for two other spectral types are adopted. We take $C = 0.00$ for A0, and 1.22 for dK5+ (being the mean of Seares's average for the components of 61 Cygni, 1.18[22], and W. Becker's photoelectric color index reduced to the international system, 1.25). With the aid of Table 13[21] we then find $c_2/T = 5.19$, which happens to be very near to the value 5.22 for gM6 given by Table 13. Much significance cannot be attached to this result; only radiometric observations of Barnard's star will solve the problem of the effective temperatures of the later M dwarfs.

Since the temperatures for giants and dwarfs seem to be nearly the same for M6 as well as for M2, the temperature scale of the giants will be used also for the dwarfs.

The mean densities, ρ, and the values of the surface gravity, g, given in Table 6 are in c.g.s. units. The variation of g along the main sequence is seen to be quite small. The mean densities vary from 0.5 to 0.6 for Mizar A and Sirius A to about 3 for K and M dwarfs.

The last column gives the Einstein gravitational red shift. It ap-

[23] Seares, *Pub. A.S.P.*, **28,** 281, 1916.

[24] *Contr. Mt. W. Obs.*, No. 356, 3, 1928.

[25] For the reasons given, the treatment of the M dwarfs in papers by Öpik and Gabovits, who assume equal *TiO* absorption in the visual region for giants and dwarfs, and who adopt a constant difference between the color indices (0.3 mag., the dwarfs being bluer), is not correct, although the errors in the two assumptions tend to compensate. Cf. *Pub. Tartu*, **28,** Nos. 3 and 5, 1935–1936; **30,** No. 1, 1938.

pears to diminish slightly along the main sequence. Only for the white dwarfs is the red shift appreciable, although in statistical studies dealing with the F, G, and K stars it should not be overlooked that the standard radial velocity system is corrected by an amount of 0.64 km/sec, the red shift of the sun, in order that the sun would show zero radial velocity. The giants of these spectral types should, therefore, show a small negative K term.

The two white dwarfs of Table 6 will be discussed, together with similar objects, in a forthcoming paper.

A theoretical discussion of the masses, radii, and luminosities derived here will not be given, since Drs. Chandrasekhar and Strömgren intend to undertake such a discussion with the methods they have developed.

TABLE 7

ADS	M_{pv}	Sp.	M_{bol}	log L	Δ log T_e	log R	log m	Wt.
3264.....	3.02	F0	2.90	+0.69	+0.118	+0.11	+0.07	1½
3483.....	3.66	F5	3.62	+ .40	+ .054	+ .09	+ .04	1
3135.....	4.48	F6	4.44	+ .07	+ .046	− .06	− .195	½
3169.....	4.52	F8	4.47	+ .06	+ .032	− .03	− .21	½
3475.....	4.59	F7	4.54	+ .03	+ .039	− .06	− .19	3
3210.....	5.65	G5	5.55	−0.37	−0.028	−0.13	−0.44	2

The values themselves are shown graphically in Figures 1 and 2. Figure 1 contains also objects of lower weight, taken from Table 5, and the binaries in the Hyades, given in Table 7. The latter table is a revision of a table published previously;[26] for ADS 3135 a new orbit was published by van den Bos,[27] who used measures up to date. As mentioned in the previous paper, the mean of the six objects in the Hyades should give a reliable determination of the hydrogen content, but deviations from the mean are not considered significant. In due time the pair 68 Tauri ($M_{pv} = +1.4$, $M_{bol} = +0.9$); discovered recently by the writer,[28] will be valuable in settling the question of possible variations of composition with absolute magnitude.

The companion to Procyon was entered in Figure 1 as a probable

[26] *Ap. J.*, **86**, 176, Tables 4 and 5, 1937.

[27] *Circ. Union Obs.*, No. 98, 1937.

[28] *Pub. A.S.P.*, **49**, 341, 1937.

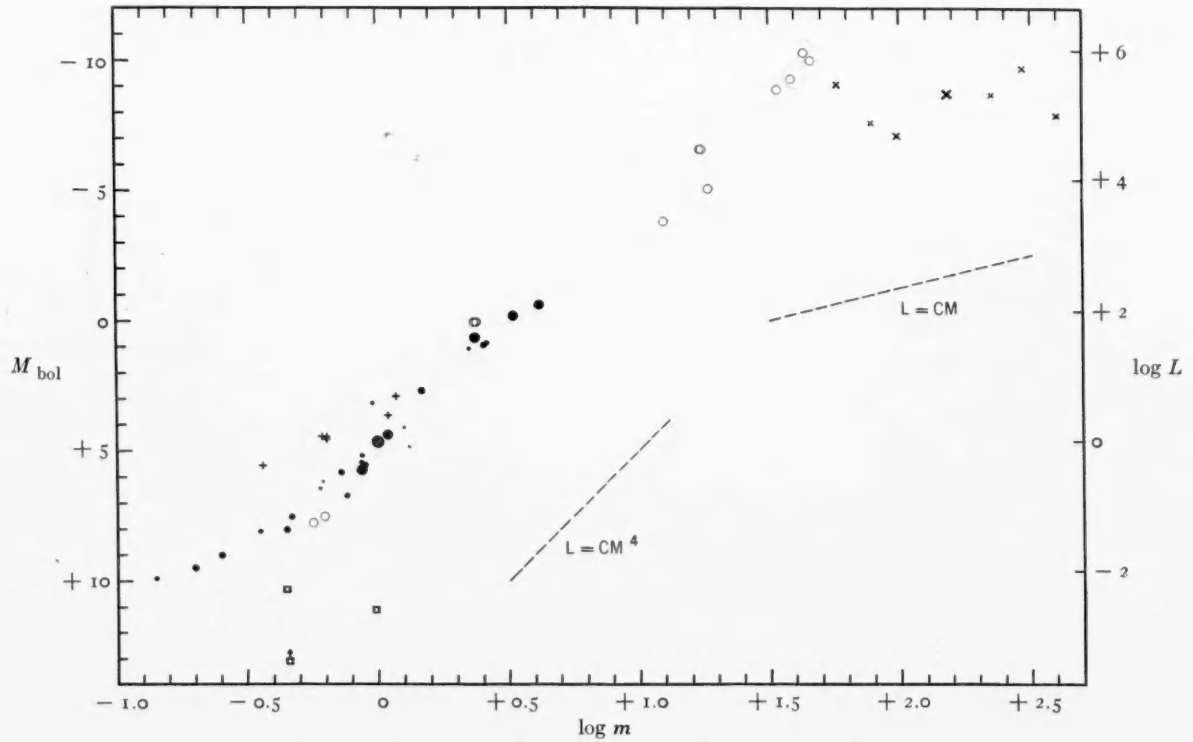

FIG. 1.—The empirical mass-luminosity relation. Closed dots: visual binaries; open circles: spectroscopic binaries; vertical crosses: Hyades; diagonal crosses: Trumpler's stars; square's: white dwarfs.

white dwarf for the following reason. Observations show that the correlation between absolute visual magnitude and spectral type is close for the lower part of the main sequence. The deviation of Procyon B from the empirical mass-luminosity relation may therefore be computed under the assumption that the star is a normal dwarf. The deviation is in that case 2 mag., or over 0.4 in log m. Until other large deviations are found in this region of the mass-luminosity diagram, we may conclude that Procyon B is probably not a normal red dwarf.

The dots in Figure 1 define an average empirical mass-luminosity relation which is useful in the discussion of such problems as that presented by ϵ Aurigae. Since, however, different selection factors operate for the different groups of stars used, it is doubtful whether this mean empirical relation has any definite physical significance; no interpolation-curve was therefore drawn. Some stars, such as the Hyades and ζ Herculis, are seen to be brighter than the average star of the same mass; these differences are considered real. Other differences, particularly among the stars of low accuracy, are probably spurious. The conclusion, therefore, is that we are not dealing with only *one* mass-luminosity relation but with many such relations, involving still a parameter different from the mass. Strömgren has identified this parameter with the hydrogen (or hydrogen and helium) content. This conclusion is based on another result, by Strömgren and Chandrasekhar, that the stars of mass smaller than five to ten times the sun are built essentially on the same model, so that changes in model cannot be held responsible for the differences in luminosity for stars of the same mass. For the more massive stars, however, Chandrasekhar has found very striking differences in model, which must be largely responsible for the scatter in the mass-luminosity relation in that region.

For the stars with masses smaller than $0.6\odot$ the slope of the mass-luminosity relation changes;[29] the exact slope will depend, of course, on the bolometric corrections used, but there is no doubt that the change is real. The explanation may be simply that the stars Krüger 60 and o_2 Eridani C have a small hydrogen content, as would follow

[29] The change found now is better determined than in Fig. 1 of *Ap. J.*, **86**, 194, 1937; cf. also Parenago, *loc. cit.*, Gabovits, *Pub. Tartu*, **30**, No. 1, 1938 (see n. 25).

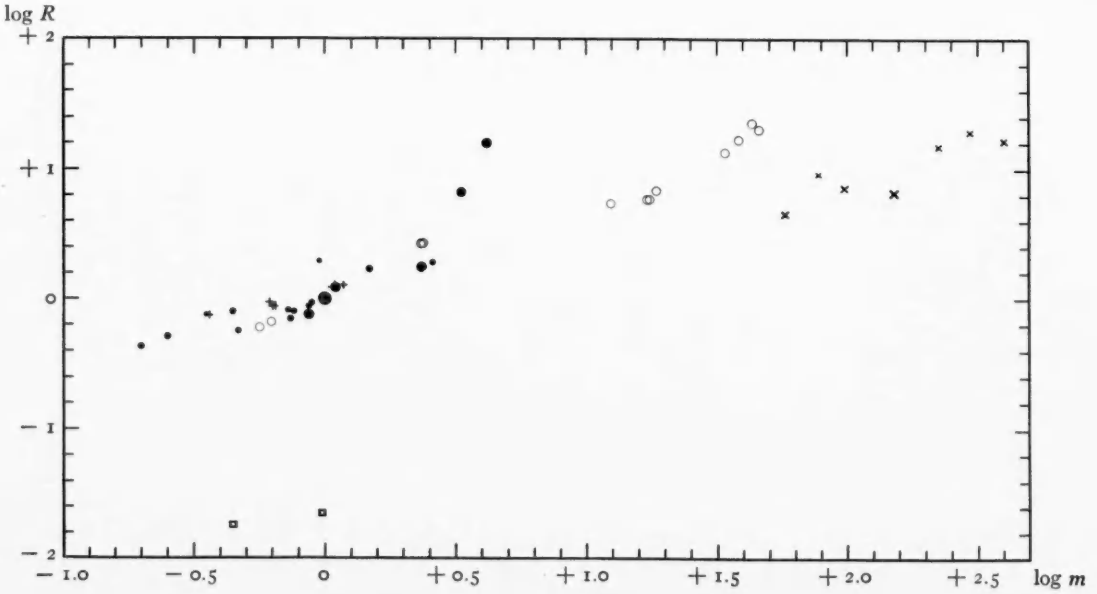

FIG. 2—Mass-radius diagram. Symbols as in Fig. 1

from an extrapolation of Strömgren's tables. A more detailed theoretical investigation of these low-temperature stars will be needed before this conclusion can be accepted. If it holds, it may be expected that stars will be found which deviate strongly from the mean relation in Figure 1, toward the fainter side. It is of great interest that the white dwarf o_2 Eridani B (also) has a very small hydrogen content, which follows from the data in Table 6 and Chandrasekhar's theoretical relations. Castor C, connected with the A-type star Castor AB, has probably a fairly high hydrogen content. Furthermore, the brighter component of μ Herculis (A) lies well above the main sequence and may therefore be expected to be relatively poor in hydrogen. It would, therefore, not be surprising to find BC somewhat bright for its mass. It is also noteworthy that both components of η Cassiopeiae deviate in the same sense from the mean relation of Figure 1.

These remarks are all of a provisional nature, but they indicate the direction in which future research may be continued. The accuracy of the observations (parallaxes, temperatures) will set the limits to which discussion is profitable.

In conclusion, in Table 8 the visual binaries are collected which promise to be of future interest in the study of the empirical mass-luminosity relation. They are of special importance in parallax and double-star observations. Spectral types marked with an asterisk are my own determinations. Of particular importance is Wolf 424, which will provide a significant extension of the mass-luminosity relation beyond Krüger 60 B. The value of the spectral parallax of this star has been unusually uncertain because of the great steepness of the main sequence in this region. A change of M8 to M7 corresponds to a change of 1.7 in M_v or a factor 2.2 in the spectral parallax. That means that even estimates of spectral type with a probable error of only one-half of one-tenth will still give quite uncertain results for types later than dM6.[30]

The limits set in the compilation of Table 8 are necessarily arbitrary. If the evidence available indicated that the parallax is (or may be) in excess of $0''.050$, the pair was included, provided the projected separation between the components did not exceed about

[30] *Ap. J.*, **87**, 593, Fig. 1, 1938.

sixty times the parallax (this limit will already include many pairs of periods over five hundred years). For stars of very large parallax, the limit was taken somewhat wider, since a much greater relative accuracy may be obtained for such pairs (on account of the larger angular scale of the orbit and the applicability of the photographic method of observation; further, mass ratios may be determined for such pairs from relatively short arcs). Boundary-line cases are entered in parentheses.

The magnitudes, m_{AB}, are reduced to the IPv system wherever possible; values depending on estimates are indicated by a colon. Of the magnitude differences, Δm, however, many values depend on estimates. Two systems, ADS 1322 and 9476, were excluded as probably optical, the spectral parallaxes derived by the author being very much smaller than the computed dynamical parallaxes.

Not mentioned in the table is Ross 614, found by Reuyl to have a variable motion; if the pair can be resolved at maximum separation, it would be a most interesting addition to Table 8. Other stars of particular interest are ADS 9655 and 16644. All these objects deserve a prominent place in parallax and double-star observations.

Other objects not mentioned are those for which interferometer observations could be combined with the spectrographic observations. They will be few in number but of great importance individually (luminous stars).

Finally, Ross 492[31] and a pair announced by Luyten,[32] may appear to have parallaxes in excess of 0".050.

SOME SELECTED SPECTROSCOPIC BINARIES

1. After a discussion of the visual binaries it is natural to collect all the data on spectroscopic binaries which have a bearing on the problem of the mass-luminosity relation. These data fall into two groups: (1) double-line spectroscopic binaries that are also eclipsing variables (for these objects the masses and radii may be found and the luminosities computed by means of the stellar temperature scale); (2) double-line spectroscopic binaries for which the mass ratio may be measured and the magnitude difference found from photometry in the spectrum.

[31] *Pub. A.S.P.*, **47**, 282, 1935. [32] *Harvard Bull.*, No. 906, 1937.

TABLE 8*

Star	R.A.	Decl.	m_{AB}	Δm	Spec.	d''	P	1000 Parallax			Source $\pi(d)$
								tr.	*dy.*	*sp.*	
ADS 48	0^h00^m4	+45° 16′	8.1	0.1	*K6, K6	5″	.....	89±5	120	79	930
(ADS 61)	0 01.0	+57 53	6.0	0.8	G3	.....	106.	14±8	53	39	930, 91
PASP **47**,282	0 07.7	+68 47	12.2:	0.3	*M5	0.7	.....	56±7	.....	.....	.....
ADS 433	0 26.0	+66 42	10.2	1.9	*M3	3	.....	103±7	.....	69	.....
ADS 490	0 30.1	− 4 09	5.2	0.6	F7	.....	7.	52±8	(51)	46	930
−69°44	1 11.6	−69 21	7.4:	0.6	G5	.....	128.	.....	52	.....	98
−30°529 AB	1 30.4	−30 25	7.2	0.2	G5	.....	4.6	36±9	56	.....	91
AB, C	.....	.....	.....	4.9	.....	1.5	.....	.....	59	.....	93
ADS 1733	2 11.1	−18 42	7.8	1.0	*K3	2.	.....	.....	74	(42)	930
ADS 1865	2 22.5	+ 3 59	8.6:	0.2	*K6	.....	25.	.....	61	.....	98
α For	3 07.8	−29 23	4.2	3.5	F5	1.	.....	72±5	55	87	93
+68°278 BC	3 38.2	+68 21	10.8	0.0	*M2+	0.4	.....	54±9	.....	60	.....
(ADS 2995)	4 00.9	+37 49	7.1	1.3	*K2	1	.....	36±6	58	44	930
68 Tau	4 19.7	+17 42	4.4	4.0	A2	1.5	.....	Hyad	.....	25	.....
ADS 3248	4 23.3	+15 56	6.6	1.0	F8	.....	40.	Hyad	28	.....	98
ADS 3321 CD	4 30.2	+16 19	11.2:	2.4	*K6	1.7	.....	Hyad	.....	.....	.....
HR 1504	4 38.6	−59 08	6.4	0.2	G0	1.	.....	.....	50	.....	93
104 Tau	5 01.5	+18 31	5.1	0.0	G1	0.1	2±?	58±8	.....	46	.....
α Aur Hh	5 10.0	+45 44	10.1	3.5	*M1+	2.	.....	73±3	Intf. = 63		.....
(ADS 3900)	5 14.1	− 3 11	7.9:	2.8	*K4	4.	.....	66±5	110	58	930
−51°1540	5 31.2	−51 08	9.3:	0.2	K0	1.	.....	.....	110	.....	93
BDS 3112 AB	5 56.6	−31 03	7.6	0.4	*K5+	< 1.	.....	53±11	79	(78)	93
AB, C	.....	.....	.....	0.1	.....	2.	.....	.....	51	.....	93
HR 2162	6 02.2	−48 27	6.5	0.4	G5	2.	.....	.....	52	.....	93
−46°3046	7 14.6	−46 49	7.6:	1.1	K0	1.	.....	73±9	14	.....	93
ADS 6487	7 52.9	− 0 33	8.3:	5.0	*K4	3.	.....	.....	81	(69)	485
HR 3430	8 34.8	−22 19	5.1	1.8	G6	1.	.....	62±6	36	76	93
ADS 7067	8 46.0	+71 11	8.6	0.2	*K6, K6	3.	.....	93±4	90	66	930
ι UMa BC	8 52.4	+48 26	10.2	0.0	M1	.....	35±	66±6	.....	30	.....
A, BC	.....	.....	3.2	7.1	A5	6.	.....	.....	91	63	930
10 UMa	8 54.2	+42 11	4.0	2.0	F2	0.6	.....	72±6	.....	66	.....
(σ_2 UMa)	9 01.6	+67 32	4.9	3.3	F4	1.5	.....	53±6	40	50	91
(ADS 7251)	9 07.7	+53 07	7.2	0.0	*K6, K6	19.	.....	162±3	(240)	(152)	930
ADS 7284	9 12.0	+29 00	7.2	0.0	*K3	.....	34.	60±8	57	48	930, 91
ψ Arg	9 26.8	−40 02	3.7	1.2	F0	.....	35.	70±9	61	55	930, 91
11 LMi	9 29.7	+36 16	5.4	7.5	K0	2.	.....	95±5	.....	91	.....
−60°2911	11 20.3	−61 06	7.4:	1.2	K5	.....	234.	67±13	104	.....	91
Wolf 424	12 28.4	+ 9 34	11.9	0.0	*M7(+)	1.	.....	(220)	.....	(320)	†
78 UMa	12 56.4	+56 54	5.0	2.4	F0	.....	90.	UMa(?)	47	24	BAN 305
42 Com	13 05.1	+18 04	4.7	0.0	F4	.....	26.	57±7	56	43	930, 91
(ADS 8841)	13 11.9	+17 34	6.4	2.7	K3	5.	.....	68±7	94	79	930
ADS 8887	13 18.9	+29 45	8.9	0.4	*K6	0.6	.....	67±11	19	46	930‡
ADS 9031	13 44.5	+27 29	7.0	0.4	K6, K6	.....	156.	60±9	79	66	91
ADS 9090	13 58.5	+46 49	9.3	0.1	*M1, M1	3.	.....	79±6	.....	95	.....
(ADS 9446)	14 51.6	−20 58	5.4	2.2	K5, M2	19.	.....	172±4	(200)	(174)	93
ADS 9544	15 08.8	− 0 58	6.5	0.0	G8	0.1	2±?	60±4	.....	42	.....
η CrB	15 19.1	+30 39	5.1	0.3	F9	.....	42.	68±8	(57)	44	930
ADS 9716	15 32.5	+40 08	6.7	0.3	*K3	.....	57.	46±9	47	54	§
ψ Ser	15 39.0	+ 2 50	5.9	6.3	G5	3.	.....	46±10	89	52	485

* Spectral types marked by an asterisk (*) are my own determinations. The last column gives the references for the dynamical parallaxes; 930 = *A.J.*, No. 930; 91, 93, 95, and 98 are the numbers of the *Union Observatory Circulars;* 451 and 485 are the numbers of the *Lick Observatory Bulletins*.

† Two good spectra available for this star give M7+ and M7, respectively. The star is, therefore, definitely somewhat earlier than Wolf 359.

‡ The spectral parallax is about 0″.06. It seems unlikely that the parallax should be much less than 0″.05 or 0″.04, as the dynamical parallax would indicate. The value of the latter was confirmed by the inclusion of recent measures. Hence, the orbital inclination must be high (in which case the binary should soon close in rapidly), or the mass of the binary is unusually small. Additional trigonometric determinations will be valuable.

§ Derived from Pitman's orbit, *Pub. A.S.P.*, **46**, 196, 1934.

TABLE 8—*Continued*

STAR	R.A.	DECL.	m_{AB}	Δm	SPEC.	d''	P	1000 PARALLAX			SOURCE $\pi(d)$
								tr.	*dy.*	*sp.*	
+45°2505	17h09m2	+45° 50′	9.4	0.4	*M3+	< 1.	.....	143±6	.....	115	.....
36 Oph	17 09.2	−26 27	4.4	0.0	K1, K3	4.	.....	179±5	52	174	93‖
ADS 11632	18 41.7	+59 29	8.5	0.8	*M4, M4	16.	.....	282±4	(240)	(282)	930
γ CrA	18 59.7	−37 12	4.2	0.0	F7, F7	.....	119.	.....	62	51	91
17 Lyr C	19 03.6	+32 21	11.2	0.4	*M5	0.2	.....	123±6	.....	.....	.....
Ross 165	19 41.7	+26 55	12.2	0.9	*M5+	0.7	.....	116±11	.....	.....	.....
ADS 12889	19 41.8	+33 22	7.7	0.2	*K3	1.	.....	48±5	57	44	930¶
HR 7703	20 04.6	−36 21	5.2	5.4	K4	8.	.....	177±9	.....	191	.....
+4°4510	20 34.6	+ 4 37	7.9	1.0	*K5	0.7	.....	57±4	.....	87	.....
Furuh 54	20 56.2	+39 41	10.0	1.9	*M2+	1.	.....	97±8	.....	87	.....
(61 Cyg)	21 02.4	+38 15	4.9	0.7	*K5, K6	26.	.....	299±3	(360)	(276)	930
−58°7893	21 39.4	−58 08	8.6:	0.1	Ma	.....	6.8	49±5	54	.....	95
(μ Cyg)	21 39.7	+28 17	4.5	1.4	F6, F3	< 1.	.....	46±8	66	44	930**
HR 8501	22 11.7	−54 06	5.5	5.1	G0	3.	.....	80±7	.....	.....	.....

‖ Another case (n. ‡, above) where the dynamic parallax is much too small.

¶ Strand (*B.A.N.*, **8**, 206, 1937) has computed a provisional orbit for this star and found the dynamical parallax 0″117. It is almost certain that this value is too large, probably as a result of the fact that the orbital inclination found by Strand is too close to 90°. The trigonometric parallax, the Mount Wilson spectroscopic parallax, and my spectral parallax (0″050) agree very well. Also Strand's doubt whether this binary is physically connected with 17 Cygni seems unjustified. Proper motion, radial velocity, and parallax suggest that the connection is real.

The nature of this case is apparently the opposite of cases ‡ and ‖, above.

** The secondary was classified at Mount Wilson earlier than the primary.

The first group gives fundamental data for the problem of stellar structure, and the second group is useful in a study of the scatter of the mass-luminosity relation[33] and in giving data that may be used statistically in a determination of the mean position of the mass-luminosity relation (the mean absolute magnitude may be determined from the spectral types; the mean mass, by substitution of the mean value of $\sin^3 i$ into the mean value of $\boldsymbol{m} \cdot \sin^3 i$).

A review of the available data showed that for many close pairs contradictions seem to be present;[34] it was clear that for many objects new observations would be required in order to find the interpretation of such discrepancies. Particularly close pairs with very unequal components are likely to present apparent anomalies; the systems with nearly identical components, however, are more easily interpreted. In the present paper we shall discuss only a few objects of the latter class; the discussion of additional spectroscopic binaries will be made later by Dr. Morgan and the present writer.

[33] Cf. *Pub. A.S.P.*, **47**, 144, 1935; the scatter found in this manner will be a minimum value, since the components of binaries seem, at least statistically, to have common properties (hydrogen content). Cf. *Harvard Bull.*, No. 903, 1936.

[34] E.g., Wyse, *Bull. Lick Obs.*, No. 464, 1934.

2. It is well known that in many classes of light-curves the ratio of the radii cannot be found with any great precision. It is therefore necessary to determine the ratio of the total brightnesses from the relative strength of the two superimposed spectra; in combination with the ratio of the surface brightnesses determined from the light-curve the ratio of the radii is found. All our discussions of the radii will be made in this manner. Fortunately, the only cases which are of interest here are binaries which show two spectra.

3. A second question in connection with the determination of the radii arises when the pair is very close, so that the components are ellipsoidal in shape. We have a good theoretical evidence that the stars possess strong central concentrations; only certain classes of very massive stars may be exceptions to this rule.[35] Hence the Roche, or point-mass, model should give a close approximation in the determination of the equipotential surfaces; the boundaries of the components will, in general, be two of these surfaces. Since for the present we shall limit ourselves to pairs of nearly identical stars, the model considered will have two equal components with envelopes of negligible mass, in which the periods of rotation are equal to the orbital period. In this case the equipotential surfaces are given by the formula[36]

$$\Omega = -GM\left[\frac{1}{r_1}+\frac{1}{r_2}+\frac{x^2+y^2}{a^3}\right]. \qquad (3)$$

The symbols have the following meaning: Ω is the potential for which a constant value is adopted; G is the gravitational constant; and M is the mass of each component. The orbit is supposed to be circular, with radius a; the xy-plane is assumed to coincide with the orbital plane, and $x = y = 0$ with the center of gravity; r_1 and r_2 are the distances of any point (x, y, z) from the centers of the two stars; x, y, z refer to a rotating co-ordinate system.

With the aid of this formula the writer has computed a family of curves, $\Omega = C$, both for the xy-plane and for a plane parallel to the yz-plane through the center of one of the components. The results were plotted on large-scale diagrams from which the ratio of the

[35] Chandrasekhar, *op. cit.*, chap. viii.

[36] E.g., Jeans, *Problems of Cosmogony*, p. 162, 1919.

axes, a_1, b_1, and c_1, were read off for a given a_1/a (if a is the distance between the components). A certain amount of rounding-off was applied to the pointed sides of the stars facing each other, since theoretically the intensity of these points (apart from reflection effects) should be low. We are interested in knowing the mean stellar radius, $R = \sqrt[3]{a_1 b_1 c_1}$, whereas the light-curve gives a_1, or a_1 and b_1. We shall therefore tabulate R/a_1 against a_1/a, so that the former quantity may be found from the latter, which is observed. The quantity b_1/a_1 to be expected from the Roche model is also given, since this

TABLE 9

a_1/a	R/a_1	b_1/a_1	a_1/a	R/a_1	b_1/a_1
0.10	1.00	1.00	0.35	0.945	0.935
.15	0.995	0.995	.40	.915	.90
.20	0.99	0.99	.45	.885	.86
.25	0.98	0.98	0.48	0.88	0.855
0.30	0.965	0.96			

ratio may be obtained observationally. Table 9 contains the results, rounded off to the nearest half of 0.01. It should be noted that for $a_1/a = 0.43$, the two components just touch each other; for larger values of a_1/a there will be a bridge between them, which, as mentioned above, may be expected to have a low intensity (apart from reflection effects), so that in the photometric solution the components will still appear separated.

Before applying the tabular values to actual stars, we may consider the results of Wesselink's discussion of SZ Camelopardalis.[37] From an unusually accurate light-curve he finds $b_1/a_1 = 0.9323 \pm .0020$ (m.e.) in the uniform solution, for which $a_1/a = 0.38$, $a_2/a = 0.27$, and $\Delta m = 1.0$. The mean value of a_i/a (weighed according to intensity) is 0.35. For the darkened solution he found $b_1/a_1 = 0.9579 \pm .0013$. The theoretical darkening coefficient for this star is about 0.1, and we may adopt the empirical value $b_1/a_1 = 0.935 \pm .002$ (m.e.). This happens to agree precisely with the tabular value. (Wesselink had already pointed out this agreement with the Roche model.)

[37] Dissertation, Leiden, 1938.

4. Finally, the *reflection effect* should be taken into account in the determination of the masses. Since the centers of light on the two disks do not project themselves precisely on the centers of mass, but are displaced toward the center of gravity, the amplitudes measured are found too small even if the components are of similar brightness. The reflection effect will increase the bolometric brightness on certain areas of the stars; in order to find the photographic increase of

TABLE 10

CORRECTION OF MASSES FOR REFLECTION EFFECT

a_1/a	$\Delta \log m$	a_1/a	$\Delta \log m$
0.10	0.000	0.35	0.021
.15	.001	.40	.032
.20	.003	.45	.046
.25	.007	(0.50)	(0.066)
0.30	0.013		

TABLE 11

FACTOR TO APPLY TO THE CORRECTION OF TABLE 10

Spec.	Factor	Spec.	Factor
O7	0.45	Fo	0.95
Bo	.45	dF5	1.15
B5	.5	dGo	1.4
Ao	.65	dKo	1.5
A5	0.8	dK6	2.5

intensity, the ratio of photographic increase to bolometric increase has to be known, which will depend on the spectral type. The simplest procedure is to tabulate the correction to log m as a function of a_1/a for bolometric intensities; this correction will then have to be multiplied by a factor giving the rate of increase of photographic intensity for a given increase of bolometric intensity. This factor is readily found from Table 3, or from Tables 9 and 13, of the preceding paper, and a table of color indices; the result is found in Table 11. The correction to log m for bolometric intensities is given in Table 10; Eddington's formula for the reflection effect[38] was used.

[38] *The Internal Constitution of the Stars*, p. 212, formula 144.3, 1926.

The reflection has, of course, also its effect on the determination of $a \sin i$, and hence on R (involving a) and L (involving a^2), as well as on m (involving a^3). The corrections are of less importance than those for the masses, but may be taken from the same tables (10 and 11), after multiplication by $1/3$ for $\log R$, and by $2/3$ for $\log L$.

After these preparations, some close binaries with nearly equal components will be discussed.

5. *Castor C.*—From the discussion in the preceding article[39] we have $\log \bar{R} = -0.198$. The ratio of the radii follows from the ratio of the intensities of the two spectra, 5:4, and the equality of the surface brightnesses. We find $\log R_1 = -0.18$ and $\log R_2 = -0.22$.

The direct determination of the effective temperature gave $\log T_e = 3.550 \pm 0.014$;[39] from the spectral type K6+ and the stellar temperature scale[40] we have $\log T_e = 3.562$. We adopt the mean, 3.556. Hence,[41] $\log L_1 = -1.16$, $\log L_2 = -1.24$; $M_{bol}(1) = +7.53$, $M_{bol}(2) = +7.73$. With $i = 86°.0$ the masses are given by[42] $\log m_1 = -0.204$; $\log m_2 = -0.250$. With $R/a = 0.16$, the correction for the reflection effect is about $+0.003$, making $\log m = -0.201$ and -0.247, respectively.

6. *β Aurigae.*—The photographic magnitudes are nearly equal,[43] and also the surface brightnesses.[44] Hence, the radii are nearly equal: $\log R_1 = \log R_2 = 0.431$.[45] The direct determination of T_e gave $\log T_e = 3.99 \pm 0.04$; from the spectral type A1 we have $\log T_e = 4.01$; we adopt 4.00. Then $\log L_1 = \log L_2 = 1.83$; $M_{bol(1,2)} = +0.04$.

With $\cos i = 0.223$[45] and Baker's orbit the masses are found: $\log m = 0.376$ and 0.370, respectively. The reflection effect found from $a_1/a = 0.15$ adds less than 0.001 to $\log m$.

7. *μ_1 Scorpii.*—From our former discussion[46] we take $\log R_1 = \log R_2 = 0.73$. The direct determination of T_e was $\log T_e = 4.20 \pm 0.05$. From the spectral type B3 of the average component

[39] P. 458.

[40] Table 13, p. 34, of the preceding paper.

[41] Formula 1, p. 475.

[42] Joy and Sanford, *Ap. J.*, **68**, 253, 1926. Computed from K, P, and i.

[43] Baker, *Pub. Allegheny Obs.*, **1**, 173, 1910.

[44] Stebbins, *Ap. J.*, **34**, 126, 1911.

[45] P. 442 of the preceding paper.

[46] P. 443 of the preceding paper.

we have log $T_e = 4.27$. We adopt 4.23. Hence log $L = 3.35$ and $M_{bol} = -3.76$; this value applies to the average of the components. Since the mass ratio for this binary is not known, we shall use the average mass of the components in connection with the average log L. With $i = 62\overset{\circ}{.}0$, the average uncorrected mass is log $\boldsymbol{m} = 1.082$; the correction for reflection ($a_1/a = 0.370$) is 0.012, and log $\boldsymbol{m} = 1.094$.

8. *V Puppis.*—The mass ratio is not known; therefore we shall use the average component. The strength of the companion is about 0.7 of that of the primary.[47] Roberts' photometric observations being visual, the amount of darkening toward the limb must be negligible; hence Shapley's uniform solution[48] will be used. Then $J_b/J_f = 1.27 = 1/0.79$. This value in connection with the ratio of the total brightnesses indicates substantially equal radii, as Shapley has remarked. Shapley finds the mean of a_i/a to be 0.438, and $b_i/a_i = 0.813$. The Roche model gives $b_i/a_i = 0.87$. Since the light-curve near the minimum depends much more on b_i than on a_i, we shall use the value of $(3b_i + a_i)/4$ as found by Shapley, and compute R by means of the Roche model. The result is $\overline{R}/a = 0.373$. With Shapley's value of cos i (0.219) and Maury's value of a sin i we find log $\overline{R} = 0.821$. The mean spectral type being B2 (Maury), log $T_e = 4.31$, and the mean log L is 3.85. From P, K, e, and i, we further find log $\overline{m} = 1.249$. From the computed value $a_i/a = 0.409$ we find Δ log $\boldsymbol{m} = 0.016$ and Δ log $L = 0.011$; the corrected values for the mean component are log $\boldsymbol{m} = 1.265$, log $R = 0.83$, and log $L = 3.86$ ($M_{bol} = -5.04$).

9. *Y Cygni.*—As Redman[49] and Dugan[50] have pointed out, the observations for this binary are not all satisfactorily explained (possibility of a third body, etc.), so that some caution should be exercised in using the results. Yet it is doubtful whether the chief quantities, R and $\boldsymbol{m}$, are much affected by these difficulties.

The spectra are of nearly equal intensity (Plaskett, Redman) and the minima are of equal depth (Dugan); hence the radii are nearly

[47] A. C. Maury, *Harvard Ann.*, **84**, 173, 1920.

[48] *Princeton Pub.*, No. 3, 1915.

[49] *M.N.*, **90**, 754, 1930; *Pub. Dom. Ap. Obs. Victoria*, **4**, 341, 1931.

[50] *Pub. Princeton Obs.*, No. 12, 1931.

equal. Dugan found $R_1 = R_2 = 0.206a = 5.86\odot$ (uniform solution, which will be used since the darkening must be small). The ellipticity effect is negligible because the width of the minimum determines b_i, which is nearly equal to R if $R/a < 0.25$.

The writer is under obligation to Dr. Morgan, who obtained an accurate spectral class for the star from the plates available at the Yerkes Observatory. This was of importance, in view of the discordant values published: B2 in the *Henry Draper Catalogue*, B2 by J. S. Plaskett,[51] O9.5 by Pearce, and O9 in the Victoria catalogue of radial velocities of O and B stars. Dr. Morgan finds the type to be certainly as early as O9, but probably not much earlier than O9. He suggests the value O9 as the best obtainable from the data at hand.

From Dugan's dimensions we now have: $\log R = 0.768$; $\log L_1 = \log L_2 = 4.51$; $M_{\text{bol}(1,2)} = -6.6$. The masses are 17.1 and 17.3 (Dugan, Redman), $\log \boldsymbol{m} = 1.233$ and 1.238; the correction for reflection to $\log \boldsymbol{m}$ is only $+0.002$.

10. *AO Cassiopeiae.*—Pearce has made four photometric solutions, corresponding to $\Delta m = 0.25$, 0.50, 0.80, and 1.11 mag.[52] He estimates the ratio of the intensities from the spectrum to be 2.6:1, but this may perhaps be an upper limit and we shall adopt the solution for $\Delta m = 0.80$ mag. The mean value of a_i/a is then 0.500; of b_i/a, 0.478. This is not possible for completely separated stars built on the Roche model, for which $b_i/a < 0.38$. If the photometric solution is correct, it is probable that the components have a common envelope; and since the stars are not identical, it is then further probable that the system is not in equilibrium. This possibility should be borne in mind if comparisons with other stars are made.

It is in this case uncertain what values for the radii should be used; since, according to Table 9, b_i and R are never very different, we shall use the values of b_i: $R_1/a = 0.549$ and $R_2/a = 0.406$.

In the case of unequal components, the effect of reflection on the constants of the system is slightly more complicated than in the case of identical components. With the ratio of the radii given and with equal surface temperatures (both spectra are O8.5), Δm is

[51] *Pub. Dom. Ap. Obs. Victoria*, **1**, 213, 1920.

[52] *Ibid.*, **3**, 297, 1926. Cf. also: M. Güssow, *A.N.*, **207**, 321, 1930.

found to be 0.65. In order to make Δm(pg) = 0.80, we shall have to make the temperatures slightly different: $\Delta \log T_e = 0.03$, which makes Δm(bol) = 1.0.

The reflection effect on the amplitudes, K, is one-third of that on the masses, which is found from Tables 10 and 11. For equal components and $a_i/a = 0.50$, the effect on log K is $\frac{1}{3}(0.066) \cdot (0.45) = 0.010$. With the intensity ratio $2\frac{1}{2}:1$, the effect on log K_1 will be about $0.4 \times 0.010 = 0.004$, and on log K_2, $2\frac{1}{2} \times 0.010 = 0.025$. Applying these corrections to the observed values, we have $K_1 = 220$; $K_2 = 248$; $m_2/m_1 = 0.887$; log $a\odot/ = 1.625$; log $R_1 = 1.365$; log $R_2 = 1.234$; log $L_1 = 5.97$, log $L_2 = 5.58$; $M_{\text{bol}(1)} = -10.3$, $M_{\text{bol}(2)} = -9.3$; log $m_1 = 1.634$, log $m_2 = 1.582$; $m_1 = 43.0\odot$; $m_2 = 38.2\odot$.

In allowing for the reflection effect we have increased the masses by a fair amount and have made them more unequal, which is more favorable to the difference in dimensions found for the two components (since they are probably in contact) and in better agreement with the difference in brightness.

However, perhaps the main uncertainty about this system is the value of the inclination, which enters seriously in the determination of the masses. This is particularly evident if a comparison is made with the ellipsoidal systems, π^5 Orionis, b Persei, and ζ Andromedae, discovered by Stebbins. A smaller inclination would obviously increase the derived ellipticity of the components, which is now found to be smaller than is possible for two stars which are just in contact. It will remain for a new photometric study of this system to settle this question.

The extremely high luminosity of this system is noteworthy (a smaller value of the inclination would even increase the luminosity). With the provisional values of the constants, it lies well above the mean empirical mass-luminosity relation; even a somewhat decreased inclination would not change that feature. This fact was interpreted by Chandrasekhar[35] to be a result of strong mass concentration, contrary to the massive stars found by Trumpler and even stars like V Puppis, which are less centrally condensed than Eddington's standard model. In that respect AO Cassiopeiae seems to resemble the stars of lower mass, whereas Trumpler's stars are

really the stars that deviate from a theoretical mass-luminosity relation based on the standard model. It will be of interest to discover which of the two classes of massive stars is the most frequent in nature.

On account of the uncertainties mentioned in connection with AO Cassiopeiae, it is very fortunate that a second system is known with similar properties. This system is 29 Canis Majoris.

11. *29 Canis Majoris.*—Spectroscopic orbits have been published by Harper,[53] Pearce,[54] and Luyten and Ebbighausen.[55] Pearce has measured both components and finds the spectral types both O7; the secondary is very faint. Furthermore, $K_1 = 217 \pm 5$ km/sec; $K_2 = 288 \pm 7$ km/sec; $P = 4.3935d$; and $e = 0.156 \pm 0.017$. Luyten and Ebbighausen found a smaller value of e, 0.077 ± 0.019.

The star was found to be an eclipsing variable by S. Gaposchkin,[56] who derived photometric elements from a light-curve based on photographic estimates. Recently Elvey and Rudnick have observed the star photoelectrically at the McDonald Observatory. They have very kindly made their provisional results available to the writer. Two solutions were made, of which one, with $k = 0.8$, fitted the observations best. This solution, in which the orbital eccentricity was neglected, is

$a \sin i = 3.01 \times 10^7$	$a_2 = 18.1\odot$
$m_1 \sin^3 i = 32.2\odot$	$b_1 = 16.6\odot$
$m_2 \sin^3 i = 24.3\odot$	$b_2 = 13.2\odot$
$k = 0.8$	$b_i/a_i = 0.73$
$i = 64°$	$m_1 = 44.3\odot$
$a_1 = 22.7\odot$	$m_2 = 33.4\odot$

It is seen that Gaposchkin's elements are in good general agreement with those derived by Elvey and Rudnick. The range being 0.4 mag., the star is photometrically a much better case than AO Cassiopeiae.

Dr. Morgan has very kindly examined the Yerkes plates of this star which were measured and discussed by Luyten and Ebbighausen, and he confirms the presence of the extremely faint com-

[53] *Pub. Dom. Obs. Ottawa*, **4**, 115, 1917.

[54] *Pub. Dom. Ap. Obs. Victoria*, **6**, 50, 1932.

[55] *Ap. J.*, **83**, 246, 1935.

[56] *Bull. Harvard Obs.*, No. 902, 1936.

panion but finds the spectral class of the primary later than S Monocerotis (=O7 or O7.5) and perhaps a trace earlier than 9 Camelopardalis (O9). Morgan classifies it as O9–O8. In the Victoria catalogue of O and B stars, this star is given as O9; Pearce classifies it as O7. We shall adopt O8.5.

From Elvey and Rudnick's figures we find $a_1/a = 0.471$, $a_2/a = 0.376$. The average of a_i/a is 0.424; if we average according to brightness, we find 0.441. The theoretical values of b_i/a_i are, then, 0.877 and 0.863, respectively, compared with the empirical 0.73. We shall, as before, adjust the photometric solution by leaving $(3b_1 + a_1)/4$ the same and by using the theoretical ellipticity constant. We then find $a_1/a = 0.400$ and $a_2/a = 0.319$. Gaposchkin found $a_1/a = 0.44$ and $a_2/a = 0.35$; his ellipticity constant 0.9 is equal to the theoretical value. In view of the fact that Elvey and Rudnick's results are still provisional, we shall adopt the average values: $a_1/a = 0.415$ and $a_2/a = 0.33$. For the inclination Gaposchkin finds $68^\circ.3$; Elvey and Rudnick, 64°. We adopt 65°.

We have not yet used the condition that the total brightnesses of the components should correspond to the relative intensities of the spectra. It would seem that Δm(pg) is about 1.0 mag. Taking the small difference in surface brightness into account, we find that the ratio a_2/a_1 should be about $2/3$. Leaving $a_1 + a_2$ unchanged, so that the representation of the light-curve will be little affected, we find $a_1/a = 0.45$; $a_2/a = 0.30$; hence $R_1/a = 0.42$ and $R_2/a = 0.28$.

Following the procedure of applying the correction for reflection used for AO Cassiopeiae, we have: correction to log K_1, 0.002, to log K_2, 0.010; $K_1 = 218$; $K_2 = 294$; log $a/\odot = 1.686$; log $R_1 = 1.309$, log $R_2 = 1.133$; furthermore, allowing for the small difference in surface brightness, log $L_1 = 5.84$, log $L_2 = 5.39$; $M_{\mathrm{bol}(1)} = -10.0$; $M_{\mathrm{bol}(2)} = -8.9$; log $m_1 = 1.66$, log $m_2 = 1.53$; $m_1 = 45.7\odot$, $m_2 = 33.9\odot$.

The striking similarity between 29 Canis Majoris and AO Cassiopeiae has been already pointed out by Gaposchkin. But in 29 Canis Majoris the components appear to be separated; this fact and the deeper minima make this star of greater importance for the mass-luminosity relation.

In conclusion, the data on spectroscopic binaries thus far discussed are collected in Table 12.

The data are included in the mass-luminosity diagram (Fig. 1) and the mass-radius diagram (Fig. 2). The two binaries AO Cassiopeiae and 29 Canis Majoris stand out by their great luminosity; Y Cygni appears to be an intermediate case.

TABLE 12

SOME SELECTED SPECTROSCOPIC BINARIES

Star	log m	log L	log R	M_{bol}
Castor C_1	−0.201	−1.16	−0.18	+ 7.53
C_2	−0.247	−1.24	−0.22	+ 7.73
β Aur A	+0.378	+1.83	+0.43	+ 0.04
B	+0.370	+1.83	+0.43	+ 0.04
μ_1 Sco $\overline{AB}$	+1.094	+3.35	+0.73	− 3.76
V Pup $\overline{AB}$	+1.265	+3.86	+0.83	− 5.04
Y Cyg A	+1.240	+4.51	+0.77	− 6.6
B	+1.235	+4.51	+0.77	− 6.6
AO Cas A	+1.634	+5.97	+1.36	−10.3
B	+1.582	+5.58	+1.23	− 9.3
29 CMa A	+1.66	+5.84	+1.31	−10.0
B	+1.53	+5.39	+1.13	− 8.9

TRUMPLER'S MASSIVE STARS

The method, used by Trumpler, of determining the masses of the very luminous O and B stars in galactic clusters from the Einstein gravitational red shift has, at least for main-sequence stars, extended the study of stellar masses to near the upper limit. For the most luminous of these objects are not appreciably exceeded in brightness (and probably not in mass) by any other known stars of classes O and B. Trumpler's method is, of course, capable of being extended to visual binaries, although the fact that only one comparison star can be used will be a disadvantage.

Table 13 gives the observational data for seven stars taken from Trumpler's paper.[57] The spectrum of the third star is classed O7 by Trumpler, O7 at Victoria, and O7.5 by E. G. Williams. We have used the average value. The temperatures and bolometric correc-

[57] *Pub. A.S.P.*, **37**, 249, 1935.

tions are taken from Table 3 of the preceding paper; the color index C was supposed to be -0.2 for all the stars. Log L follows from M_{bol} and $M_{bol}(\text{sun}) = 4.62$; log R from log L, log T_e, and log $T_e(\text{sun}) = 3.757$. It is seen that log $\boldsymbol{m}$ is roughly twice as large as log R; this shows that the surface gravity is about the same as that of the sun, as was supposed in adopting the temperature scale for log $g = 4.4$.

The last column gives the order of reliability of the measured red shifts, according to a private communication by Dr. Trumpler.

TABLE 13

TRUMPLER'S STARS

Star	E	$\log \frac{\boldsymbol{m}}{R}$	M_{pg}	Sp.	$\log T_e$	B.C. $- C$	M_{bol}	$\log L$	$\log R$	$\log \boldsymbol{m}$	Q
NGC 2244, 15	7.9	1.10	−4.4	O6	4.8:	−4.7	−9.1	5.49	0.66:	1.76:	3
..... 8	8.5	1.13	4.1	O9	4.50	3.0	7.1	4.69	0.86	1.99	2
NGC 2264, 60	14.6	1.36	4.7	O7(+)	4.68	4.0	8.7	5.33	0.82	2.18	1
NGC 2362, 1	9.9	1.19	6.4	O8.5	4.55	3.3	9.7	5.73	1.28	2.47	4
NGC 6871, 2	9.4	1.17	5.7	O9w	4.50	3.0	8.7	5.33	1.18	2.35	6
..... 5	15.2	1.38	5.4	Bo	4.40	2.5	7.9	5.01	1.22	2.60	5
NGC 7380, 1	5.4	0.93	−4.6	O9	4.50	−3.0	−7.6	4.89	0.96	1.89	7

The data of the last columns are shown graphically in Figures 1 and 2. The general position of Trumpler's stars in these diagrams is explained by the observational selection for large values of $\boldsymbol{m}/R$, in connection with an intrinsic scatter of the O and B stars in these diagrams.

The spectroscopic binaries Plaskett's star and HD 698, studied by Pearce, for which $\boldsymbol{m}_1 \sin^3 i = 76\,\odot$ and $113\odot$, respectively, are probably objects similar to Trumpler's cluster stars, whereas AO Cas and 29 CMa are very luminous but of only medium large mass. The latter stars form a continuation of the less massive stars, both in stellar model (Chandrasekhar) and in the mass-luminosity relation, which for these stars is approximately

$$L = \boldsymbol{m}^{3\frac{1}{2}} \qquad (\tfrac{1}{3} < \boldsymbol{m} < 40)\,. \tag{4}$$

Considering the smaller masses only, the relation

$$L = \boldsymbol{m}^{4\frac{1}{2}} \qquad (\tfrac{1}{2} < \boldsymbol{m} < 2\tfrac{1}{2}) \tag{5}$$

fits the data considerably better. This conclusion is consistent with the theoretical mass-luminosity relation

$$L = c.\frac{m^{5\frac{1}{2}}(\mu\beta)^{7\frac{1}{2}}}{\kappa_0 R^{\frac{1}{2}}} \tag{6}$$

in connection with the theoretical result $\beta \cong 1$, with the theoretical variation of κ_0 and the empirical variation of R, if we assume μ to be constant.

Formula (4) is only roughly correct, and its interpretation is less direct since the decrease of β with increasing m has also to be taken into account.

YERKES OBSERVATORY
June 1938

TABLES FACILITATING THE CALCULATION OF LINE ABSORPTION COEFFICIENTS

F. HJERTING

ABSTRACT

A table of the integral $\frac{a}{\pi}\int_{-\infty}^{+\infty}\frac{e^{-v^2}dy}{a^2+(v-y)^2}$ is calculated by numerical quadratures for values of a up to 0.2, and, with somewhat less accuracy, for values of a up to 0.5.

The coefficient of line absorption resulting as a consequence of natural damping, collision damping, and Doppler broadening is given by the well-known expression[1]

$$\frac{\kappa_\nu}{\kappa_0}=\frac{a}{\pi}\int_{-\infty}^{+\infty}\frac{e^{-v^2}dy}{a^2+(v-y)^2}. \tag{1}$$

The following notation is used:

κ_ν Line absorption coefficient at frequency ν

κ_0 Fictitious absorption coefficient at the center of the line, when the damping is vanishing [eq. (8)]

$b^{(\nu)}$ Doppler width $b^{(\nu)}=\sqrt{\frac{2kT}{Am_0}}\cdot\frac{\nu}{c}$, in frequency units

A Atomic weight in units of m_0

δ' Effective natural line width [eq. (9)]

v Deviation from the center of the line in units of the Doppler width, i.e., $v=\frac{\nu-\nu_0}{b^{(\nu)}}$

a Ratio of effective natural line width to Doppler width, i.e., $a=\frac{\delta'}{b^{(\nu)}}$. We use the same definition of a as do Mitchell and Zemansky. Other authors denote by a a quantity equal to twice our a

The integral in (1) can be evaluated with the aid of series expressions or by numerical quadratures. For $a\geqq 0.5$ convenient series ex-

[1] E.g., M. Born, *Optik*, § 93, Berlin, 1932; A. C. G. Mitchell and M. W. Zemansky, *Resonance Radiation and Excited Atoms*, pp. 319 ff., Cambridge, 1934; A. Unsöld, *Physik der Sternatmosphären*, § 44, Berlin, 1938.

pressions have been given by Zemansky,[2] who also gives tables of the integral for $a = 0.5$, 1.0, and 1.5. Born[3] gives series expressions for large values of a, and tables for $a = 0.5$, 1.0, 2.0, and 10.0. Mitchell and Zemansky[4] give an expression for small values of a, 0.01 or less, and convenient tables for the numerical calculation of the integral in this case. Thus, the intermediate region of a-values between 0.01 and 0.5 is not so well covered. At the suggestion of Professor B. Strömgren I have, with the aid of numerical quadratures, calculated a table of the integral in (1) as a function of v and a, for values of a up to $a = 0.20$. Larger values of a will not normally occur in astrophysical applications. In the calculations an accuracy in κ_ν/κ_0 of one-tenth of 1 per cent, or better, was maintained.

Two different procedures were used in calculating the integral in (1). For moderate values of v ($v \leqq 3.5$) the following procedure was used. The transformation of the integral in (1) to the following form, first given by Reiche,[5] is well known:

$$\frac{\kappa_\nu}{\kappa_0} = \frac{1}{\sqrt{\pi}} \int_0^\infty e^{-ax-(x^2/4)} \cos(vx)dx \,. \tag{2}$$

For small values of a it is natural to expand the factor e^{-ax} in the integrand in powers of a. Retaining only the first two terms in the expansion, the expression referred to results

$$\frac{\kappa_\nu}{\kappa_0} = e^{-v^2} + \frac{2a}{\sqrt{\pi}}\left[-1 + 2ve^{-v^2}\int_0^v e^{x^2}dx\right] . \tag{3}$$

Mitchell and Zemansky[4] give tables with argument v of e^{-v^2} and of the function in brackets.

The following equation is valid quite generally:

$$\left.\begin{aligned}\frac{\kappa_\nu}{\kappa_0} = e^{-v^2} + \frac{2a}{\sqrt{\pi}}\left[-1 + 2ve^{-v^2}\int_0^v e^{x^2}dx\right] \\ + \frac{1}{\sqrt{\pi}}\int_0^\infty [e^{-ax} - 1 + ax]e^{-x^2/4}\cos(vx)dx\end{aligned}\right\} \tag{4}$$

[2] *Phys. Rev.*, **36**, 219, 1930; cf. also Mitchell and Zemansky, *op. cit.*, p. 329.

[3] *Op. cit.* Born's η is $1/a$, his x is v/a, and κ_ν/κ_0 is $-1/(a\sqrt{\pi})$ times Born's ψ.

[4] *Loc. cit.* Cf. also D. H. Menzel, *Pub. Lick Obs.*, **17**, 229, 1931; E. F. M. v. d. Held, *Zs. f. Phys.*, **70**, 508, 1931.

[5] *Verh. d. D. Phys. Ges.*, **15**, 3, 1913.

or

$$\frac{\kappa_\nu}{\kappa_0} = e^{-v^2} + a \cdot \varphi(v) + \psi(a, v) . \tag{5}$$

For relatively small values of a this equation is a more convenient basis for numerical quadratures than (2), since the product of the first and the second factor is then always quite small. With increasing values of v, however, the calculations become increasingly laborious, because the largest interval that can be conveniently used in the numerical quadratures is inversely proportional to v. Equation (4) was used up to $v \leqq 3.5$, and for $a \leqq 0.10$ up to $v \leqq 4.0$.

For moderately large, and large, values of v, equation (1) is quite a convenient basis for the numerical quadratures. Generally, for the relatively small values of a in question the denominator of the integrand in (1) varies in such a way in the neighborhood of $y = v$ as to make the equation unsuitable as a basis for numerical quadratures. When, however, v is large, the numerator is so small for $y = v$ as to make the contribution of the immediate neighborhood of $y = v$ to the integral practically negligible.

The two procedures of calculation thus supplement each other. A few values were calculated by both procedures so that a check on the calculations was obtained.

For $a \leqq 0.2$ and $v \geqq 5$ the integral in (1) is independent of a within an accuracy of better than two-tenths of 1 per cent [eqs. (6) and (7)]. Thus, a table with one argument, equivalent to the table given by Mitchell and Zemansky[4] of the bracketed function in (3), suffices for $v \geqq 5$.

The following asymptotic series expression [eq. (4)] was used to check the calculations for moderately large values of v ($v \geqq 4$):

$$\left.\begin{aligned} \frac{1}{\sqrt{\pi}}\int_0^\infty [e^{-ax} - 1 + ax]e^{-x^2/4} \cos(vx)dx \\ = -\frac{a^3}{\sqrt{\pi}v^4}\left[1 + \frac{5}{v^2} + \frac{105}{4v^4} + \ldots .\right]. \end{aligned}\right\} \tag{6}$$

Also[4] for large values of v

$$\frac{\kappa_\nu}{\kappa_0} = \frac{a}{\sqrt{\pi}v^2}\left[1 + \frac{3}{2v^2} + \frac{15}{4v^4} + \ldots .\right]. \tag{7}$$

The results of the calculations are given in the tables that follow. It was not necessary to carry out numerical quadratures for all the values given, interpolation being used as far as the resulting interpolated values were deemed sufficiently accurate.

A table of less accurate values is also given for a up to 0.5. The accuracy of the calculation of these values was about 1 per cent. The table may be of use in certain problems of theoretical physics.

The arrangement of the tables is as follows. Table 1 contains numerical values of the third term in (4) and (5) —i.e., $\psi(a, v)$—together with two-figure values of κ_ν/κ_0. The purpose of Table 1 is to show the relative importance of the third term for various values of a and v. For $a = 0.03$ the third term is always less than 0.5 per cent, for $a = 0.10$ it is less than 3 per cent, and for $a = 0.20$ it is less than 9 per cent. Thus, our calculations show that when an accuracy of, say, 10 per cent is sufficient, the expression $e^{-v^2} + a \cdot \varphi(v)$ can be used up to $a \leqq 0.2$, i.e., considerably farther than was anticipated.[4] Table 2 gives numerical values of κ_ν/κ_0 with arguments a and v up to $v = 5$. Table 3 gives $(1/a)\ (\kappa_\nu/\kappa_0)$ with argument v for $v \geqq 5$. Table 4 contains two-figure values of κ_ν/κ_0 up to $a = 0.5$ for $v \leqq 5$. For $v \geqq 5$ Table 3 gives two-figure accuracy up to $a = 0.5$.

TABLE 1

v	$a=0.01$		$a=0.05$		$a=0.10$		$a=0.20$	
	κ_ν/κ_0	$100\psi(a, v)$	κ_ν/κ_0	$100\psi(a, v)$	κ_ν/κ_0	$100\psi(a, v)$	κ_ν/κ_0	$100\psi(a, v)$
0.00	0.99	+0.01	0.95	+0.24	0.90	+0.93	0.81	+3.5
0.25	.93	+ .01	.89	+ .20	.85	+ .77	.77	+2.9
0.50	.77	.00	.75	+ .10	.72	+ .38	.66	+1.4
0.75	.57	.00	.56	− .01	.55	− .04	.52	−0.1
1.0	.37	.00	.37	− .08	.37	− .32	.37	−1.2
1.5	.11	.00	.12	− .09	.13	− .35	.16	−1.3
2.0	.021	.000	.030	− .031	.040	− .13	.059	−0.52
2.5	.0032	.0000	.0084	− .0058	.015	− .024	.027	− .12
3.0	.00091	.00000	.0040	− .0008	.0079	− .0036	.016	− .021
3.5	.00054	.00000	.0027	− .0001	.0053	− .0008	.011	− .0060
4.0	.00039	.00000	.0020	− .0001	.0039	− .0003	.0078	− .0028
4.5	.00030	.00000	.0015	.0000	.0030	− .0002	.0060	− .0017
5.0	0.00024	0.00000	0.0012	0.0000	0.0024	−0.0001	0.0048	−0.0010

TABLE 2

a	v										
	0.00	0.25	0.50	0.75	1.00	1.25	1.50	1.75	2.00	2.25	2.50
0.00	1.000	0.939	0.779	0.570	0.368	0.210	0.105	0.0468	0.0183	0.00633	0.00193
.01	0.989	.930	.772	.567	.369	.212	.109	.0497	.0206	.00806	.00323
.02	0.978	.920	.766	.565	.370	.215	.112	.0525	.0229	.00979	.00452
.03	0.967	.910	.760	.562	.370	.217	.115	.0553	.0252	.0115	.00581
.04	0.956	.901	.753	.560	.371	.220	.118	.0581	.0274	.0132	.00710
.05	0.946	.892	.747	.558	.371	.222	.121	.0608	.0296	.0149	.00838
.06	0.936	.883	.741	.555	.372	.224	.123	.0635	.0318	.0166	.00966
.07	0.926	.874	.735	.552	.372	.226	.126	.0660	.0339	.0182	.0109
.08	0.916	.865	.729	.550	.373	.229	.129	.0687	.0360	.0198	.0122
.09	0.906	.856	.723	.548	.373	.231	.131	.0713	.0381	.0215	.0134
.10	0.896	.848	.718	.545	.373	.232	.134	.0737	.0402	.0231	.0147
.11	0.887	.840	.712	.542	.374	.234	.136	.0762	.0422	.0247	.0160
.12	0.878	.831	.706	.540	.374	.236	.139	.0786	.0442	.0263	.0172
.13	0.869	.823	.701	.538	.374	.238	.141	.0810	.0463	.0279	.0184
.14	0.860	.815	.695	.535	.374	.240	.144	.0833	.0482	.0294	.0196
.15	0.851	.807	.690	.532	.374	.241	.146	.0856	.0502	.0310	.0208
.16	0.842	.799	.684	.530	.374	.243	.148	.0879	.0520	.0325	.0221
.17	0.834	.792	.679	.527	.374	.244	.150	.0901	.0540	.0340	.0233
.18	0.825	.784	.674	.525	.374	.246	.152	.0922	.0558	.0356	.0245
.19	0.817	.777	.668	.522	.373	.247	.154	.0943	.0576	.0371	.0256
0.20	0.809	0.770	0.663	0.520	0.373	0.248	0.157	0.0964	0.0595	0.0385	0.0268

TABLE 2—*Continued*

a	v										
	2.50	2.75	3.00	3.25	3.50	3.75	4.00	4.25	4.50	4.75	5.00
0.00	0.00193	0.00052	0.000123	0.000026	0.000005	0.000001	0.000000	0.000000	0.000000	0.000000	0.000000
.01	.00323	.00151	.000908	.000666	.000539	.000455	.000393	.000343	.000302	.000269	.000241
.02	.00452	.00251	.00169	.00130	.00107	.000910	.000785	.000686	.000605	.000538	.000482
.03	.00581	.00350	.00248	.00194	.00161	.00136	.00118	.00103	.000907	.000806	.000722
.04	.00710	.00449	.00326	.00258	.00214	.00182	.00157	.00137	.00121	.00108	.000963
.05	.00838	.00548	.00404	.00322	.00268	.00227	.00196	.00171	.00151	.00134	.00120
.06	.00966	.00646	.00483	.00386	.00321	.00273	.00236	.00206	.00181	.00161	.00144
.07	.0109	.00745	.00561	.00450	.00374	.00318	.00275	.00240	.00212	.00188	.00169
.08	.0122	.00843	.00639	.00513	.00428	.00364	.00314	.00274	.00242	.00215	.00192
.09	.0134	.00940	.00717	.00577	.00481	.00409	.00353	.00308	.00272	.00242	.00217
.10	.0147	.0104	.00794	.00641	.00534	.00454	.00392	.00343	.00302	.00269	.00241
.11	.0160	.0114	.00872	.00704	.00587	.00500	.00432	.00377	.00332	.00295	.00265
.12	.0172	.0123	.00949	.00768	.00640	.00545	.00471	.00411	.00362	.00322	.00289
.13	.0184	.0133	.0103	.00831	.00693	.00590	.00510	.00445	.00392	.00349	.00313
.14	.0196	.0142	.0110	.00894	.00746	.00635	.00549	.00479	.00423	.00376	.00337
.15	.0208	.0152	.0118	.00957	.00799	.00680	.00588	.00513	.00453	.00403	.00361
.16	.0221	.0162	.0126	.0102	.00852	.00726	.00627	.00547	.00483	.00429	.00385
.17	.0233	.0171	.0133	.0108	.00905	.00771	.00666	.00581	.00513	.00456	.00409
.18	.0245	.0180	.0141	.0115	.00958	.00816	.00705	.00615	.00543	.00483	.00433
.19	.0256	.0190	.0149	.0121	.0101	.00860	.00744	.00649	.00573	.00510	.00457
0.20	0.0268	0.0199	0.0156	0.0127	0.0106	0.00906	0.00783	0.00683	0.00603	0.00536	0.00481

With the aid of the tables, the calculation of the line absorption coefficient within an absorption line originating from the ground state runs as follows. Let τ be the mean lifetime corresponding to the

TABLE 3

v	$\frac{\kappa_\nu/\kappa_0}{a}$	v	$\frac{\kappa_\nu/\kappa_0}{a}$	v	$\frac{\kappa_\nu/\kappa_0}{a}$
5.0	0.0241	10.0	0.00573	15.0	0.00251
5.5	.0197	10.5	.00519	15.5	.00235
6.0	.0164	11.0	.00472	16.0	.00221
6.5	.0139	11.5	.00432	16.5	.00208
7.0	.0119	12.0	.00396	17.0	.00196
7.5	.0103	12.5	.00365	17.5	.00185
8.0	.00903	13.0	.00337	18.0	.00175
8.5	.00798	13.5	.00312	18.5	.00166
9.0	.00710	14.0	.00290	19.0	.00157
9.5	.00636	14.5	.00270	19.5	.00149
10.0	0.00573	15.0	0.00251	20.0	0.00142

TABLE 4

v	κ_ν/κ_0					
	$a=0.0$	$a=0.1$	$a=0.2$	$a=0.3$	$a=0.4$	$a=0.5$
0.00	1.00	0.90	0.81	0.74	0.67	0.62
0.25	0.94	.85	.77	.70	.64	.59
0.50	0.78	.72	.66	.62	.57	.53
0.75	0.57	.54	.52	.50	.47	.44
1.00	0.37	.37	.37	.37	.36	.36
1.25	0.21	.23	.25	.26	.27	.27
1.50	0.10	.13	.16	.17	.19	.20
1.75	0.047	.074	.096	.12	.13	.14
2.00	0.018	.040	.060	.076	.090	.103
2.50	0.002	.015	.027	.038	.049	.058
3.00	0.0001	.0079	.016	.023	.030	.037
3.50	0.0000	.0053	.011	.016	.021	.026
4.00	0.0000	.0039	.0078	.012	.016	.019
4.50	0.0000	.0030	.0060	.0090	.012	.015
5.00	0.0000	0.0024	0.0048	0.0072	0.0096	0.012

transition between the two stationary states k (upper state) and 1 (lower state) in question. Then

$$\kappa_0 = \frac{1}{\tau}\frac{q_k}{q_1}\frac{\lambda^2}{8\pi\sqrt{\pi}}\frac{1}{b^{(\nu)}}\cdot N_1 = \frac{1}{\tau}\frac{q_k}{q_1}\frac{\lambda^3}{8\pi\sqrt{\pi}}\sqrt{\frac{A m_0}{2kT}}\cdot N_1\,, \qquad (8)$$

where q_k and q_i are the statistical weights of the states k and i, c the velocity of light, $b^{(\nu)}$ the Doppler width in frequency units, and N_i the number of absorbing atoms in state i per gram. Further,

$$\delta' = \frac{1}{4\pi}\sum_{r<k} a_{kr} + \frac{1}{2\pi} S\,, \tag{9}$$

where S is the number of broadening collisions[6] per second, and

$$\left.\begin{aligned} b^{(\lambda)} &= \sqrt{\frac{2kT}{Am_0}}\,\frac{\lambda}{c} \\ b^{(\nu)} &= \sqrt{\frac{2kT}{Am_0}}\,\frac{1}{\lambda} \end{aligned}\right\}, \tag{10}$$

$b^{(\lambda)}$ and $b^{(\nu)}$ being the Doppler width in wave-length and frequency units, respectively. Then if $\lambda-\lambda_0$ is the deviation of the wave length considered from the center of the line, in wave-length units,

$$v = \frac{\lambda - \lambda_0}{b^{(\lambda)}} \tag{11}$$

and, further,

$$a = \frac{\delta'}{b^{(\nu)}}\,. \tag{12}$$

Now, Table 2 gives κ_ν/κ_0 as a function of a and v, then κ_ν follows immediately, since κ_0 is given by (8). In making calculations of line contours, or equivalent widths, the values of $\lambda-\lambda_0$ can usually be chosen such that interpolation in Table 2 with respect to v is avoided.

For a subordinate line the calculation runs quite similarly if it is permissible to assume that the atoms in the lower state are distributed according to the normal distribution. In that case it is only necessary to use the well-known Weisskopf-Wigner equation corresponding to equation (9).

OBSERVATORY, COPENHAGEN
June 1938

[6] E.g., Mitchell and Zemansky, *loc. cit.*; Unsöld, *loc. cit.*, and the references there given.

ON THE INTEGRATION OF THE EQUATION OF RADIATIVE TRANSFER

P. SWINGS AND L. DOR

ABSTRACT

The equation of the radiative transfer has been integrated by a generalization of Spitzer's method, which makes use of Bessel functions.

1. In solving the equation of radiative transfer appropriate to the problem of the formation of absorption lines, it is necessary to take into account the variation of the Planck intensity B_ν as function of the total optical depth within the line. To a sufficient approximation, B_ν may be expected to be a linear function of the form $a_\nu + b_\nu\tau$, where τ is the optical depth in the continuous spectrum; τ is defined with respect to the Rosseland mean absorption coefficient over the whole spectrum. On the other hand, we cannot, in general, expect B_ν to be a linear function of the optical depth t_ν. The point at issue here is the circumstance to which Strömgren[1] has recently drawn attention:

> Line absorption affects the intensity within the radiated spectrum in two ways. First, it cuts down the intensity as would increased continuous absorption, the effect depending upon the existence of a temperature gradient in the stellar atmosphere. Second, it causes a deviation from Kirchhoff's law, in the sense that emission is reduced, so that there is a further reduction in the radiated intensity.

Spitzer's recent solution[2] of the equation of transfer in terms of Bessel functions is seen to take into account the second of the foregoing two effects "rigorously," while the first effect is taken into account by assuming for B_ν a linear function in t_ν (which assumption cannot generally be valid). For this reason the perturbation theory, developed by Strömgren,[1] is of greater value inasmuch as Strömgren's method in fact allows quite a considerable variation in η_ν.[3]

However, it is of some interest to supplement Spitzer's analysis

[1] *Ap. J.*, **86**, 1, 1937.

[2] *Ap. J.*, **87**, 1, 1938.

[3] *Ap. J.*, **86**, 1, 1937, Table II.

by calling attention to the fact that several other possibilities of rigorous solutions exist for the equation of radiative transfer. Such possibilities are indicated here in a summarized form, no analytical discussion or expression of the residual intensity being added, as this would proceed along the same line as in Spitzer's paper. In any special example (i.e., for a definite model and frequency), it will be possible to select the analytical case which best approximates the physical conditions.

2. Using classical notations, the equation of radiative transfer may be written

$$\frac{d^2J_\nu(t_\nu)}{dt_\nu^2} = 3\,\frac{(1+\epsilon\eta_\nu)}{1+\eta_\nu}\left\{J_\nu(t_\nu) - \frac{1+\epsilon\eta_\nu Q}{1+\epsilon\eta_\nu}\,B_\nu(t_\nu)\right\}, \tag{1}$$

where

$$dt_\nu = (1+\eta_\nu)d\tau_\nu\,. \tag{2}$$

We assume, as usual,

$$\frac{1+\epsilon\eta_\nu Q}{1+\epsilon\eta_\nu}\,B_\nu(t_\nu) = a_\nu + p_\nu t_\nu\,, \tag{3}$$

and substitute

$$y(t_\nu) = J_\nu(t_\nu) - (a_\nu + p_\nu t_\nu) \tag{4}$$

$$\lambda(t_\nu) = \frac{1+\epsilon\eta_\nu}{1+\eta_\nu} \tag{5}$$

Thus, we get instead of (1)

$$\frac{d^2y}{dt_\nu^2} = 3\lambda(t_\nu)\cdot y(t_\nu)\,. \tag{6}$$

Spitzer's treatment consists essentially in finding adequate substitutions which convert equation (6) into a Bessel equation of the type

$$\frac{d^2y}{dw^2} + \frac{1}{w}\cdot\frac{dy}{dw} - \left(1+\frac{n^2}{w^2}\right)y = 0\,. \tag{7}$$

Solution I of Spitzer is

$$\lambda = \frac{1}{A}\,(1 + mt_\nu)^{-s/s+1}\,,$$

with

$$m = (s + 1)\,\frac{D}{A}\,,$$

s, A, and D being constants.

Solution II is

$$\lambda = L + Me^{-ut_\nu}\,,$$

L, M, and u being constants.

3. Substituting

$$z = \alpha + \beta t_\nu\,, \tag{8}$$

(6) keeps its essential form and becomes

$$\frac{d^2y_1}{dz^2} = \frac{3\lambda(z)}{\beta^2} \cdot y_1(z)\,. \tag{9}$$

We may try to find a substitution of independent variable $w(z)$ and of unknown

$$y(z) = u(z) \cdot y_1(z)\,, \tag{10}$$

which transforms (7) into (9).

After some easy algebra, it is found that we need, therefore,

$$\frac{d^2z}{dw^2} + \frac{1}{w} \cdot \frac{dz}{dw} + \left(\frac{2}{u} \cdot \frac{du}{dz}\right) \cdot \left(\frac{dz}{dw}\right)^2 = 0 \tag{11}$$

$$-\frac{3\lambda}{\beta^2} = \frac{1}{u} \cdot \frac{d^2u}{dz^2} + \frac{1}{\left(\frac{dz}{du}\right)^2} \cdot \left[\frac{1}{u} \cdot \frac{du}{dz}\left(\frac{d^2z}{dw^2} + \frac{1}{w}\frac{dz}{dw}\right) - \left(1 + \frac{n^2}{w^2}\right)\right] = 0\,. \tag{12}$$

Solution I of Spitzer corresponds to

$$z = aw^b\,; \quad u = z^{-1/2}\,; \quad z = 1 + mt_\nu\,,$$

a, b, and m being constants which may be immediately related to Spitzer's coefficients.

Solution II corresponds to

$$w = ae^{bz} ; \quad u = \text{const.} ; \quad z = t_\nu .$$

The equations (11) and (12) generalize Spitzer's results; (11) may be replaced immediately by a first-order linear equation which brings

$$\frac{dz}{dw} = \frac{1}{w\left[\text{const.} + \int\left(\frac{2}{u} \cdot \frac{du}{dz}\right) \cdot \frac{dw}{w}\right]} . \tag{13}$$

We may take, for instance,

$$u = e^z ; \quad z = a + bt_\nu ; \quad w = \left[\frac{1}{A} \cdot e^{Be^{2(a+bt)}}\right]^{1/2} ;$$

then λ has the following form

$$3\lambda = b^2 + b^2n^2B^2e^{4z} + \frac{b^2B^2}{A} \cdot e^{4z+Be^{2z}} , \tag{14}$$

a, b, A, B, and n, being constants. and the solution is, accordingly,

$$y = e^{-(a+bt_\nu)} \cdot [c_1 \cdot I_n(w) + c_2 \cdot K_n(w)] . \tag{15}$$

$I_n(w)$ and $K_n(w)$ are the usual Bessel functions of imaginary argument.

Obviously, instead of transforming (6) into (7), we could have taken the other Bessel equation, or, more generally, any other well-known type of differential equation of the second order, namely, that providing the orthogonal polynomials.

4. Equation (6) being linear and homogeneous with regard to y and d^2y/dt^2, the substitution

$$y = e^{\int u dt} \tag{16}$$

will transform (6) into a Riccati equation

$$\frac{du}{dt} + u^2 = 3\lambda(t) ,$$

and a solution by quadratures is always obtainable when

$$3\lambda(t) = \frac{d\mu}{dt} + \mu^2 , \tag{17}$$

μ being any function of t.

The solution is actually

$$u = \mu - \frac{1}{v} , \tag{18}$$

with

$$v = e^{2\int \mu dt} \left\{ c_1 - \int e^{-2\int \mu dt} dt \right\} . \tag{19}$$

For instance, if

$$\mu = \frac{f'(t)}{f(t)} \quad \text{or} \quad 3\lambda(t) = \frac{f''(t)}{f(t)} , \tag{20}$$

$f(t)$ being any function, we have

$$y = c_1 f(t) + c_2 f(t) \cdot \int \frac{dt}{f^2(t)} . \tag{21}$$

The simple case $f(t) = At^m$ brings

$$3\lambda(t) = \frac{m(m-1)}{t^2} \quad \text{and} \quad y = c_1 t^m + c_2 t^{-m+1} . \tag{22}$$

5. Let

$$y = f(t) \tag{23}$$

be a solution of (6); suppose we may write $t = F(y)$. Then (6) becomes

$$\frac{d^2y}{dt^2} = 3\lambda[F(y)] \cdot y = \varphi(y) \cdot y . \tag{24}$$

Thus

$$dt = [2\int\varphi(y)\cdot y\cdot dy + c_1]^{-1/2}\cdot dy\,. \tag{25}$$

By quadrature we shall find t as a function of y.

In other words, if we take any function $\varphi(y)$, we shall get $y = f(t)$ by quadrature, and then

$$3\lambda(t) = \varphi(y) = \varphi[f(t)]\,. \tag{26}$$

For instance, if

$$\varphi(y) = \frac{A}{y}\,,$$

we find

$$y = \frac{A}{2}t^2 + Bt + C\,,$$

with

$$3\lambda = \frac{2A}{At^2 + 2Bt + 2C}\,,$$

A, B, and C being constants.

6. Summarizing, we may state: (1) Spitzer's method introducing Bessel functions may be generalized by formulae (11) and (12) [Example: formula (15)]; (2) and substitution (16) give a solution by quadrature when $\lambda(t)$ verifies the general relation (17) [Examples: formulae (20) and (21)]; (3) another integration by quadrature is given by formula (26); this may in some cases give simple solutions.

Our thanks are due to S. Chandrasekhar for valuable suggestions.

UNIVERSITY OF LIÉGE, BELGIUM
DEPARTMENT OF ASTROPHYSICS
April 10, 1938

NOTES

ON COLLAPSED NEUTRON STARS

ABSTRACT

Some consequences are discussed of the hypothesis that certain stars and cores of stars are composed mainly of neutrons. On the assumption that supernovae represent rapid transitions of ordinary stars into neutron stars, the large red shifts observed in the spectra of the recent bright supernovae are interpreted as gravitational red shifts. The neutron-star hypothesis, in conjunction with the general theory of relativity, leads to a theory of critical stellar masses.

In view of the rapid advances made recently in the observation of supernovae, it seems appropriate to give here a brief summary of some conclusions of a series of theoretical investigations concerning the properties of highly collapsed neutron stars, which it is hoped may be ready for publication in the near future.

The neutron-star hypothesis was first introduced by Baade and myself[1] in an effort to account for the tremendous liberation of energy in supernovae. We suggested the existence of stars and cores of stars the average density of which is comparable with the density of matter ordinarily encountered only inside of atomic nuclei. With the designation "neutron star" we do not wish to imply, however, that such a star is to be regarded as a giant nucleus composed of separate neutrons of precisely the same character as free neutrons. We only suggest, that, in contradistinction to ordinary stellar matter, in neutron stars already minute regions whose linear dimensions are larger than $\delta = e^2/m_e c^2 = 2.8 \times 10^{-13}$ cm are electrically neutral.

We here briefly describe some of the properties of neutron stars, as well as some new observations of supernovae which tend to support the neutron-star hypothesis.

a) Cold neutron stars, according to present knowledge, represent states of lowest energy that matter may assume without being completely transformed into radiation.

[1] W. Baade and F. Zwicky, *Proc. Nat. Acad. Sci.*, **20**, 259, 1934, and *Phys. Rev.* **45**, 138, 1934, and **46**, 67, 1934; F. Zwicky, *Scientific Monthly*, **40**, 461, 1935. More recently the neutron-star hypothesis has also been considered by G. Gamow, *Atomic Nuclei*, p. 234, Oxford, 1937; L. Landau, *Nature*, **141**, 334, 1938; and others.

b) According to the general theory of relativity, a *limiting mass* of stars exists for every given average density (Schwarzschild limit).[2] At this limit the energy liberated because of gravitational packing is

$$E = \left(1 - \frac{4}{3\pi}\right) Mc^2 = 0.58\, Mc^2 ,$$

where M is the proper mass of the star. For an average density $\rho = 10^{14}$ gm/cm^3 the limiting mass is $M_L = 6.4 \times 10^{34}$ gm. The derivation of these results which was obtained in discussion with Professor R. C. Tolman will be communicated in a joint paper with Professor Tolman.

A star which has reached the Schwarzschild limiting configuration must be regarded as an object between which and the rest of the universe practically no physical communication is possible. For instance, the velocity of light on such a star is infinitely small, so that it requires light from this star an infinitely long time to reach any external point. Also, the gravitational red shift is complete in the sense that light originating on the star arrives at any external point with the energy zero. It is, therefore, impossible to observe physical conditions in stellar bodies which have reached the Schwarzschild limit. It should, however, be possible to observe stellar bodies in stages intermediate between the ordinary configurations and the collapsed configurations of limiting mass just described, provided that such are accessible.

c) We may express the limiting mass M_L of collapsed neutron stars in terms of the universal gravitational constant

$$\Gamma = 6.66 \times 10^{-8}\ \text{gm}^{-1}\ \text{cm}^3\ \text{sec}^{-2} ,$$

the charge of the electron e and the masses m_e, m_p, and m_n of the electron, the proton, and the neutron, respectively. We obtain

$$M_L = \alpha R^{3/2} m_n , \tag{1}$$

where

$$R = \frac{e^2}{\Gamma m_p m_e} = 2.3 \times 10^{39} \tag{2}$$

[2] See, e.g., R. C. Tolman, *Relativity, Thermodynamics and Cosmology*, p. 247, Oxford, 1934.

is the ratio of the electrical to the gravitational attraction between an electron and a proton and where α is a dimensionless number of the order 1. The number of neutrons in the mass M_L is $N = \alpha R^{3/2}$. According to an idea first discussed by H. Weyl,[3] the ratio R may play a role in the determination of large numbers, such as the total number of particles in the universe and the ratio between the "radius" of the universe and the radius of the proton. The fact that M_L is proportional to $R^{3/2}$ suggests possible observational tests of Weyl's idea, which will be discussed in another place.

d) If supernovae are transitions from ordinary stars into neutron stars, the observation of light-curves and spectra of supernovae should furnish us with direct evidence of the neutron-star hypothesis. For instance, the surface of the central star of a supernova should be exceedingly hot, the acceleration of gravity very high, and light coming from this surface should be subject to enormous gravitational red shifts. Now, it is a significant fact, first observed by Dr. R. Minkowski in the spectrum of the recent bright supernova in IC 4182, which was at its maximum brightness in August, 1937, that all of the permanent features of this spectrum have gradually shifted toward the red, until in June, 1938, a stage S was reached when this shift amounted to 100 angstroms.[4] On our hypothesis we may tentatively interpret this red shift as a gravitational red shift. Assuming that the central star has a mass $M_c = 2 \times 10^{33}$ gm, equal to that of the sun, the following characteristics for the central star in the stage S may be derived: radius $r = 74$ km; average density $\rho = 1.2 \times 10^{12}$ gm/cm^3. Since the supernova in the stage S was about one million times brighter than the sun, it follows that the effective surface temperature $T > 1.8 \times 10^7$ degrees absolute. For the limiting mass $M_L = 6.3 \times 10^{34}$ gm we obtain $r = 3700$ km, $\rho = 1.2 \times 10^9$ gm/cm^3, and $T > 3.1 \times 10^6$ degrees. The neutron-star hypothesis in conjunction with observations on supernovae may therefore lead to some new and far-reaching tests of the general

[3] H. Weyl, *Raum, Zeit, Materie*, 5th ed., p. 277, Springer, Berlin, 1923. See also *Naturwissenschaften*, **22**, 145, 1934.

[4] The spectra of the supernovae in NGC 1003 (1937) and NGC 4273 (1936) exhibit similar effects. I am indebted to Dr. Minkowski for the permission to make use here of these unpublished observational facts, which he will present in detail in a paper shortly to be published in this *Journal*.

theory of relativity. Also, the fascinating problem now presents itself of investigating how certain well-known physical processes, such as nuclear reactions, will be modified when they take place inside of highly collapsed stars in which the very properties of time and space are drastically altered.

F. ZWICKY

CALIFORNIA INSTITUTE OF TECHNOLOGY
PASADENA, CALIFORNIA
August 8, 1938

SPECTRAL TYPES AND RADIOMETRIC OBSERVATIONS OF STARS OF LARGE INFRARED INDEX

In a recent paper Hetzler[1] announced the discovery of a number of red stars with exceptionally large infrared indices, some of the values being as large as 10 mag. If one uses these indices as a basis for temperature determinations, on the assumption of black-body radiation, the large indices will yield temperatures of about 1000°. The objects of infrared magnitudes 4 to 6 having this temperature would be within easy reach of a vacuum thermocouple, the radiometric magnitudes being of the order of 0 to −2. For this reason it was considered worth while to study the stars radiometrically. At the same time a determination of their spectral types seemed desirable.

The radiometric measurements were made with a vacuum thermocouple[2] at the 24-inch reflector with a junction of bismuth against 95 per cent bismuth plus 5 per cent tin and with a highly sensitive galvanometer. Provisional results were obtained with the equipment not yet developed to its full sensitivity; at the time of the measurements a star of radiometric magnitude 3 gave a measurable deflection. The measurements consisted of a comparison of three of the more promising stars of large infrared index with α Orionis and α Tauri. The visual magnitudes of the chosen stars were 11.5, 12.5, and 14.0; the first two stars are included in Table 1. No deflection

[1] *Ap. J.*, **86**, 509, 1937.

[2] A more complete description of the radiometric equipment will be given later.

of the galvanometer was observable in the case of the selected stars, indicating that their radiometric magnitudes must be fainter than 3.0.

The spectra were obtained at the 40-inch refractor with the one-prism spectrograph designed by Dr. Kuiper.[3] Twenty stars have been observed, their infrared indices ranging from 2.0 to 8.0 mag.

TABLE 1

Star	1855		Infrared Index (Hetzler)	Spectrum†
	R.A.	Decl.		
IV:3*	19^h26^m1	$+23°\ 20'.3$	$8^m.0$	S_3
V:1	1 17.6	54 23.9	7.5	M9
V:2	1 51.0	57 54.6	6.8	M7
I:5	22 1.1	58 5.3	6.6	M7
IV:5	19 18.5	21 11.5	6.5	(M8)
IV:6	19 17.0	26 52.8	6.2	S_3
V:5	1 32.4	55 46.7	6.1	(M7)
I:9	21 47.6	55 17.7	6.0	M7
IV:7	19 17.2	26 42.6	5.9	M8
I:15	21 40.4	58 11.2	5.6	M7
FI Lyr	18 36.4	28 49.0	5.5	M9
II:3*	4 54.0	56 25.6	5.1	M6
V:3	1 24.2	57 0.9	5.0	R or N‡
V:14	1 34.1	58 4.5	4.9	M6
V:13	1 30.2	58 58.5	4.5	$S_3\pm$
V:19	1 34.6	55 36.8	4.2	M_5
RV Cam	4 18.7	57 5.2	4.0	M6
BD+53°413	1 44.3	53 31.6	3.8	M1
V:18	1 15.9	58 4.4	3.5	M_5
BD+22°3792	19 41.9	22 24.6	3.2	$K_4\pm$
VX Cas	0 23.2	61 12.0	.....	M_2
T Per	2 9.0	58 17.3	2.0	K_1
EP Lyr	19 12.5	27 35.0	.....	F8
X Lyr	19 7.2	+26 32.0	.....	M_5

† The S and M stars are classified very easily. The values in parentheses are uncertain and provisional.

‡ In the spectral region used, these spectral types look very similar.

Table 1 gives the spectral types obtained. The stars are designated by their field and chart numbers as given by Hetzler, the Roman numerals representing the field, the Arabic numerals the chart. Columns 2 and 3 give the position for 1855, column 4 the infrared index, and the last column the spectral type. The stars marked with an asterisk were observed radiometrically.

[3] *Ap. J.*, **87**, 592, 1938.

PLATE XX

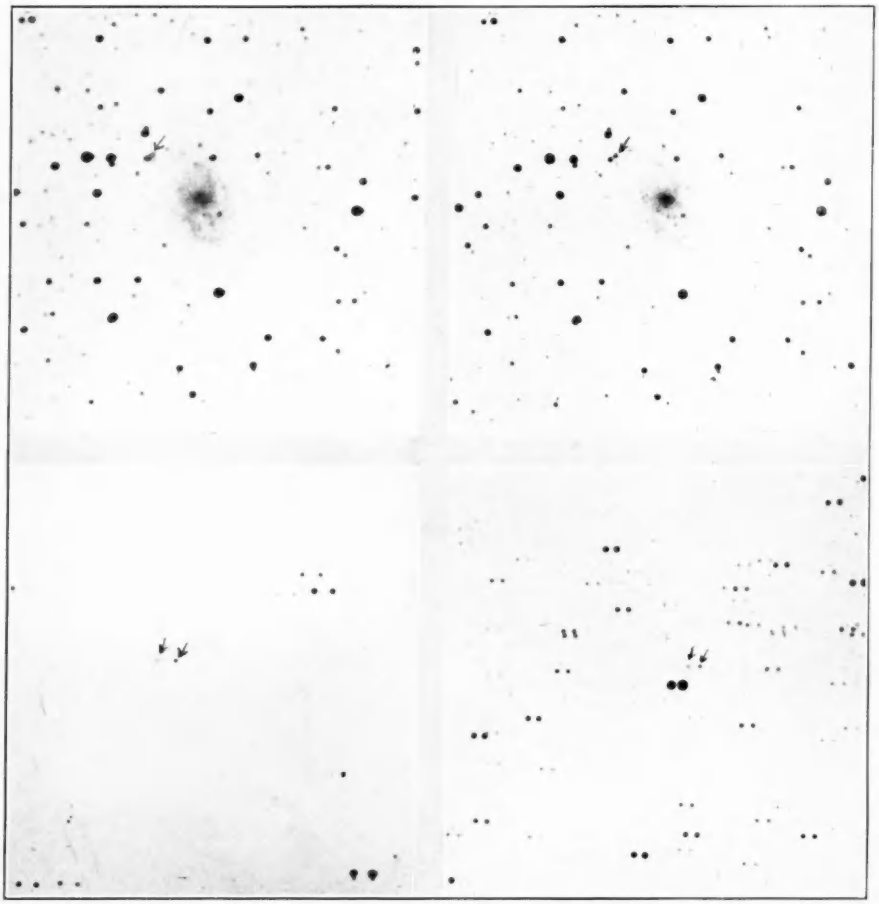

a) A double exposure of the planetary nebula NGC 7027. The right-hand exposure was obtained with a focal setting at $H\alpha$, while the faint diffuse image on the left was taken with the focal setting to the violet of $H\alpha$. The exposures were five minutes each.

b) The spiral nebula M 33, photographed on August 22/23, 1938 (on the right), with a six-hour exposure and with a focal setting appropriate for $H\alpha$.

c) Was obtained with a six-hour exposure on August 21/22, with a focal setting of 2.5 mm to the violet of $H\alpha$. The strongest emission condensation is marked by an arrow.

d) A new Wolf-Rayet star. The exposure on the right is for $H\alpha$, and that on the left is toward the violet of $H\alpha$. The exposure time was twenty minutes each.

All four exposures were obtained on Agfa Superpan Press film with filter 23A.

Table 1 shows that this sample of red stars belongs to classes M and S; no new types are found among the stars observed. Accordingly, the great redness of the stars must be interpreted as being caused by heavy band absorption and not by excessively low temperature. The radiometric observations lead to the same conclusion.

I am indebted to Professor G. P. Kuiper for the suggestion of the problem and for helpful discussions.

CARL F. RUST

YERKES OBSERVATORY
October 15, 1938

A METHOD FOR THE DETECTION OF SMALL OBJECTS HAVING EMISSION SPECTRA

During the course of an investigation of the colors of knots in extragalactic nebulae, a method was devised to detect objects having strong $H\alpha$ emission in their spectra. Briefly, the method is as follows: The suspected object is photographed through a refracting telescope on a red-sensitive plate behind a red filter. One exposure is made with the telescope focused at $H\alpha$, and another exposure is made on the same emulsion at a shorter wave length chosen in such a way that the images of normal stars on the plate are equal in size at the two focal settings. If the object in question has an emission spectrum, the image will be sharply in focus at $H\alpha$ and will be considerably out of focus at the other wave-length setting, whereas the two images of a normal star will be of equal size.

Plate XX shows some of the results that have been obtained by this method with a 6-inch refractor, at the McDonald Observatory. All the exposures were made on Agfa Super Pan Press film exposed behind a Wratten No. 23*A* filter.

Plate XX*a* is an enlargement of two five-minute exposures on the planetary nebula NGC 7027, and shows the effectiveness of the method very clearly. For the nebula, the $H\alpha$ image is quite strong, whereas the image taken to the violet of $H\alpha$ is so weak that it has practically disappeared.

Plate XX*b* and XX*c* are enlargements from two six-hour exposures on the extragalactic nebula, M33, taken at *Hα* and to the violet of *Hα*, respectively. The emission character of the three brightest knots, first announced by Hubble,[1] is confirmed by the increased strength of these knots photographed in *Hα* light. In addition, two fainter knots, hitherto not observed spectroscopically, are found by this method to be emission nebulae.

Plate XX*d* shows a photograph of a new Wolf-Rayet star discovered by this method. The position of the star is $\alpha 19^h19^m46^s.7$, $\delta + 29°28'.4$ (1900), about 4′ northwest of the fifth-magnitude star 2 Cygni. Two objective-prism plates of this object showed *Hα*, *Hβ*, and *Hγ* in emission. The fact that the lines N1 and N2 are absent from the spectrum indicates that the object is probably not a planetary nebula.

This method of detecting objects having emission spectra has two limitations: first, it can be used only on objects of approximately stellar size as seen on the photographic plate; and second, it cannot be used with a reflecting telescope because of the absence of chromatic aberration. It is expected that this method will prove useful for detecting and confirming suspected planetary nebulae and Wolf-Rayet stars which are too faint to be observed spectroscopically.[2]

CARL K. SEYFERT

McDONALD OBSERVATORY
October 1938

[1] *Ap. J.*, **63**, 236, 1926.

[2] A somewhat similar method was used by Barnard (*Ap. J.*, **14**, 151, 1901) for visual and photographic observations of novae and planetary nebulae.

ERRATUM

On Plate XVI in the October issue the pointer indicating the line *Hα* was inadvertently displaced to the left. It should have been placed in line with the heavy emission at the extreme right of the reproductions.